Aalto University
School of Science
Degree Programme in Engineering Physics and Mathematics

Juho Andelmin

Optimal routing of electric vehicles

Master's Thesis
Espoo, July 31, 2014

Supervisor: Assistant Professor Enrico Bartolini
Instructor: Assistant Professor Enrico Bartolini

Aalto University
School of Science
Degree Programme in Engineering Physics and Mathematics

ABSTRACT OF MASTER'S THESIS

Author:	Juho Andelmin		
Title: Optimal routing of electric vehicles			
Date:	July 31, 2014	**Pages:**	89
Professorship:	Systems and Operations Research	**Code:**	Mat-2
Supervisor:	Assistant Professor Enrico Bartolini		
Instructor:	Assistant Professor Enrico Bartolini		

In this thesis, a vehicle routing problem (VRP) variant tailored for plug-in battery electric vehicles (BEVs) is studied. The studied problem involves a fleet of identical BEVs located at a central depot, a set of customers that must be serviced within given time windows, and a set of charging stations where the vehicles can recharge their batteries. The objective is to design a set of vehicle routes, each starting and ending at the depot, so that each customer is serviced exactly once and the total energy cost of the vehicle routes is minimized. Since BEVs have limited battery capacity and low recharging rate, charging station visits and recharging times must be explicitly considered in the route planning, wherefore most VRP variants are not sufficient in modeling the studied problem.

Optimal routing of electric vehicles is not much studied in the optimization literature. The two most relevant models are the *Green Vehicle Routing Problem* (G-VRP) by Erdoğan & Miller-Hooks (2012) and the *Electric VRP with Time Windows* (E-VRPTW) by Schneider et al. (2013). The model considered in this thesis generalizes the E-VRPTW by also allowing the possibility of recharging a variable amount of energy at charging stations (*variable recharging scheme*) rather than performing a full recharge at every visit (*fixed recharging scheme*).

This thesis introduces *energy paths* (e-paths) and proposes a new formulation of the studied problem based on non-dominated e-paths between every customer pair. The new formulation reduces the number of decision variables in the model and eliminates the need of imposing an artificial upper bound on the number of stops to a charging station, as is commonly done in previous models to keep their size acceptable. Some new preprocessing steps and valid inequalities are also presented to strengthen the LP-relaxation of the proposed formulation.

Computational tests indicate that the new formulation provides considerable improvements over the standard formulation. Moreover, it is shown that significant reductions in the routing cost can be obtained in real-world routing problems by adopting the variable recharging scheme over the fixed one.

Keywords:	vehicle routing problem, VRP, electric vehicle routing, plug-in battery electric vehicle, BEV, e-path
Language:	English

Aalto-yliopisto
Perustieteiden korkeakoulu
Teknillisen fysiikan ja matematiikan koulutusohjelma

DIPLOMITYÖN TIIVISTELMÄ

Tekijä:	Juho Andelmin		
Työn nimi: Sähköautojen optimaalinen reititys			
Päiväys:	31. heinäkuuta 2014	**Sivumäärä:**	89
Professuuri:	Systeemi- ja operaatiotutkimus	**Koodi:**	Mat-2
Valvoja:	Apulaisprofessori Enrico Bartolini		
Ohjaaja:	Apulaisprofessori Enrico Bartolini		

Tässä työssä tutkitaan ajoneuvon reititysongelman (*Vehicle Routing Problem*, VRP) variaatiota, joka on räätälöity ladattavia sähköautoja varten. Tutkittu ongelma käsittää laivueen identtisiä sähköautoja, jotka sijaitsevat keskusvarikolla; joukon asiakkaita, joiden luona tulee vierailla annettujen aikaikkunoiden määräämissä rajoissa; sekä joukon latausasemia, joissa autot voivat käydä lataamassa akkunsa. Ongelman tavoitteena on suunnitella joukko ajoreittejä, alkaen varikolta ja päättyen varikolle, siten, että jokainen asiakas on palveltu tasan kerran ja ajoreittien yhteenlaskettu energiakustannus on pienin mahdollinen. Koska sähköautojen toimintasäde on lyhyt ja akun lataaminen kestää suhteellisen kauan, tulee sekä latausasemakäynnit että lataukseen kuluva aika ottaa erityisesti huomioon reitin suunnittelussa, minkä vuoksi useimmat ajoneuvon reititysongelman variaatiot eivät ole riittäviä mallintamaan tutkittua ongelmaa.

Sähköautojen optimaalista reititystä ei ole tutkittu paljon alan kirjallisuudessa. Kaksi keskeisintä mallia ovat *Green VRP* (G-VRP) (Erdoğan & Miller-Hooks, 2012) ja *Electric VRP with Time Windows* (E-VRPTW) (Schneider et al., 2013). Tässä työssä tutkittu malli on yleistys E-VRPTW -mallista, joka mahdollistaa lisäksi mielivaltaisen energiamäärän lataamisen latausasemilla toisin kuin alkuperäisessä mallissa, jossa sähköautojen akut ladataan täyteen jokaisella käynnillä.

Tässä työssä esitetään *energiapolku* (e-path) ja kehitetään uusi formulaatio tutkitulle ongelmalle perustuen ei-dominoituihin energiapolkuihin asiakasparien välillä. Uusi formulaatio vähentää päätösmuuttujien lukumäärää mallissa ja poistaa tarpeen asettaa mielivaltaisen ylärajan latausasemakäyntien lukumäärälle, kuten on tavallisesti tehty aikaisemmissa malleissa pitääkseen niiden koot kohtuullisina. Työssä esitetään myös uusia esikäsittelyjä sekä valideja epäyhtälöitä.

Laskennalliset testit osoittavat, että työssä kehitetty uusi formulaatio on huomattavasti tehokkaampi kuin alkuperäinen vastaava. Lisäksi mallintamalla ladattu energiamäärä muuttujana, toisin kuin suorittamalla täysi lataus jokaisella latausasemakäynnillä, voidaan kuljetuskustannuksia vähentää merkittävästi.

Asiasanat:	ajoneuvon reititysongelma, kauppamatkustajan ongelma, sähköauton reititysongelma, sähköauto, energiapolku
Kieli:	Englanti

Acknowledgements

This research has been supported by the Aalto Energy Science Initiative (ESCI) of Aalto University School of Science.

First and foremost, I wish to thank my instructor and supervisor Professor Enrico Bartolini for his excellent guidance and motivation throughout this thesis. I wish to thank Professor Ahti Salo for guiding me in the right direction, and both Ahti and Dr. Juuso Liesiö for initially giving me the opportunity to work at the Systems Analysis Laboratory. I also wish to thank Professor Jukka Nurminen from the Department of Computer Science and Engineering for providing valuable ideas during the several meetings we had with Jukka, Ahti and Enrico.

I also wish to thank my family for all their support. Most importantly, I wish to express my deepest gratitude to my soulmate Riikka for her love and support.

Finally, I dedicate this thesis to the memory of my friend Tommi, who sadly passed away as the final version was nearing completion.

Salo, July 31, 2014

Juho Andelmin

Contents

Abbreviations

$\mathcal{P}(\Psi_{ij})$	Set of feasible paths between i and j
$\mathscr{P}_{ij}$	Index set of non-dominated paths between i and j
Ψ_{ij}	E-path between i and j
A	Arc set
a_i	Time window beginning of vertex i
b_i	Time window end of vertex i
C	Vehicle load capacity
$c(P)$	Cost of path P
c_{ij}	Cost of arc (i, j)
F	Charging station vertices
G	Graph $G = (V, A)$
g	Recharging rate
K	Energy consumption rate
m	Number of vehicles
N	Customer vertices
n_C	Number of customers
N_P	Number of non-dominated paths
Q	Vehicle battery capacity
T	Maximum route duration
V	Vertex set

x_{ij}^p	Path variable $x_{ij}^p \in \{0, 1\}$
x_{ij}	Arc variable $x_{ij} \in \{0, 1\}$
BEV	Plug-in battery electric vehicle
CVRP	Capacitated vehicle routing problem
E-VRPTW	Electric vehicle routing problem with time windows
G-VRP	Green vehicle routing problem
ICE	Internal combustion engine
MDVRP	Multi-depot vehicle routing problem
MDVRPI	Multi-depot vehicle routing problem with inter-depot routes
Model 1	Formulation (3.2) - (3.16)
Model 2	Formulation (4.16) - (4.29)
R-VRP	Recharging vehicle routing problem
TSP	Traveling salesman problem
VRP	Vehicle routing problem
VRPIRF	Vehicle routing problem with intermediate replenishment facilities
VRPPD	Vehicle routing problem with pickup and delivery
VRPSF	Vehicle routing problem with satellite facilities
VRPTW	Vehicle routing problem with time windows

Chapter 1

Introduction

1.1 Background and motivation

Global warming has become a prevalent issue in recent years, evoking ongoing political and public debate across the world. One of the main causes of this phenomenon is believed to be the increased amount of greenhouse gas emissions resulting from human-induced activities such as cement production, deforestation and the burning of fossil fuels (National Research Council, 2010). Specifically, the vast amount of carbon dioxide (CO_2) emissions from fossil fuel combustion has been identified as a potential major contributor in the rise of the Earth's average surface temperature (Intergovernmental Panel on Climate Change, 2013). Consequently, in order to mitigate the global warming, various laws and regulations aimed at reducing the amount of CO_2 emissions have been progressively implemented and adopted across different economic sectors.

Transportation sector, in particular, is estimated to account for over 30% of global CO_2 emissions, road transport being the largest contributing subsector (Ehsani et al., 2009); this is mainly because over 95% of consumed vehicle fuels are based on petroleum, a fossil fuel derivative (Ehsani et al., 2009; Fulton et al., 2009). Moreover, the transportation sector is estimated to expend more than 25% of the available fossil fuels, an amount that is expected to increase with the growing transportation demand (Polski Instytut Spraw Miedzynarodowych, 2009). However, as fossil fuels are becoming scarce and further reductions in CO_2 emissions are being required, satisfying this demand in the future poses significant challenges. In fact, it will likely become necessary for both organizations and individuals to eventually start deploying alternative fuel vehicles that are (i) not dependent on fossil fuels, (ii) emit only small amounts of greenhouse gases and (iii) utilize low-emission energy sources.

Among the viable candidates for replacing the conventional internal combustion engine (ICE) powered vehicles, plug-in battery electric vehicles (BEVs) appear promising with their zero tailpipe CO_2 emissions (European Parliament & European Council, 2011) and the possibility of exploiting their batteries to provide ancillary services in the future, such as frequency regulation on electric distribution systems (Kempton et al., 2008). Moreover, BEVs are inherently more efficient than ICE vehicles due to their regenerative breaking capabilities, i.e., their ability to recuperate energy during deceleration phases. On the other hand, it is important to note that the environmental impact of BEVs cannot be estimated based solely on their tailpipe emissions, but rather on how the electricity they consume is generated. For example, given the current energy mix in the U.S., some estimates state that the reductions in CO_2 emissions could be as large as 40% in regions with a high percentage of renewable energy sources such as wind power, or, conversely, close to zero or even negative in regions with a high concentration of coal based electricity generation (see, e.g., Kintner-Meyer et al., 2007). Consequently, in order to achieve the true potential of BEVs, it is crucial to ensure that emission free energy sources are utilized to produce the extra electricity required by the entire fleet.

Wider adoption of BEVs has not succeeded in earlier years for various reasons, including short driving range, slow battery charging, limited charging infrastructure and high associated costs. However, motivated by the environmental concerns and the potential scarcity of fossil fuels, BEVs have been actively studied and technological advances have since been made that mitigate many of these previous issues. Nevertheless, some challenges still remain that undermine the promotion of BEVs as viable alternatives to conventional ICE powered vehicles.

Most importantly, the driving range of a commercial BEV is still relatively short, ranging approximately from 100 km to 350 km depending on various factors such as weather, battery type, vehicle speed and traffic congestion (Chan, 2002, 2007; Jha, 2012). Moreover, the charging infrastructure is still very limited; i.e., the number of charging stations is significantly smaller than, for example, the number of gasoline stations. Furthermore, in Finland, for instance, most charging stations are currently aggregated around major cities, thus making it difficult to recharge the battery in between trips from one major city to another.

The short driving range along with limited charging infrastructure may consequently cause issues related to range anxiety, i.e., the fear of not having enough battery charge to reach the desired destination (or the nearest charging station) (Franke et al., 2012), unless the vehicle is used exclusively in an area with a high concentration of charging stations, for example, within a major city. However, limiting the use of BEVs to such restricted areas is not a viable option for either most individuals, or organizations that are planning to convert their fleets to alternative fuel vehicles and are considering BEVs as potential candidates.

Fortunately, range anxiety can be effectively mitigated by careful route planning; for example, by planning in advance when and where to recharge the battery so that the total energy consumption and the risk of battery depletion are minimized. However, optimal routing of electric vehicles is not much studied in the optimization literature. The motivation behind this thesis is to facilitate this shortcoming by developing an optimization model for route planning problems involving BEVs.

1.2 Related studies

Route planning problems are generally modeled as *Vehicle Routing Problems* (VRPs). The first VRP variant was introduced by Dantzig & Ramser (1959) in the context of a truck dispatching problem, more generally known as the *Capacitated VRP* (CVRP), in which a set of customers have positive demands, a fleet of vehicles have limited capacities for supplying the customers and the task is to find a set of minimum cost vehicle routes so that all customers are serviced and the sum of the customer demands in one route does not exceed the vehicle capacity. Many VRP variants have since been developed, such as the VRP with distance constraints, in which the driving range of the vehicles is limited (Laporte, Desrochers, & Nobert, 1984), and the *VRP with Time Windows* (VRPTW), in which a set of customers must be visited within specified time intervals (see, e.g., Laporte, 2009; Golden et al., 2008 for recent surveys). However, most VRP variants are not directly applicable to routing problems involving BEVs, because they do not incorporate visits to charging stations. Moreover, the distance constraint imposed by the battery capacity is subject to change as a consequence of recharging en route.

Relatively few studies have been published that focus specifically on the optimal routing of electric vehicles; instead, most related studies concentrate on the following aspects: (i) minimizing vehicle fuel consumption and emissions in general, (ii) optimizing the placement of charging stations and (iii) finding the shortest energy paths (i.e., paths with smallest energy-related routing costs) between two locations (see, e.g., Demir et al., 2013 for a recent review). In fact, this thesis is aware of only two routing models that incorporate both the charging station visits and the distance constraints that are subject to change: the green VRP (G-VRP) model proposed by Erdoğan & Miller-Hooks (2012) and the electric VRP with time windows (E-VRPTW) presented in (Schneider et al., 2013). Moreover, the main focus of these studies is to develop approximate (heuristic) solution methods that provide suboptimal solutions with no guarantees on their quality. Such methods can be useful in practice, because they are typically significantly faster than exact optimization techniques; however, care must generally be taken before making important decisions based on a heuristic solution, because it could be far from the optimal one (see, e.g., Cordeau et al., 2002).

1.3 Objectives and contributions

This thesis focuses on the optimal routing of BEVs from an operational viewpoint. The aim is to contribute towards the development of a framework that supports the user in designing optimal routing plans in scenarios, where a set of locations (e.g., customers) is to be visited within given time windows using one or more BEVs, and where the tour length exceeds the initial driving range, thus making it necessary to recharge at charging stations en route. Towards this end, an optimization model is developed that finds the minimum cost vehicle routes with regard to energy consumption for a fleet of vehicles starting their tour from a depot, visiting a set of locations (e.g., customers) within specified time windows, stopping to recharge when necessary, and finally returning back to the depot. This problem is known as the Electric Vehicle Routing Problem with Time Windows (E-VRPTW) introduced by Schneider et al. (2013), which in turn builds on the ideas presented in (Erdoğan & Miller-Hooks, 2012) and (Bard et al., 1998). The problem considered in this thesis is a generalization of the E-VRPTW, which also allows the possibility of recharging a variable amount of energy at the charging stations (*variable recharging scheme*) rather than performing a full recharge at every visit (*fixed recharging scheme*).

This thesis proposes a new formulation of the problem which does not model the charging stations explicitly, but replaces them with a set of non-dominated energy paths between every customer pair. The new formulation reduces the number of decision variables in the model and is shown to provide significant computational improvements with respect to the standard formulation. Moreover, it removes the need of imposing an artificial upper bound on the number of stops to a charging station, as is commonly done in previous models to keep their size acceptable. Some new preprocessing steps and valid inequalities are also presented to strengthen the LP-relaxation of the developed model.

Both the standard and the new formulation are implemented in C programming language and solved with CPLEX (ILOG, 2013) using the CPLEX 12.5 callable library interface functions. The models are compared on a set of small benchmark instances proposed by Schneider et al. (2013), which are based on the benchmark instances for the VRPTW proposed by Solomon (1987). Furthermore, the solutions obtained with the variable recharging scheme are compared to those obtained with the fixed recharging scheme used in the previous models, showing that the variable recharging scheme can provide significant improvements to the solution quality.

Finally, an illustrative test instance based on the road network of southwestern Finland is constructed by using the network data obtained from openstreetpmap.org, and a set of test cases are generated to simulate potential real-world BEV routing problems by taking into account the existing charging infrastructure. The results of these test cases are finally reported and evaluated.

1.4 Structure

The rest of this thesis is structured as follows. Chapter 2 reviews the relevant literature regarding BEVs, vehicle routing problems and green logistics in general. Chapter 3 presents the standard mathematical formulation for the E-VRPTW and describes how to reduce the number of variables by means of different preprocessing techniques. Chapter 4 presents the new formulation and introduces some new preprocessing steps and valid inequalities to strengthen the formulation. Chapter 5 presents computational results for a set of small benchmark instances and evaluates the two models in more detail. Chapter 6 presents a case study based on the road network of southwestern Finland; a set of test cases are generated to simulate potential real-world BEV routing problems. Finally, Chapter 7 provides concluding remarks.

Chapter 2

Literature review

This Chapter reviews the essential literature related to this thesis. The aim is to provide a brief overview of green logistics and demonstrate the central role of plug-in battery electric vehicles (BEVs) in achieving sustainable green logistics solutions. This is followed by a more comprehensive review of studies related to vehicle routing problems and specifically to the optimal routing of BEVs and other alternative fuel vehicles.

2.1 Green logistics and battery electric vehicles (BEVs)

Green logistics originates from the mid-1980s, when it was first referred to as a "concept to characterize logistics systems and approaches that use advanced technology and equipment to minimize environmental damage during operations" (Thiell et al., 2011). In general, green logistics can be thought of comprising a whole range of measures that provide sustainable logistics solutions while minimizing their environmental impacts (e.g., CO_2 emissions). Some examples of green logistics approaches include: more efficient packing, route optimization, load optimization and the use of alternative fuel vehicles for both manufacturing and shipping (Tambovceva & Tambovcevs, 2012).

Traditionally, the main focus in most logistics operations has been cost minimization. However, environmental concerns and the potential scarcity of fossil fuels have driven governments to enact laws and regulations that require organizations to emphasize green logistics approaches in their operations, starting with the deployment of alternative fuel vehicles where possible (see, e.g., Becker et al., 2009). This has achieved some success; for example, in the package shipping industry, several big companies have started using BEVs for last-mile deliveries in areas with a sufficient charging infrastructure (for surveys of this subject, see Edwards et al., 2010; Finnegan et al., 2005).

Several governments have also started establishing tax incentives for BEVs to promote them to individuals, and thus facilitate their market penetration (see, e.g., Becker et al., 2009). Moreover, projects around the world have been initiated that aim at building wide charging infrastructures to support the growing number of BEV fleets (see, e.g., Wiederer & Philip, 2010). Notably, as of December 2013, Estonia became the first country in the world with a nationwide fast charging infrastructure to support a full scale adoption of BEVs. The ultimate goal, for instance in Denmark and probably eventually across the world, is the extensive adoption of BEVs fueled by electricity from sustainable energy sources to replace the conventional internal combustion engine (ICE) powered vehicles (see, e.g., Bigliani & Gallotti, 2009; Binding et al., 2010).

Some challenges still remain, however, that undermine the promotion of BEVs as viable alternatives to ICE powered vehicles. Most importantly, the driving range of commercial BEVs is still relatively short (ranging from 100 km to 350 km), which causes range anxiety, that is, the fear of not having enough battery charge to reach the desired destination (or the nearest charging station) (Franke et al., 2012). Several studies have shown that range anxiety is a relevant issue, which acts as a potential barrier to a wider adoption of electric vehicles, especially in places with a limited charging infrastructure (see, e.g., Franke et al., 2012; Daziano, 2013).

Fortunately, range anxiety can be effectively mitigated by careful route planning; for example, by planning in advance when and where to recharge the battery in a given vehicle route so that the total energy consumption and the risk of a battery depletion are minimized. Since the time to recharge is rather long and affects the route planning, it is also important to determine how much should be recharged. Such decision support could provide significant benefits to both individuals and organizations, and further facilitate the adoption of BEVs. However, optimal routing of electric vehicles is not much studied, despite the increasing importance of green logistics in the optimization literature (see, e.g., Demir et al., 2013 for a recent review).

2.2 Related studies

Route planning problems are generally modeled as *Vehicle Routing Problems* (VRPs). The VRP seeks to service a set of customers using a fleet of vehicles such that the total routing cost (e.g., traveled distance) is minimized. The VRP can be considered as a generalization of the *Traveling Salesman Problem* (TSP), in which for a given set of cities the objective is to find the shortest possible route that visits each city exactly once, eventually returning to the city of departure (see, e.g., Flood, 1956). As the TSP is known to be an NP-hard problem, the VRP is also NP-hard.

The first VRP variant was originally introduced by Dantzig & Ramser (1959) in the context of a truck dispatching problem, in which a fleet of delivery trucks with limited capacities are based at a depot, and a set of service stations (or customers) is to be visited by the fleet so that the station demands are satisfied and the total distance traversed by the entire fleet is minimized. This problem is more commonly known as the *Capacitated Vehicle Routing Problem* (CVRP).

Several variants of the VRP have since been developed, including the VRP with distance constraints, in which the driving range of each vehicle is limited (see, e.g., Laporte, Desrochers, & Nobert, 1984), and the *VRP with Time Windows* (VRPTW), in which customers must be visited within specified time intervals (see, e.g., Laporte, 2009; Golden et al., 2008 for recent surveys and advances). The high computational complexity of VRP and its variants renders most exact solution methods inadequate for many real-world applications (for a review of recent exact algorithms, see Baldacci et al., 2012), wherefore most studies focus on heuristic solution methods instead (see, e.g., Toth & Vigo, 2001; Golden et al., 2008).

Unfortunately, most VRP variants are not directly applicable to routing problems involving BEVs, because they do not incorporate visits to charging stations. Moreover, the driving range of a BEV is subject to change whenever the battery is recharged, whereas in the traditional distance constrained VRP, for instance, the driving range of a vehicle remains constant. Modeling the increase in the vehicle driving range upon recharging/refueling plays a key role in BEV routing; however, it has received only limited interest in earlier years due to the widespread availability of petrol stations and the long driving range of gasoline powered vehicles.

Some related studies focus on military applications, where the objective is to maximize the total traveled distance of a selected vehicle or a group of vehicles within a larger fleet using a sequential recharging scheme, in which available fuel is allocated and transferred between the vehicles based on their priority and type (e.g., from fuel carrying tankers to other vehicles) (see, e.g., Mehrez et al., 1983; Mehrez & Stern, 1985; Melkman et al., 1986). In the studied applications, however, refueling can be performed regardless of the vehicle location, whereas in BEV routing recharging can occur only at charging stations.

In a more recent study, Gonçalves et al. (2011) extend the *VRP with Pickup and Delivery* (VRPPD), in which a fleet of vehicles is based at a depot, and the objective is to transport customers from specific origin locations to specific destination locations so that the traversed distance of the entire fleet is minimized (see, e.g., Toth & Vigo, 2001). The proposed extension incorporates a mixed fleet of BEVs and conventional ICE vehicles with the possibility of recharging or refueling en route. The objective of the model is to minimize a combination of fixed and variable routing costs (e.g., fixed costs of deploying a BEV and varying fuel consumption costs based on the traveled distance). The total time to recharge a BEV is estimated based on the traveled distance by taking into account the maximum driving range imposed by the battery capacity. However, no specific locations for the charging stations are presented in this model.

In another related study, Ichimori et al. (1983) present a simple model that incorporates refueling stations at specific locations. In this model, a single vehicle, based at a depot, visits a single customer after receiving a service call, and finally returns to the depot, possibly refueling en route if necessary. The model allows extending the vehicle driving range via refueling to serve customers that are initially unreachable with regard to the length of the round trip between the customer and the depot. However, the presented model is a variant of the shortest path problem, which cannot be generalized in a straightforward way to include multiple customers or vehicles.

Bard et al. (1998) present a CVRP variant that incorporates intermediate stations denoted as *satellite facilities*, where the vehicles can replenish (i.e., restock their supply) and thus increase their operational range by allowing them to serve additional customers before returning to the depot. This variant is referred to as the *VRP with Satellite Facilities* (VRPSF), and it is the first VRP variant this thesis is aware of that models such intermediate stations at specific locations. The VRPSF is originally intended for goods distribution problems, where vehicles can stop at the satellite facilities to replenish or unload; however, the satellite facilities could also be regarded as charging stations, where BEVs could recharge their battery and thus increase their driving range. Bard et al. (1998) also discuss the issue that arises when incorporating such replenishment stations: multiple visits to a same station must be explicitly modeled. This issue is specifically addressed later in this thesis. In terms of solving the VRPSF, Bard et al. (1998) develop a branch-and-cut algorithm and report optimal solutions to instances with up to 18-20 customers and 0-2 satellite facilities.

Another VRP variant that is capable of modeling charging station visits is presented in (Crevier et al., 2007) as an extension of the *Multi-Depot Vehicle Routing Problem* (MDVRP), in which vehicle fleets are based at several depots, every customer is to be visited exactly once, and each vehicle route starts and ends at the same depot (see, e.g., Laporte, Nobert, & Arpin, 1984). In the proposed extension, the depots can act as intermediate replenishment facilities along the vehicle route; the extension is accordingly referred to as *MDVRP with Inter-Depot Routes* (MDVRPI). The MDVRPI is originally motivated by a real-life grocery distribution problem, in which a fleet of delivery trucks, based at one of several depots, can stop at the intermediate depots to replenish their food supply. Even though Crevier et al. (2007) present the MDVRPI as a multi-depot problem, they propose benchmark instances where all the vehicles are based at a single central depot.

Tarantilis et al. (2008) rename the problem as *Vehicle Routing Problem with Intermediate Replenishment Facilities* (VRPIRF) to "emphasize both the replenishment role of the intermediate facilities and the use of a single central station for the fleet of vehicles". On the other hand, the VRPIRF appears similar to the VRPSF presented by Bard et al. (1998), with the exception that the replenishment facilities are referred to as satellite facilities. Problems similar to the MDVRPI (or VRPIRF) arise, for example, in waste collection (Kim et al., 2006), but with a slightly different objective: instead of minimizing the traveled distance, the objective is extended to include workload balancing between the vehicles. In terms of solving the MDVRPI and VRPIRF, some heuristic procedures are developed in (Crevier et al., 2007) and (Tarantilis et al., 2008), respectively.

2.3 Routing models for electric vehicles

Conrad & Figliozzi (2011) present the first VRP variant this thesis is aware of that is specifically tailored for BEV routing. The proposed variant is referred to as the *Recharging Vehicle Routing Problem* (RVRP), and it extends the VRPTW by implementing the possibility of recharging the BEVs at the customer locations en route, and thus increasing their driving range. The primary objective of the RVRP is to minimize the number of vehicles used, and the secondary objective is to minimize a cost function comprising costs related to the traveled distance, service time delays and the number of recharging occurrences. However, since recharging is allowed only at the customer locations upon service, the model is rather limited and not applicable to more general situations, where charging stations are located separately from the customers and a single charging station can be visited more than once. Moreover, the model assumes constant recharging times, a shortcoming which is later addressed in this thesis. In terms of solving the RVRP, Conrad & Figliozzi (2011) describe a heuristic algorithm based on ”an iterative construction and improvement algorithm” for the VRPTW (Figliozzi, 2010). In addition, the impact of the vehicle battery capacity, time windows and recharging time are studied by solving a set of test instances derived from the benchmark instances proposed by Solomon (1987).

Erdoğan & Miller-Hooks (2012) present the *Green Vehicle Routing Problem* (G-VRP), a VRP variant which builds on the VRPSF formulation presented in (Bard et al., 1998). The G-VRP is the first VRP variant this thesis is aware of that allows vehicles to refuel (or recharge) at specific locations denoted as refueling stations. The G-VRP models the refueling (or recharging) stations similarly to the satellite facilities in the VRPSF formulation (Bard et al., 1998), thus ensuring that several visits to a single station can be performed. According to Erdoğan & Miller-Hooks (2012), the key difference between the VRPSF and the G-VRP is that the VRPSF does not incorporate distance constraints on the vehicles based on their fuel tank capacity, wherefore running out of fuel en route to a customer (or a satellite facility or a depot) is not considered. Moreover, in the G-VRP, fuel is consumed along the network edges, whereas in the VRPSF goods are consumed at the network vertices, wherefore the capacity limitations associated with the VRPSF are not sufficient to model fuel consumption limitations. The primary objective of the G-VRP is to minimize the total traveled distance of the entire fleet. The G-VRP provides a basis for the *Electric Vehicle Routing Problem with Time Windows* (E-VRPTW) studied in this thesis; however, unlike the E-VRPTW, the G-VRP assumes a constant refueling time and incorporates no customer time windows. Erdoğan & Miller-Hooks (2012) propose two heuristic methods for solving the G-VRP: the Modified Clarke and Wright Savings (MCWS; Clarke & Wright, 1964) and the Density-Based Clustering Algorithm (DBCA; Ester et al., 1996).

Finally, Schneider et al. (2013) present the *Electric Vehicle Routing Problem with Time Windows* (E-VRPTW), which extends the G-VRP by introducing customer time windows, customer demands and vehicle capacities (i.e., the E-VRPTW generalizes both the CVRP and the VRPTW). Additionally, the E-VRPTW introduces a new recharging scheme, in which the time to recharge depends on the battery state-of-charge upon arriving at a charging station. However, a full recharge is enforced at every station visit. In terms of solving the E-VRPTW, Schneider et al. (2013) propose a heuristic solution method which combines the Variable Neighborhood Search (VNS) and the Tabu Search (TS) heuristics (see Mladenović & Hansen, 1997; Glover & Laguna, 1999). The performance of the proposed heuristic is assessed by solving a set of instances with up to ~100 customers derived from the VRPTW dataset of Solomon (1987). Moreover, the heuristic solutions are compared with the best solutions obtained by the integer programming solver CPLEX on a set of small instances with up to 15 customers.

The formulation introduced in Chapter 3 is based on the G-VRP and the E-VRPTW formulations presented in (Erdoğan & Miller-Hooks, 2012) and (Schneider et al., 2013), respectively, but allows the possibility of recharging a variable amount of energy at the charging stations.

Chapter 3

Electric Vehicle Routing Problem with Time Windows

This Chapter describes the *Electric Vehicle Routing Problem with Time Windows* (E-VRPTW) and presents a mathematical model for solving the problem. The proposed model corresponds to the formulation presented in (Schneider et al., 2013), but allows the possibility of recharging a variable amount of energy at charging stations, in contrast to performing a full recharge at every visit. Additionally, a theoretical upper bound on the number of possible visits to a single charging station is provided, instead of assigning an arbitrary bound as in the previous studies. Furthermore, a new preprocessing step is introduced that eliminates redundant decision variables.

3.1 Problem description

The description of the E-VRPTW is as follows. A fleet of identical electric vehicles is to visit a set of *customers* at different locations. Each customer is associated with a *service time* and a *time window* within which the service must begin. The vehicles start their tour from a predefined *origin depot* and end their tour end at a predefined *destination depot*; additionally, the total duration of each vehicle route is limited. The vehicles' batteries must not run out of energy; to prevent this, the vehicles can stop to recharge at any of the available charging stations between the customer visits. The objective is to determine an optimal routing plan for the entire fleet so that (i) all customers are visited exactly once within the specified time windows and (ii) the total energy cost of the vehicle routes is minimized.

3.2 Modeling assumptions

It is assumed that the problem can be defined on a road network describing the area of interest. Moreover, it is assumed that this network can be modeled as a directed graph $G' = (V', A')$ with vertices V' corresponding to network locations (e.g., customers, charging stations and road intersections) and arcs A' corresponding to road segments between the vertices. Each road segment $(i, j) \in A'$ between two vertices $i, j \in V'$ is assumed to be associated with a distance value d_{ij}, a constant travel speed v, and a travel time $t_{ij} = d_{ij}/v$.

The proposed model for the E-VRPTW is based on the following assumptions:

1. Energy consumption of the vehicles is proportional to the traveled distance: the energy cost of traversing an arc $(i, j) \in A'$ is defined as

$$c_{ij} = K d_{ij}, \tag{3.1}$$

   where K denotes the constant energy consumption rate. Consequently, the shortest path is also the most energy-efficient.

2. Vehicle speed v is constant over the arcs.

3. Vehicle battery is charged with a constant rate; i.e., the charging function is linear over time. Additionally, the charged amount is not fixed in advance, and is limited only by the battery capacity Q.

4. Time is discretized into time steps (e.g., into one minute steps).

Furthermore, it is assumed that there are no vertices in the network graph representing both a customer and a charging station. Instead, such vertices are modeled by duplicating them into two distinct vertices, one representing the customer and the other one the charging station.

Following the assumptions presented in (Erdoğan & Miller-Hooks, 2012), the proposed model differentiates between visits to charging stations from those to customers and depots. This assumption is necessary, because each charging station can be visited more than once (or not at all), whereas each customer *must* be visited exactly once. In order to allow multiple visits to the same charging station, each such potential visit is modeled as a separate instance (i.e., vertex) representing the same station in the network graph (Bard et al., 1998). Erdoğan & Miller-Hooks (2012) suggest that the number of such *dummy* vertices for each charging station should remain small in order to prevent the network graph from expanding too much, but large enough not to restrict beneficial visits to the station. However, no theoretical upper bound on the number of these dummy vertices was given. The following Lemma provides such a bound.

Lemma 1. *Suppose that the number of customers in an E-VRPTW instance is n_C. Then, in an optimal solution, the number of visits to a single charging station is at most $n_C + m^*$, where m^* denotes the number of vehicles used in the solution.*

Proof. Let n_l denote the number of customers visited by vehicle v_l for all $l \in \{1, \ldots, m^*\}$. In an optimal solution, each charging station is visited at most once between two consecutive customer visits, amounting to a maximum of $n_l - 1$ visits for each vehicle v_l. Moreover, each vehicle may visit a charging station after leaving the origin depot and before arriving at the destination depot. Thus, the number of visits to a single charging station is at most $\sum_{l=1}^{m^*}(n_l - 1 + 2) = \sum_{l=1}^{m^*} n_l + \sum_{l=1}^{m^*} 1 = n_C + m^*$. □

E-VRPTW instances where the optimal solution contains $n_C + m^*$ visits to a single charging station can be easily constructed, wherefore setting an arbitrary limit on the number of charging station visits might not produce an optimal solution. Therefore, in the following, it is assumed that every charging station is modeled as a set of $n_C + m$ dummy vertices, where m corresponds to the upper limit set on the number of vehicles.

3.3 Formal description of the model

The E-VRPTW is modeled on a directed graph $G = (V \cup \{0\} \cup \{n+1\}, A)$, where the vertex set $V = N \cup F$ is composed of the subsets $N = \{1, \ldots, n\}$ and F that comprise the vertices representing the customers and charging station visits, respectively, whereas the vertices $\{0\}$ and $\{n+1\}$ correspond to the origin and destination depots, respectively. The arc set $A = \{(i, j) \mid i, j \in V \cup \{0\} \cup \{n + 1\}, i \neq j\}$ contains one arc (i, j) for each pair of vertices $i, j \in V \cup \{0\} \cup \{n + 1\}$ representing the shortest path from i to j in G' with respect to distances d_{ij}. These paths can be obtained, for instance, with Dijkstra's shortest path algorithm (Dijkstra, 1959). The energy cost and travel time of an arc $(i, j) \in A$ are denoted by c_{ij} and t_{ij}, respectively.

For notational convenience, the following sets are also defined:

$$\begin{aligned} V_0 &= V \cup \{0\}, \quad & V_{n+1} &= V \cup \{n+1\}, \quad & V_{0,n+1} &= V \cup \{n+1\} \cup \{0\}, \\ F_0 &= F \cup \{0\}, \quad & F_{n+1} &= F \cup \{n+1\}, \quad & F_{0,n+1} &= F \cup \{n+1\} \cup \{0\}, \\ N_0 &= N \cup \{0\}, \quad & N_{n+1} &= N \cup \{n+1\}, \quad & N_{0,n+1} &= N \cup \{n+1\} \cup \{0\}. \end{aligned}$$

Each customer $i \in N$ is associated with a *service time* s_i and a *time window* $[a_i, b_i]$, where a_i and b_i denote the earliest and the latest times at which the customer can be visited, respectively. Additionally, the origin and destination depots are associated with time windows $[a_0, b_0]$ and $[a_{n+1}, b_{n+1}]$, respectively, representing the feasible time intervals within which the origin depot must be departed from and the destination depot arrived at. The scalar b_{n+1}, specifically, corresponds to the maximum route duration, which is also denoted by T.

The vehicles have identical batteries with a maximum capacity Q, and each vehicle departs from the origin depot with a full battery; however, it is possible to adjust the battery's initial state-of-charge if necessary. Upon entering a charging station, the vehicle battery is recharged with a constant rate g. Any amount can be recharged, as long as the battery charge remains below the maximum capacity Q.

To represent a mathematical formulation for the E-VRPTW, the following decision variables are defined:

- $x_{ij} \in \{0, 1\}$: $x_{ij} = 1$ if an arc (i, j) is traversed, $x_{ij} = 0$ otherwise; defined for all $i \in V_0$, $j \in V_{n+1}$, $i \neq j$.
- $\tau_i \in \mathbb{R}_+$: the arrival time at a vertex $i \in V_{0,n+1}$.
- $y_i \in \mathbb{R}_+$: the vehicle battery charge upon arriving at a vertex $i \in V_{0,n+1}$.
- $r_i \in \mathbb{R}_+$: the recharged amount at a charging station $i \in F$.

Using these variables, the E-VRPTW is modeled as the following mixed-integer linear programming (MILP) problem:

$$\min \sum_{(i,j)\in A} c_{ij}x_{ij} \tag{3.2}$$

subject to

$$\sum_{j\in V} x_{0j} = \sum_{j\in V} x_{j\,n+1} \leq m, \tag{3.3}$$

$$\sum_{j\in V_0} x_{ji} = 1, \ \forall i \in N, \tag{3.4}$$

$$\sum_{j\in V_0} x_{ji} \leq 1, \ \forall i \in F, \tag{3.5}$$

$$\sum_{j\in V_0} x_{ji} - \sum_{j\in V_{n+1}} x_{ij} = 0, \ \forall i \in V, \tag{3.6}$$

$$\tau_j \geq \tau_i + (s_i + t_{ij})x_{ij} - \max\{0, b_i - a_j\}(1 - x_{ij}), \ \forall i \in N_0, j \in N_{n+1}, \tag{3.7}$$

$$\tau_j \geq \tau_i + t_{ij}x_{ij} + gr_i - (T + gQ)(1 - x_{ij}), \qquad \forall i \in F, j \in V_{n+1}, \tag{3.8}$$

$$\tau_j \geq \tau_i + (s_i + t_{ij})x_{ij} - T(1 - x_{ij}), \qquad \forall i \in N_0, j \in F, \tag{3.9}$$

$$a_i \leq \tau_i \leq b_i, \ \forall i \in N_{0,n+1}, \tag{3.10}$$

$$\tau_{n+1} \leq T, \tag{3.11}$$

$$0 \leq y_j \leq y_i - c_{ij}x_{ij} + Q(1 - x_{ij}), \qquad \forall i \in N_0, j \in V_{n+1}, \tag{3.12}$$

$$0 \leq y_j \leq y_i - c_{ij}x_{ij} + r_i + Q(1 - x_{ij}), \ \forall i \in F, j \in V_{n+1}, \tag{3.13}$$

$$y_i + r_i \leq Q, \ \forall i \in F, \tag{3.14}$$

$$r_i \geq 0, \qquad \forall i \in F, \tag{3.15}$$

$$x_{ij} \in \{0, 1\}, \ \forall (i,j) \in A. \tag{3.16}$$

The objective (3.2) minimizes the total energy cost of the vehicle routes, including visits to charging stations. Constraints (3.3) ensure that at most m vehicles depart from the origin depot and arrive at the destination depot. Constraints (3.4) impose that each customer is visited exactly once, whereas constraints (3.5) guarantee that each vertex representing a charging station is visited at most once. Constraints (3.6) establish route connectivity by imposing that the number of incoming arcs must equal the number of outgoing arcs for each vertex.

Constraints (3.7) - (3.9) ensure the consistency of arrival times and prevent the formation of subtours. Constraints (3.10) guarantee that customers are visited within the specified time windows, and constraint (3.11) imposes an upper limit T on the duration of each vehicle route. Constraints (3.12) and (3.13) establish the consistency of the battery state-of-charge at each vertex, while constraints (3.14) impose that the battery charge remains below the maximum capacity Q. Finally, constraints (3.15) ensure that the recharged amount remains positive and (3.16) enforce integrality on the arc variables.

Note that by removing the constraints (3.3) completely, the routing plan with the minimum energy cost is always obtained. The constraints (3.4), (3.6) and (3.7) - (3.9) ensure that every customer is visited exactly once and the number of vehicles arriving at the destination depot equals the number of vehicles departing from the origin depot. Consequently, a set of distinct vehicle routes is formed upon solving the problem. These routes can be identified by following each path in the solution that begins with an arc between the origin depot and a customer or a charging station vertex $j \in N \cup F$ with $x_{0j} = 1$.

3.3.1 Hierarchical objective

An option with multiple vehicles is to use a hierarchical objective, in which the primary objective is to minimize the number of vehicles required to service all the customers and the secondary objective is to minimize the total energy cost of the vehicle routes. A potential strategy for solving E-VRPTW instances with the hierarchical objective is to first solve the problem without the constraints (3.3) to obtain the optimal solution with minimum energy cost; subsequently imposing an upper bound $m^* - 1$ on the number of vehicles, where m^* denotes the number of vehicles used in the optimal solution; and finally attempting to solve the problem with this upper bound. If a feasible solution is found, the number of vehicles can be decreased and the new optimal solution is computed. On the other hand, if the problem becomes infeasible, the primary objective cannot be improved and the previous solution is optimal. However, since determining the feasibility of a VRP instance is in itself a difficult problem, this strategy cannot be used efficiently in general.

Another option is to add an integer variable μ representing the number of vehicles to the objective function with a large enough cost coefficient M, that is, replacing (3.2) with the following objective function

$$\min\Big(\sum_{(i,j)\in A} c_{ij}x_{ij} + M\mu\Big), \tag{3.17}$$

and replacing (3.3) with

$$\sum_{j\in N} x_{0j} = \mu. \tag{3.18}$$

Setting the value of M large enough (i.e., larger than the energy cost of any feasible vehicle route), the objective (3.17) minimizes first the number of vehicles μ, and then the energy cost of the vehicle routes. However, this option is likely to be computationally demanding in larger problems.

Implementing the hierarchical objective efficiently is itself a difficult problem, wherefore it is more commonly associated with heuristic solution methods, whereas most exact algorithms focus solely on routing cost minimization. Incorporating the hierarchical objective is not examined further in this thesis; however, this provides an interesting opportunity for future study.

3.3.2 Customer demands

The formulation (3.2) - (3.16) can be extended to include customer demands (e.g., demands for certain types of goods) and vehicle supply capacities (i.e., the amount of goods that can be carried by a vehicle is limited). Towards this end, the following decision variable is defined:

- $u_i \in \mathbb{R}_+$: the free vehicle capacity upon arriving at a vertex $i \in V_{0,n+1}$.

Additionally, let q_i denote the demand of a of vertex $i \in V_{0\,n+1}$ (for others than customers, $q_i = 0$), and let C denote the maximum vehicle capacity. It is assumed that each vehicle has the same maximum capacity. Using this notation, the customer demands can be implemented by adding the following constraints to the model:

$$0 \leq u_j \leq u_i - q_i x_{ij} + C(1 - x_{ij}), \quad \forall i \in V_0, j \in V_{n+1}, \tag{3.19}$$

$$0 \leq u_0 \leq C. \tag{3.20}$$

Accordingly, (3.19) imposes that when traveling directly from $i \in V_0$ to $j \in V_{n+1}$ (i.e., $x_{ij} = 1$), the vehicle capacity u_j at j is obtained by subtracting the demand q_i at i from the vehicle load u_i at i. Furthermore, (3.20) ensures that each vehicle departs from the origin depot with at most the maximum capacity C. The maximum initial capacity can be imposed by setting $u_0 = C$.

3.3.3 Fixed recharging scheme

It is possible to enforce a full recharge at every charging station visit by replacing (3.14) with

$$y_i + r_i = Q, \quad \forall i \in F. \tag{3.21}$$

However, this may affect the optimal solution or even the feasibility of the problem instance: some customers may not be serviced in time, or the end depot may not be reached within the maximum route duration if recharging takes too long. Consequently, solutions obtained using the fixed recharging scheme cannot be better than those obtained with the variable recharging scheme.

3.4 Preprocessing

A common practice in most vehicle routing problems is to apply a set of *preprocessing* steps before solving the problem (see, e.g., Psaraftis, 1983; Savelsbergh, 1985). Preprocessing is an essential part of the solution process, especially with exact solution methods. Preprocessing methods include, for example, the elimination of infeasible arcs from the network graph, and the tightening of certain inequality constraints (e.g., time window constraints) to improve the linear programming relaxation of the problem formulation. Applying different preprocessing steps can potentially eliminate a significant number of decision variables and provide a stronger formulation, thus reducing the problem size and decreasing the computation time required to solve the problem. In the following, two preprocessing techniques are presented: arc elimination and time window tightening.

3.4.1 Arc elimination

Arc elimination aims at removing infeasible arcs from the network graph G before solving the problem (see, e.g., Psaraftis, 1983; Savelsbergh, 1985). Such arcs may be identified by (i) constructing a set of inequalities that must hold for every feasible arc and (ii) systematically evaluating each arc with regard to the constructed inequalities: if an arc violates these inequalities, it is declared infeasible and removed from the graph.

The following inequalities are based on time window and battery capacity constraints. Any arc $(i, j) \in A$ satisfying either of the inequalities (3.22) - (3.23) is infeasible and can be removed from G.

$$i \in N_0, j \in N \wedge a_i + s_i + t_{ij} > b_j, \tag{3.22}$$

$$i \in N_0, j \in N \wedge a_i + s_i + t_{ij} + s_j + t_{j\,n+1} > T. \tag{3.23}$$

Furthermore, any arc $(i, j) \in A$ satisfying either of the following sets of inequalities (3.24) and (3.25) is infeasible and can be removed from G.

$$i \in N, j \in N \wedge c_{si} + c_{ij} + c_{jt} > Q, \qquad \forall s \in F_0, t \in F_{n+1}, \tag{3.24}$$

$$j \in N \wedge c_{ij} + c_{jk} > Q, \qquad \forall i \in V_0, k \in V_{n+1}. \tag{3.25}$$

The inequalities (3.22) - (3.23) are "well-known preprocessing steps" (Schneider et al., 2013) exploiting customer time windows and maximum route duration T, whereas the inequalities (3.24) and (3.25) are problem specific and exploit the maximum battery capacity Q. The set of inequalities (3.24) is similar to the one presented in (Schneider et al., 2013), which states that an arc $(i, j) \in A$, $i, j \in N$ is infeasible if the energy cost of the path $P = (s, i, j, t)$ is greater than the maximum battery capacity Q for all $s \in F_0$ and $t \in F_{n+1}$. As far as this thesis is aware of, the inequalities (3.25), instead, constitute a new preprocessing step, which states that an arc $(i, j) \in A$, $i \in V_0$, $j \in N$ is infeasible if the energy cost of the path $P = (i, j, k)$ is greater than Q for every $k \in V_{n+1}$.

Note that in order to obtain a full benefit from these preprocessing steps, they should be applied several times until no changes occur in the problem variables. Computational tests indicate that a combination of (3.24) and (3.25), in particular, eliminates a significant number of feasible arcs in many of the problem instances studied in this thesis. A more detailed analysis is presented in Chapter 5.

3.4.2 Time window tightening

Customer time windows can be tightened based on the following procedures. First of all, in accordance with Kontoravdis & Bard (1995), the earliest time for a vehicle to arrive at a customer corresponds to the travel time of the shortest route from the origin depot to the customer. In addition, the latest time a vehicle can leave a customer cannot be more than the maximum route duration T minus the travel time from that customer to the end depot, because otherwise the maximum route duration would be exceeded. Thus, for every customer $i \in N$, the time windows can be tightened by replacing $[a_i, b_i]$ with

$$\Big[\max\{a_0 + t_{0i}, a_i\}, \min\{T - t_{i\,n+1} - s_i, b_i\}\Big]. \tag{3.26}$$

Additionally, Desrochers et al. (1992) introduce four conditions to further tighten the customer time windows. In the following, these conditions are altered slightly to account for customer service times. In order to apply these conditions efficiently, potential *predecessors* and *successors* of every customer are first identified. Towards this end, let $N_i^- = \{j \in N_0 \mid (j,i) \in A\}$ and $N_i^+ = \{j \in N_{n+1} \mid (i,j) \in A\}$ denote the potential predecessor and successor customers, respectively, of a customer $i \in N$. The following conditions are applied sequentially to every customer $i \in N$ and repeated iteratively until no changes occur in the time windows.

1. Minimal arrival time from predecessors:

$$a_i = \max\{a_i, \min_{k \in N_i^-}\{a_k + s_k + t_{ki}\}\}. \tag{3.27}$$

2. Minimal arrival time to successors:

$$a_i = \max\{a_i, \min\{b_i, \min_{k \in N_k^+}\{a_k - t_{ik} - s_i\}\}\}. \tag{3.28}$$

3. Maximal departure time from predecessors:

$$b_i = \min\{b_i, \max\{a_i, \max_{k \in N_k^-}\{b_k + s_k + t_{ki}\}\}\}. \tag{3.29}$$

4. Maximal departure time to successors:

$$b_i = \min\{b_i, \max_{k \in N_k^+}\{b_k - t_{ik} - s_i\}\}. \tag{3.30}$$

The first step attempts to adjust the start time of a time window so that it corresponds to the earliest arrival time when arriving from any potential predecessor vertex. The second step, on the other hand, aims to reduce excess waiting time in situations where the potential successor vertices cannot be serviced immediately upon arrival. The third and the fourth step apply the same principles as the first and the second step, respectively, with the attempt to adjust the end time of the time window.

Chapter 4

Improved formulation

This Chapter develops a new formulation for the E-VRPTW presented in Chapter 3. The key difference is that the new formulation eliminates the need of modeling every possible charging station visit as a separate vertex in the network graph. Moreover, it removes the need of imposing an artificial upper bound on the number of visits to a charging station, as is commonly done in previous models to keep their size acceptable. This results in a significantly smaller number of decision variables, especially in larger problem instances, thus allowing solving problems with more customers and charging stations optimally. The new formulation removes the charging station vertices completely from the network graph and replaces them with a set of elementary paths between the remaining vertices (i.e., the customers and the depots). These paths are constructed so that they account for all the charging station visits that may be included in an optimal vehicle route.

In the following, the same notation as in Section 3.3 is used, with the exception that the vertex set F now contains only one vertex per each charging station. Additionally, let $\mathcal{T}$ denote an E-VRPTW tour corresponding to a vehicle route that starts from the origin depot, visits a set of customers within their time windows, stops to recharge when necessary, and finally arrives at the destination depot within the maximum route duration. Furthermore, let m^* denote the number of E-VRPTW tours in an optimal solution and n_l the number of customers serviced by vehicle v_l in a tour $\mathcal{T}_l$ for all $l \in \{1, \dots, m^*\}$. Finally, let n_C denote the number of customers in an E-VRPTW instance. Note that since the optimal solution constitutes all m^* tours $\mathcal{T}_l$, $l \in \{1, \dots, m^*\}$, it must be that $n_1 + \dots + n_{m^*} = n_C$.

4.1 Decomposition of optimal vehicle tours

In the following, it is shown that any E-VRPTW tour $\mathcal{T}_l$ associated with a vehicle v_l visiting n_l customers can be decomposed as a sequence of $n_l + 1$ simple paths, denoted as *e-paths*, each starting from a vertex $i \in N_0$, ending at another vertex $j \in N_{n+1}$, and possibly visiting a set of charging stations in between. Subsequently, a dominance relation based on travel time and energy consumption is established for e-paths, and a smaller subset of *non-dominated* e-paths is identified that provides a sufficient characterization for a set of optimal E-VRPTW tours that constitute an optimal solution.

Definition 1. *An e-path Ψ_{ij} is a simple path $P(\Psi_{ij}) = (i \equiv i_0, \dots, i_p \equiv j)$ in G starting from $i \in N_0$ with a starting energy $e_0(\Psi_{ij}) \leq Q$, visiting a (possibly empty) set $F(\Psi_{ij}) = \{i_1, \dots, i_{p-1}\} \in F$ of charging stations and ending at $j \in N_{n+1}$. Moreover, Ψ_{ij} is associated with recharge amounts $0 \leq r_{i_k}(\Psi_{ij}) \leq Q$ for each vertex $i_k \in F(\Psi_{ij})$ with $r_i(\Psi_{ij}) = r_j(\Psi_{ij}) = 0$.*

Definition 2 introduces energy cost, total recharge amount, travel time, energy levels and energy consumption of an e-path. Note that the travel time between two vertices $i \in V_0$ and $j \in V_{n+1}$ is $t_{ij} = d_{ij}/v$, where d_{ij} denotes the distance and v the vehicle speed. In addition, the energy cost c_{ij} of arc (i, j) can be expressed as $c_{ij} = Kd_{ij}$, where K is the vehicle energy consumption rate. Consequently, the travel time from i to j can be written as

$$t_{ij} = \frac{d_{ij}}{v} = \frac{1}{Kv} c_{ij}. \tag{4.1}$$

Definition 2. *Let Ψ_{ij} be an e-path between two vertices $i \in N_0$ and $j \in N_{n+1}$ traversing a path $P(\Psi_{ij}) = (i \equiv i_0, \dots, i_p \equiv j)$.*

1. *The energy cost of Ψ_{ij} is defined as $c(\Psi_{ij}) := \sum_{k=0}^{p-1} c_{i_k i_{k+1}}$*
2. *The total recharge amount of Ψ_{ij} is defined as $R(\Psi_{ij}) := \sum_{k=1}^{p-1} r_{i_k}(\Psi_{ij})$*
3. *The travel time of Ψ_{ij} is defined as $t(\Psi_{ij}) := \sum_{k=0}^{p-1} (\frac{1}{Kv} c_{i_k i_{k+1}} + g r_{i_k}(\Psi_{ij})) = \frac{1}{Kv} c(\Psi_{ij}) + gR(\Psi_{ij})$.*
4. *The energy level of Ψ_{ij} at a vertex i_k, $k = 0, \dots, p$ is defined as $y_i(\Psi_{ij}) = e_0(\Psi_{ij})$, and $y_{i_k}(\Psi_{ij}) := \min\{Q, y_{i_{k-1}}(\Psi_{ij}) - c_{i_{k-1} i_k} + r_{i_{k-1}}(\Psi_{ij})\}$ for $k = 1, \dots, p$.*
5. *The energy consumption of Ψ_{ij} is defined as $e(\Psi_{ij}) := y_i(\Psi_{ij}) - y_j(\Psi_{ij})$.*

Definition 3. *An e-path Ψ_{ij} from $i \in N_0$ to $j \in N_{n+1}$ traversing a path $P(\Psi_{ij}) = (i \equiv i_0, \dots, i_p \equiv j)$ is feasible, if $0 \leq y_{i_k}(\Psi_{ij}) \leq Q$, $\forall k = 0, \dots, p$.*

Accordingly, Definition 3 states that an e-path is feasible if the energy level at each vertex along the path remains positive and does not exceed the maximum battery capacity Q.

Let G_F denote the subgraph of G induced by the set of charging station vertices F:

$$G_F = \{(i, j) \in A \mid i, j \in F\}. \tag{4.2}$$

An e-path Ψ_{ij} between two vertices $i \in N_0$ and $j \in N_{n+1}$ is now completely characterized by the following:

- A path $P(\Psi_{ij}) = (i \equiv i_0, \dots, i_p \equiv j)$ which is composed of either
  - (i) an arc (i, s), $s \in F$; a subpath $P_F(\Psi_{ij}) = (s \equiv i_1, \dots, i_{p-1} \equiv t)$ in G_F from s to $t \in F$ (possibly with $s = t$); and an arc (t, j), or
  - (ii) the arc (i, j) if no charging stations are visited.
- A sequence of recharge amounts $0 \leq r_{i_k}(\Psi_{ij}) \leq Q$, $k = 0, \dots, p$.
- A starting energy $y_i(\Psi_{ij}) = e_0(\Psi_{ij}) \leq Q$.

The following Definition 4 introduces a dominance relation based on energy consumption and travel time for e-paths having the same starting energy. This provides a basis for reducing the number of feasible e-paths by removing those paths that are dominated.

Definition 4. *Given two feasible e-paths Ψ_{ij} and Ψ'_{ij} from $i \in N_0$ to $j \in N_{n+1}$ with $e_0(\Psi_{ij}) = e_0(\Psi'_{ij})$, Ψ_{ij} dominates Ψ'_{ij}, denoted by $\Psi_{ij} \succ \Psi'_{ij}$, if*

$$\begin{aligned} e(\Psi_{ij}) &\leq e(\Psi'_{ij}), \\ t(\Psi_{ij}) &\leq t(\Psi'_{ij}), \end{aligned}$$

and one of the inequalities is strict.

The following proposition asserts that for any feasible E-VRPTW instance (i.e., for any instance with at least one optimal solution), each of the tours $\mathcal{T}_l^*$, $l \in \{1, \dots, m^*\}$, constituting an optimal solution to the problem can be decomposed as a sequence of non-dominated e-paths. For simplicity, the origin depot and the destination depot are also referred to as customers with zero service time.

Proposition 1. *For any feasible E-VRPTW instance, there exists at least one optimal solution constituting m^* E-VRPTW tours $\mathcal{T}_l^*$, $l \in \{1, \dots m^*\}$, each associated with a vehicle v_l visiting n_l customers, so that each such tour can be decomposed as a sequence of $n_l + 1$ non-dominated e-paths.*

Proof. Let $\mathcal{T}_\lambda$, $\lambda \in \{1, \dots, m^*\}$ be a feasible E-VRPTW tour associated with vehicle v_λ visiting n_λ customers. Consider a tour segment between two customers $i \in N_0$ and $j \in N_{n+1}$ contained in the tour that are serviced sequentially, possibly visiting some charging stations in between. According to Definitions 1 - 3, this segment corresponds to a feasible e-path Ψ_{ij} with a starting energy $y_i(\Psi_{ij}) = e_0(\Psi_{ij})$. Now, suppose that Ψ_{ij} is dominated in accordance with Definition 4. Thus, there exists another e-path $\Psi'_{ij} \succ \Psi_{ij}$ from i to j such that $y_i(\Psi'_{ij}) = y_i(\Psi_{ij}) = e_0(\Psi_{ij})$, $e(\Psi'_{ij}) \leq e(\Psi_{ij})$ and $t(\Psi'_{ij}) \leq t(\Psi_{ij})$ with at least one of the inequalities being strict. In what follows, it is shown that the energy cost $c(\Psi'_{ij})$ is less than $c(\Psi_{ij})$, which indicates that by substituting Ψ_{ij} with Ψ'_{ij} in $\mathcal{T}_\lambda$, a new feasible E-VRPTW tour $\mathcal{T}'_\lambda$ is obtained with a lower energy cost.

Towards this end, let $R(\Psi_{ij})$ and $R(\Psi'_{ij})$ be the total recharge amounts of the e-paths Ψ_{ij} and Ψ'_{ij}, respectively. It can be easily verified that the following inequalities are valid:

$$y_j(\Psi_{ij}) \leq y_i(\Psi_{ij}) - c(\Psi_{ij}) + R(\Psi_{ij}), \tag{4.3}$$
$$y_j(\Psi'_{ij}) \leq y_i(\Psi'_{ij}) - c(\Psi'_{ij}) + R(\Psi'_{ij}). \tag{4.4}$$

Furthermore, it can be assumed that $y_j(\Psi_{ij}) = y_i(\Psi_{ij}) - c(\Psi_{ij}) + R(\Psi_{ij})$ and $y_j(\Psi'_{ij}) = y_i(\Psi'_{ij}) - c(\Psi'_{ij}) + R(\Psi'_{ij})$, because otherwise it would be possible to simply reduce the recharge amounts $R(\Psi_{ij})$ and $R(\Psi'_{ij})$ in (4.3) and (4.4) until the equalities are satisfied without affecting either the feasibility or the energy cost of the tours $\mathcal{T}_\lambda$ and $\mathcal{T}'_\lambda$. Furthermore, since $y_i(\Psi_{ij}) = y_i(\Psi'_{ij}) = e_0(\Psi_{ij})$ and $e(\Psi'_{ij}) \leq e(\Psi_{ij})$ in accordance with definition 4, it must be that $y_j(\Psi_{ij}) \leq y_j(\Psi'_{ij})$ and the following must hold:

$$y_j(\Psi_{ij}) = e_0(\Psi_{ij}) - c(\Psi_{ij}) + R(\Psi_{ij}) \leq e_0(\Psi_{ij}) - c(\Psi'_{ij}) + R(\Psi'_{ij}) = y_j(\Psi'_{ij}),$$

which results in

$$c(\Psi_{ij}) - c(\Psi'_{ij}) \geq R(\Psi_{ij}) - R(\Psi'_{ij}). \tag{4.5}$$

Finally, according to Definition 4, $t(\Psi_{ij}) \geq t(\Psi'_{ij})$, which can be written as $\frac{1}{Kv}c(\Psi_{ij}) + gR(\Psi_{ij}) \geq \frac{1}{Kv}c(\Psi'_{ij}) + gR(\Psi'_{ij})$ (see Definition 2). This can be further expressed as

$$c(\Psi_{ij}) - c(\Psi'_{ij}) \geq Kvg(R(\Psi'_{ij}) - R(\Psi_{ij})). \tag{4.6}$$

It can be deduced from (4.5) and (4.6) that $c(\Psi_{ij}) - c(\Psi'_{ij}) \geq 0$. Moreover, since these inequalities are derived from the conditions of Definition 4, at least one of them must be strict. Consequently, it can be concluded that $c(\Psi'_{ij}) < c(\Psi_{ij})$, thus verifying that by substituting Ψ_{ij} with Ψ'_{ij} in the initial tour $\mathcal{T}_\lambda$, a new tour $\mathcal{T}'_\lambda$ is obtained with a strictly lower energy cost. Therefore, as long as the tour contains at least one dominated e-path, it can be replaced by a non-dominated one to obtain a new feasible tour with a lower energy cost. Since the tour consists of $n_\lambda + 1$ e-paths by definition, an optimal tour $\mathcal{T}_\lambda{}^*$ is eventually composed of $n_\lambda + 1$ such non-dominated paths. By repeating this procedure for all the tours $\mathcal{T}_l$, $l \in \{1, \ldots, m^*\}$, each such tour is finally composed of $n_l + 1$ non-dominated e-paths. □

The dominance relation of Definition 4 can be impractical, because it depends on both the starting energy and the energy consumption of Ψ_{ij}. Indeed, establishing dominance relations in accordance with Definition 4 requires knowledge of all feasible e-paths between two customers $i \in N_0$ and $j \in N_{n+1}$. To overcome this drawback, the following establishes a necessary condition for an e-path Ψ_{ij} visiting at least one charging station to be dominated that depends only on the energy cost of the path $P(\Psi_{ij})$ traversed by Ψ_{ij}. This makes it significantly easier to establish dominance relations between such e-paths and provides a basis for reducing their number efficiently. Note that the following applies to all paths except those consisting of only the single arc $(i, j) \in A$, $i \in N_0$, $j \in N_{n+1}$.

Definition 5. *Let $P = (i, s, \ldots, t, j)$ be a path from $i \in N_0$ to $j \in N_{n+1}$ with subpath $P_F = (s, \ldots, t)$ in G_F from $s \in F$ to $t \in F$ (possibly with $s = t$) of energy cost $c(P_F)$. P is said to be dominated with respect to (i, j) if there exists another path $P' = (i, s', \ldots, t', j)$ with subpath $P'_F = (s', \ldots, t')$ in G_F from $s' \in F$ to $t' \in F$ (possibly with $s' = t'$) of energy cost $c(P'_F)$ such that*

$$c_{is'} \leq c_{is},$$
$$c_{t'j} \leq c_{tj},$$
$$c(P'_F) \leq c(P_F),$$

and at least one of the inequalities is strict. Moreover, P' is then said to dominate P with regard to (i, j), denoted by $P' \succ_{(i,j)} P$.

Proposition 2. *Let Ψ_{ij} be an e-path from $i \in N_0$ to $j \in N_{n+1}$ traversing a path $P(\Psi_{ij}) = (i, s, \ldots, t, j)$, and let $P_F(\Psi_{ij}) = (s, \ldots, t)$ be the subpath of $P(\Psi_{ij})$ in G_F from $s \in F$ to $t \in F$. If $P(\Psi_{ij})$ is dominated with respect to (i, j), there exists a feasible e-path Ψ'_{ij} such that $\Psi'_{ij} \succ \Psi_{ij}$.*

Proof. The proof is constructive: a feasible e-path Ψ'_{ij} from i to j is constructed that satisfies $y_i(\Psi'_{ij}) = y_i(\Psi_{ij}) = e_0(\Psi_{ij})$, $e(\Psi'_{ij}) \leq e(\Psi_{ij})$ and $t(\Psi'_{ij}) \leq t(\Psi_{ij})$ with at least one strict inequality, thus verifying that $\Psi'_{ij} \succ \Psi_{ij}$ in accordance with Definition 4.

Since $P(\Psi_{ij})$ is dominated with respect to (i, j), there exists another path $P' = (i, s', \ldots, t', j) \succ_{(i,j)} P(\Psi_{ij})$ with a subpath $P'_F = (s', \ldots, t')$ in G_F from $s' \in F$ to $t' \in F$ such that

$$\begin{aligned} c_{is'} &\leq c_{is}, \\ c_{t'j} &\leq c_{tj}, \\ c(P'_F) &\leq c(P_F(\Psi_{ij})), \end{aligned}$$

with at least one strict inequality.

Let Ψ'_{ij} be constructed as follows: Ψ'_{ij} starts from i with energy $y_i(\Psi'_{ij}) = y_i(\Psi_{ij}) = e_0(\Psi_{ij})$, traverses a path $P(\Psi'_{ij}) = (i \equiv i_0, s' \equiv i_1, \ldots, i_{p-1} \equiv t', i_p \equiv j)$, which is composed of the arc (i, s'), the path $P_F(\Psi'_{ij}) = P'_F = (s' \equiv i_1, \ldots, i_{p-1} \equiv t')$ and the arc (t', j). In addition, let the recharge amounts r_{i_k}, $k = 1, \ldots, p-1$, be set recursively as follows:

- $r_{s'}(\Psi'_{ij}) = \max\{0, c_{s'i_2} - y_{s'}(\Psi'_{ij})\}$;
- $r_{i_k}(\Psi'_{ij}) = \max\{0, c_{i_k i_{k+1}} - y_{i_k}(\Psi'_{ij})\}$, $k = 2, \ldots, p-2$;
- $r_{t'}(\Psi'_{ij}) = r_t(\Psi_{ij}) + y_t(\Psi_{ij}) - y_{t'}(\Psi'_{ij})$.

It is now shown that (i) Ψ'_{ij} is feasible, (ii) $e(\Psi'_{ij}) \leq e(\Psi_{ij})$ and (iii) $t(\Psi'_{ij}) \leq t(\Psi_{ij})$ with at least one inequality being strict, thus verifying that $\Psi'_{ij} \succ \Psi_{ij}$.

(i) According to Definition 2, the energy level of Ψ'_{ij} at vertex $i_1 \equiv s'$ is $y_{s'}(\Psi'_{ij}) = e_0(\Psi_{ij}) - c_{is'} \geq e_0(\Psi_{ij}) - c_{is} = y_s(\Psi_{ij})$, since $c_{is'} \leq c_{is}$. Hence, since Ψ_{ij} is feasible, $0 \leq y_s(\Psi_{ij}) \leq y_{s'}(\Psi'_{ij}) \leq Q$. Furthermore, it can be verified that the above recursive equations for $r_{i_k}(\Psi'_{ij})$, $k = 2, \ldots, p-2$, imply $0 \leq y_{i_k}(\Psi'_{ij}) \leq Q$, $k = 1, \ldots, p-2$. Finally, the recharge amount set for $r_{t'}(\Psi'_{ij})$ ensures that $0 \leq y_j(\Psi_{ij}) \leq y_j(\Psi'_{ij}) \leq Q$ since $c_{t'j} \leq c_{tj}$.

Thus, $0 \leq y_{i_k}(\Psi'_{ij}) \leq Q$, $\forall k = 0, \ldots, p$ and Ψ'_{ij} is feasible in accordance with Definition 3.

(ii) According to Definition 2, the energy consumption of Ψ'_{ij} is $e(\Psi'_{ij}) = y_i(\Psi'_{ij}) - y_j(\Psi'_{ij}) = e_0(\Psi_{ij}) - y_j(\Psi'_{ij}) \leq e_0(\Psi_{ij}) - y_j(\Psi_{ij}) = e(\Psi_{ij})$, since $y_j(\Psi'_{ij}) \geq y_j(\Psi_{ij})$ as established in part (i). Thus, $e(\Psi'_{ij}) \leq e(\Psi_{ij})$.

(iii) Let $R(\Psi_{ij})$ and $R(\Psi'_{ij})$ be the total recharge amounts of Ψ_{ij} and Ψ'_{ij}, respectively. From the definition of energy levels in Definition 2, it can be deduced that

$$y_t(\Psi_{ij}) \leq y_s(\Psi_{ij}) - c(P_F(\Psi_{ij})) + R(\Psi_{ij}) - r_t(\Psi_{ij}),$$

which can be written as

$$R(\Psi_{ij}) \geq y_t(\Psi_{ij}) - y_s(\Psi_{ij}) + c(P_F(\Psi_{ij})) + r_t(\Psi_{ij}). \tag{4.7}$$

Moreover, the above defined recharge amounts $r_{i_k}(\Psi'_{ij})$, $k = 1, \ldots, p-1$ for Ψ'_{ij} imply

$$\begin{aligned} R(\Psi'_{ij}) = \sum_{k=1}^{p-1} r_{i_k}(\Psi'_{ij}) \leq \sum_{k=1}^{p-2} c_{i_k i_{k+1}} - y_{s'}(\Psi'_{ij}) + y_t(\Psi_{ij}) + r_t(\Psi_{ij}) \\ \Rightarrow R(\Psi'_{ij}) \leq y_t(\Psi_{ij}) - y_{s'}(\Psi'_{ij}) + c(P_F(\Psi'_{ij})) + r_t(\Psi_{ij}). \end{aligned} \tag{4.8}$$

Consequently, since $c(P_F(\Psi'_{ij})) \leq c(P_F(\Psi_{ij}))$ and $y_{s'}(\Psi'_{ij}) \geq y_s(\Psi_{ij})$, (4.8) can be written as

$$R(\Psi'_{ij}) \leq y_t(\Psi_{ij}) - y_s(\Psi_{ij}) + c(P_F(\Psi_{ij})) + r_t(\Psi_{ij}). \tag{4.9}$$

Finally, combining (4.7) with (4.9) results in

$$R(\Psi'_{ij}) \leq R(\Psi_{ij}). \tag{4.10}$$

The energy costs of the two e-paths can be written as follows:

$$c(\Psi_{ij}) = c_{is} + c(P_F(\Psi_{ij})) + c_{tj}, \tag{4.11}$$

$$c(\Psi'_{ij}) = c_{is'} + c(P_F(\Psi'_{ij})) + c_{t'j}, \tag{4.12}$$

and the corresponding travel times as

$$t(\Psi_{ij}) = \frac{1}{Kv}c(\Psi_{ij}) + gR(\Psi_{ij}), \tag{4.13}$$

$$t(\Psi'_{ij}) = \frac{1}{Kv}c(\Psi'_{ij}) + gR(\Psi'_{ij}). \tag{4.14}$$

By the construction of Ψ'_{ij}, it must be that: $c_{is'} \leq c_{is}$, $c_{t'j} \leq c_{tj}$ and $c(P_F(\Psi'_{ij})) \leq c(P_F(\Psi_{ij}))$ with at least one strict inequality. Thus, it can be concluded from (4.11) and (4.12) that $c(\Psi'_{ij}) < c(\Psi_{ij})$. Moreover, in (4.10) it was verified that $R(\Psi'_{ij}) \leq R(\Psi_{ij})$. Combining these results and substituting them into (4.13) and (4.14) implies $t(\Psi'_{ij}) < t(\Psi_{ij})$, indicating that $\Psi'_{ij} \succ \Psi_{ij}$.

□

Proposition 1 provides a basis for constructing an alternative formulation for the E-VRPTW by replacing the charging station vertices with a set of feasible e-paths between every customer pair. Moreover, Proposition 2 provides means for effectively discarding a significant number of e-paths by performing pairwise dominance comparisons for all possible paths between two customers $i \in N_0$ and $j \in N_{n+1}$ and removing those paths that are dominated with regard to (i, j) in accordance with Definition 5. Note, however, that this procedure does not in general produce the true non-dominated set of e-paths, but rather significantly reduces the number of possible paths that can be traversed by the e-paths. The non-dominated e-paths can subsequently be constructed from the remaining paths, since only those paths that are dominated with regard to (i, j) are removed, and Proposition 2 ensures that e-paths traversing such paths are dominated by some other e-path. Finally, it is assumed that the (feasible) paths consisting of only the arc $(i, j) \in A$ for each $i \in N_0$ and $j \in N_{n+1}$ are always included; the dominance status of such paths cannot be established in view of Definition 5 since they have no subpath in G_F.

The formulation presented in Chapter 3 models each charging station as a set of $n_C + m$ dummy vertices, one for each potential visit. In order to estimate the impact of this modeling technique with regard to problem size, let n_S denote the number of charging stations. Accordingly, the number of arcs in the network graph is of the order of $\mathcal{O}(n_C + n_S(n_C + m))(n_C + n_S(n_C + m) - 1) = \mathcal{O}(n_C^2 n_S^2)$, resulting in a significant number of decision variables, each corresponding to a single (feasible) arc.

Now, suppose that the new formulation removes all charging station vertices from the graph and replaces them with a set of non-dominated paths between every customer pair $i \in N_0$ and $j \in N_{n+1}$, with each such path being represented by a decision variable. In addition, let n_P denote the average number of non-dominated paths between each vertex pair $i \in N_0$ and $j \in N_{n+1}$. Thus, the number of path decision variables in the new formulation is of the order of $\mathcal{O}(n_C(n_C - 1)n_P) = \mathcal{O}(n_C^2 n_P)$. This indicates that if the number of paths that remain non-dominated in view of Definition 5 remains reasonable, specifically, if $n_P << n_C^2$, the number of decision variables is significantly smaller than in the previous formulation. Obviously, the set of non-dominated paths must be calculated in advance for every customer pair. However, it turns out that this set can be computed quickly for all the instances studied in this thesis.

4.1.1 Computation of non-dominated paths

Let I_{ij} denote the index set of all unique paths between $i \in N_0$ and $j \in N_{n+1}$ that can be traversed by any feasible e-path Ψ_{ij} so that $p \in I_{ij}$ if the path $P^p = (i, s, \dots, t, j)$ is composed of the following:

1. An arc (i, s) from i to $s \in F$.
2. A subpath $P_F^p = (s, \dots, t)$ in G_F corresponding to the shortest path between $s \in F$ and $t \in F$ (possibly with $s = t$).
3. An arc (t, j) from $t \in F$ to j.

Furthermore, let

$$\mathcal{P}(\Psi_{ij}) = \{P^p \mid p \in I_{ij}\} \tag{4.15}$$

denote the set of all such paths between i and j.

The set of paths that are non-dominated with regard to Definition 5 can be sequentially constructed for each customer pair $i \in N_0$ and $j \in N_{n+1}$ by first generating the path set $\mathcal{P}(\Psi_{ij})$ between the two customers, subsequently applying a suitable procedure for establishing dominance relations between the generated paths and finally eliminating those paths that are dominated by some other path. Note that the subpaths in G_F for all the paths in $\mathcal{P}(\Psi_{ij})$ correspond to the shortest paths between each charging station pair; this will significantly reduce the number of possible path combinations.

The first step is to compute the shortest paths between each charging station pair $s \in F$ and $t \in F$ in G_F. This can be achieved, for instance, by applying Dijkstra's shortest path algorithm (Dijkstra, 1959) starting from each vertex $s \in G_F$. Next, all the customer pairs are sequentially examined, and for each such pair $i \in N_0$ and $j \in N_{n+1}$, the path set $\mathcal{P}(\Psi_{ij})$ between the two customers is computed by constructing all the possible paths $P^p = (i, s, \ldots, t, j)$ starting from i, traversing a subpath $P_F^p = (s, \ldots, t)$ in G_F corresponding to the shortest path from $s \in F$ to $t \in F$, and finally ending at j. These paths are constructed by considering all the different charging station pair combinations $s \in F$ and $t \in F$ (including those with $s \equiv t$). The paths that remain feasible then constitute the set $\mathcal{P}(\Psi_{ij})$.

After the set $\mathcal{P}(\Psi_{ij})$ is obtained, the procedure presented in (Deb, 2001) is applied to find those paths that are non-dominated with regard to Definition 5. Towards this end, suppose that the number of different paths in $\mathcal{P}(\Psi_{ij})$ is N_P, that is, $I_{ij} = \{1, \ldots, N_P\}$ and

$$\mathcal{P}(\Psi_{ij}) = \{P^p \mid p \in \{1, \ldots, N_P\}\}.$$

Furthermore, let $\mathcal{P}'(\Psi_{ij})$ be an initially empty set, which is sequentially updated during the procedure until it comprises all the non-dominated paths. The procedure is described in Alg. 1.

Algorithm 1 Identifying the non-dominated set (Deb, 2001)

Input: The set $\mathcal{P}(\Psi_{ij}) = \{P^p \mid p \in \{1, \ldots, N_P\}\}$ consisting of N_P feasible paths between $i \in N_0$ and $j \in N_{n+1}$.

Returns: The set $\mathcal{P}'(\Psi_{ij})$ comprising all the non-dominated paths of $\mathcal{P}(\Psi_{ij})$ with regard to Definition 5.

Init: Initialize $\mathcal{P}'(\Psi_{ij}) = \{P^1\}$ and set solution counter $k = 2$.

Iteration:

1: Set $m = 1$.

2: Establish dominance between $P^k \in \mathcal{P}(\Psi_{ij})$ and $P^m \in \mathcal{P}'(\Psi_{ij})$.

3: If $P^k \succ_{(i,j)} P^m$, set $\mathcal{P}'(\Psi_{ij}) = \mathcal{P}'(\Psi_{ij}) \setminus \{P^m\}$. If $m < |\mathcal{P}'(\Psi_{ij})|$, increment m by one and go to step 2; otherwise, go to step 4. Alternatively, if $P^m \succ_{(i,j)} P^k$, increment k by one and go to step 1. Otherwise, go to step 4.

4: Set $\mathcal{P}'(\Psi_{ij}) = \mathcal{P}'(\Psi_{ij}) \cup \{P^k\}$. If $k < N_P$, increment k by one and go to step 1. Otherwise, stop and declare $\mathcal{P}'(\Psi_{ij})$ as the non-dominated set.

In the procedure presented in Alg 1, the dominance status of every path in the initial set $\mathcal{P}(\Psi_{ij})$ is established by comparing it with a set of potentially non-dominated paths that are included in the set $\mathcal{P}'(\Psi_{ij})$ during the execution. In the beginning, the first feasible path P^1 is added to the set $\mathcal{P}'(\Psi_{ij})$ that is initially empty. After that, every feasible path in $\mathcal{P}(\Psi_{ij})$ (starting with the second path P^2) is sequentially compared with all the paths in $\mathcal{P}'(\Psi_{ij})$. If a path $P^k \in \mathcal{P}(\Psi_{ij})$ dominates any member of $\mathcal{P}'(\Psi_{ij})$, the corresponding path is removed from $\mathcal{P}'(\Psi_{ij})$. This ensures that those paths that are dominated are eventually removed from $\mathcal{P}'(\Psi_{ij})$. Alternatively, if the path P^k is dominated by any member of $\mathcal{P}'(\Psi_{ij})$, the counter k is incremented by one and P^k is thus ignored in further iterations. Otherwise, if P^k is not dominated by any path in $\mathcal{P}'(\Psi_{ij})$, it is added to the set $\mathcal{P}'(\Psi_{ij})$. This ensures that the set $\mathcal{P}'(\Psi_{ij})$ grows with non-dominated paths. Finally, after all the feasible paths in $\mathcal{P}(\Psi_{ij})$ are examined, the remaining paths in $\mathcal{P}'(\Psi_{ij})$ constitute the non-dominated set.

Note that the procedure finds the non-dominated paths for a single customer pair only. Thus, in order to find all the non-dominated paths, it must be applied to each pair of customers separately. Fortunately, as demonstrated by Deb (2001), computing the non-dominated set from a given set of objects is not computationally too demanding. For instance, with the procedure of Alg. 1, the second path is compared with only the first path, the third path with at most two paths and so on, thus requiring at most $1+2+\cdots+(N_P-1) = N_P(N_P-1)/2$ dominance comparisons. Since each dominance comparison requires three energy cost comparisons, the non-dominated paths can be computed in $\mathcal{O}(3N_P(N_P-1)/2) = \mathcal{O}(N_P^2)$. Moreover, since the total number of customer pairs is $n_C(n_C-1)$, all the non-dominated paths can be computed in $\mathcal{O}(n_C^2 N_{P_{max}}^2)$ where $N_{P_{max}}$ denotes the maximum number of paths between any two customers. However, since these estimates are for the worst case scenarios and without estimating the impact of preprocessing, the actual computational complexity is likely smaller.

In the following, let $\mathscr{P}_{ij}$ denote the index set of all the non-dominated paths between $i \in N_0$ and $j \in N_{n+1}$ with regard to Definition 5, including the path corresponding to the single arc $(i,j) \in A$. Additionally, let c_{ij}^p denote the energy cost and t_{ij}^p the travel time of the path $P^p(\Psi_{ij})$, $p \in \mathscr{P}_{ij}$, and let h_{ij}^p and f_{ij}^p denote the energy cost of the first and the last arc, respectively. Furthermore, let the paths corresponding to the single arcs $(i,j) \in A$ for every $i \in N_0$ and $j \in N_{n+1}$ be indexed as $P^0(\Psi_{ij}) = (i,j)$; for such paths, it is assumed that $h_{ij}^0 = 0$ and $f_{ij}^0 = 0$.

4.2 Improved model

This Section develops an alternative formulation for the E-VRPTW that exploits the results of Section 4.1. The formulation is similar to the one presented in Chapter 3; however, it is defined on a multigraph $\overline{G} = (\overline{V}, \overline{A})$, where the vertex set $\overline{V} = N \cup \{0\} \cup \{n+1\}$ comprises the customer vertices, the origin depot and the destination depot, respectively; and the arc set $\overline{A} = \{(i,j)^p \mid i \in N_0, j \in N_{n+1}, p \in \mathscr{P}_{ij}\}$ contains one arc $(i,j)^p$ for every non-dominated path $p \in \mathscr{P}_{ij}$ between each customer pair $i \in N_0$, $j \in N_{n+1}$, in addition to the arc $(i,j)^0$ which corresponds to the path composed of the single arc $(i,j) \in A$.

To represent the improved formulation for the E-VRPTW, the following decision variables are defined:

- $x_{ij}^p \in \{0,1\}$: $x_{ij}^p = 1$ if an arc $(i,j)^p \in \overline{A}$ is traversed, $x_{ij}^p = 0$ otherwise; defined for all $i \in N_0$, $j \in N_{n+1}$ and $p \in \mathscr{P}_{ij}$, $i \neq j$.
- $\tau_i \in \mathbb{R}_+$: arrival time at a vertex $i \in N_{0,n+1}$.
- $y_i \in \mathbb{R}_+$: the vehicle battery charge upon arriving at a vertex $i \in N_{0,n+1}$.
- $r_{ij} \in \mathbb{R}_+$: the total recharge amount at charging stations when traversing directly from $i \in N_0$ to $j \in N_{n+1}$.

Using these variables, the improved formulation for the E-VRPTW is modeled as the following MILP problem:

$$\min \sum_{i\in N_0}\sum_{j\in N_{n+1}}\sum_{p\in\mathscr{P}_{ij}} c_{ij}^p x_{ij}^p \tag{4.16}$$

subject to

$$\sum_{j\in N}\sum_{p\in\mathscr{P}_{0j}} x_{0j}^p = \sum_{j\in N}\sum_{p\in\mathscr{P}_{j\,n+1}} x_{j\,n+1}^p \le m, \tag{4.17}$$

$$\sum_{j\in N_0}\sum_{p\in\mathscr{P}_{ji}} x_{ji}^p = 1,\ \forall i\in N, \tag{4.18}$$

$$\sum_{j\in N_0}\sum_{p\in\mathscr{P}_{ji}} x_{ji}^p - \sum_{j\in N_{n+1}}\sum_{p\in\mathscr{P}_{ij}} x_{ij}^p = 0,\ \forall i\in N, \tag{4.19}$$

$$\sum_{p\in\mathscr{P}_{ij}} x_{ij}^p \le 1,\ \forall i\in N_0, j\in N_{n+1}, \tag{4.20}$$

$$\tau_j \ge \tau_i + (s_i + t_{ij}^p)x_{ij}^p + gr_{ij} - T_{ij}(1-x_{ij}^p),\ \forall i\in N_0, j\in N_{n+1}, p\in\mathscr{P}_{ij}, \tag{4.21}$$

$$\tau_j \ge \tau_i + (s_i + t_{ij}^0)x_{ij}^0 - T_{ij}(1-x_{ij}^0), \qquad \forall i\in N_0, j\in N_{n+1}, \tag{4.22}$$

$$a_i \le \tau_i \le b_i, \qquad \forall i\in N_{0,n+1}, \tag{4.23}$$

$$0 \le y_j \le y_i - c_{ij}^p x_{ij}^p + r_{ij} + Q(1-x_{ij}^p), \qquad \forall i\in N_0, j\in N_{n+1}, p\in\mathscr{P}_{ij}, \tag{4.24}$$

$$0 \le y_j \le y_i - c_{ij}^0 x_{ij}^0 + Q(1-x_{ij}^0), \qquad \forall i\in N_0, j\in N_{n+1}, \tag{4.25}$$

$$y_i - h_{ij}^p x_{ij}^p \ge 0,\quad \forall i\in N_0, j\in N_{n+1}, p\in\mathscr{P}_{ij}, \tag{4.26}$$

$$y_j + f_{ij}^p x_{ij}^p \le Q,\ \forall i\in N_0, j\in N_{n+1}, p\in\mathscr{P}_{ij}, \tag{4.27}$$

$$r_{ij} \ge 0, \qquad \forall i\in N_0, j\in N_{n+1}, \tag{4.28}$$

$$x_{ij}^p \in \{0,1\}, \qquad \forall i\in N_0, j\in N_{n+1}, p\in\mathscr{P}_{ij}, \tag{4.29}$$

where $T_{ij} = \max\{0, b_i - a_j\}$. Furthermore, to simplify the notation, it is assumed that $a_0 = a_{n+1} = 0$ and $b_0 = b_{n+1} = T$, where T denotes the maximum route duration. Note that the variable x_{ij}^p with index $p = 0$ represents the path corresponding to the single arc $(i,j)\in A$ for every $i\in N_0$ and $j\in N_{n+1}$ with $h_{ij}^0 = 0$ and $f_{ij}^0 = 0$.

The objective (4.16) minimizes the total energy cost of the vehicle tours. Constraints (4.17) ensure that at most m vehicles depart from the origin depot and arrive at the destination depot, whereas constraints (4.18) impose that each customer is visited exactly once. Constraints (4.19) state that the number of incoming arcs must equal the number of outgoing arcs for each vertex. Constraints (4.20) impose that at most one path is traversed between two vertices. Constraints (4.21) - (4.22) ensure the consistency of arrival times and prevent the formation of subtours.

Constraints (4.23) enforce that the customers are visited within the specified time windows. Constraints (4.24) - (4.25) ensure the feasibility of the vehicle battery charge. Constraints (4.26) state that the vehicle must have enough energy to travel the first arc of a path, while constraints (4.27) impose an upper bound on the energy level upon traversing the last arc. Finally, constraints (4.28) ensure that the recharge amounts remain positive and constraints (4.29) enforce integrality on the path variables x_{ij}^p.

To see that the constraints (4.21) and (4.22) produce valid inequalities with $T_{ij} = \max\{0, b_i - a_j\}$, first consider the case where $x_{ij}^p = 1$ (or $x_{ij}^0 = 1$ for $p = 0$). Accordingly, the term $T_{ij}(1-x_{ij}^p)$ then disappears and the inequalities (4.21) and (4.22) become

$$\tau_j \geq \tau_i + s_i + t_{ij}^p + gr_{ij}, \tag{4.30}$$

$$\tau_j \geq \tau_i + s_i + t_{ij}^0, \tag{4.31}$$

which remain valid, since the vehicle travels directly from i to j either via charging station(s) (4.30) or without recharging (4.31). On the other hand, when $x_{ij}^p = 0$ (or $x_{ij}^0 = 0$ for $p = 0$), these inequalities reduce to

$$\tau_j \geq \tau_i + gr_{ij} - T_{ij}, \tag{4.32}$$

$$\tau_j \geq \tau_i - T_{ij}. \tag{4.33}$$

Since $T_{ij} = \max\{0, b_i - a_j\}$, the inequality (4.33) must hold regardless of the order in which i and j are visited. For (4.32), on the other hand, there are two different scenarios.

1. There exists some other $\hat{p} \in \mathscr{P}_{ij}$ for which $x_{ij}^{\hat{p}} = 1$ and hence $gr_{ij} > 0$. In this case, since the vehicle actually travels directly from i to j, the value of r_{ij} is set by constraints (4.24), and thus gr_{ij} corresponds to the actual recharge time spent en route from i to j and the inequality (4.32) must remain valid.

2. There exists no other $\hat{p} \in \mathscr{P}_{ij}$ for which $x_{ij}^{\hat{p}} = 1$. Hence, the vehicle does not travel directly from i to j, wherefore r_{ij} can be set to zero, and (4.33) reduces to (4.32).

As in the standard formulation, by removing the constraints (4.17) completely, the routing plan with the minimum energy cost is always obtained.

The constraints (4.18), (4.19) and (4.21) - (4.23) ensure that every customer is visited exactly once and the number of vehicles arriving at the destination depot equals the number of vehicles departing from the origin depot. Consequently, a set of distinct vehicle routes is formed upon solving the problem. These vehicle routes can be identified by following each route that begins with an e-path between the origin depot and a customer $j \in N$ with $x^p_{0j} = 1$.

4.2.1 Customer demands

Similarly to the previous model, the formulation (4.16) - (4.29) can be extended to include customer demands and vehicle supply capacities. Using similar notation as in Section 3.3.2, the customer demands can be incorporated by adding the following constraints:

$$0 \leq u_j \leq u_i - q_i x^p_{ij} + C(1 - x^p_{ij}), \quad \forall i \in N_0, j \in N_{n+1}, p \in \mathscr{P}_{ij}, \tag{4.34}$$

$$0 \leq u_0 \leq C. \tag{4.35}$$

Accordingly, (4.34) imposes that when traveling directly from $i \in N_0$ to $j \in N_{n+1}$ (i.e., $x^p_{ij} = 1$ for some $p \in \mathscr{P}_{ij}$), the vehicle capacity u_j at j is obtained by subtracting the customer demand q_i at i from the vehicle load u_i at i. Furthermore, (4.35) ensures that every vehicle departs from the origin depot with at most the maximum capacity C. The maximum initial capacity can be imposed by setting $u_0 = C$.

4.2.2 Fixed recharging scheme

Enforcing a full recharge at every charging station visit with the formulation (4.16) - (4.29) is not as straightforward as with the initial model in Section 3.3.3 due to the absence of charging station vertices. Further complications arise from the fact that more than one charging station visit may be included in an e-path. One way to implement this recharging scheme without introducing additional variables is to impose the following constraints:

$$y_i + r_{ij} \geq (Q + c^p_{ij} - f^p_{ij}) x^p_{ij}, \quad \forall i \in N_0, j \in N_{n+1}, p \in \mathscr{P}_{ij} \setminus \{0\}. \tag{4.36}$$

To see this, suppose that an e-path from $i \in N_0$ to $j \in N_{n+1}$ is traversed, that is $x_{ij}^p = 1$ for some $p \in \mathscr{P}_{ij}$. By reformulating (4.36), the following inequality is obtained:

$$r_{ij} \geq (Q - y_i) + c_{ij}^p - f_{ij}^p. \tag{4.37}$$

Accordingly, (4.37) states that the total recharge amount r_{ij} over the e-path from i to j must be greater than or equal to the amount that would be needed to refill the battery at i (i.e., $Q - y_i$) plus the energy cost of the whole path c_{ij}^p minus the energy cost f_{ij}^p of the last arc. This guarantees that the battery state-of-charge when departing from the last charging station of the path is greater than or equal to Q. Thus, since Q is the maximum battery capacity, the inequality (4.36) must hold with equality for any solution with $x_{ij}^p = 1$, thus imposing that the maximum amount is recharged over the path.

4.3 Preprocessing

The preprocessing steps introduced in Section 3.4 can be applied to reduce the initial graph G before computing the set of non-dominated paths for every customer pair. In the following, the path structure of the new formulation is exploited to devise updated versions of some of these preprocessing steps. If a customer pair $i \in N_0$ and $j \in N$ satisfies any of the following inequalities, all non-dominated paths between those customers can be removed from the multigraph $\overline{G}$.

$$i \in N_0, j \in N \wedge q_i + q_j > C, \tag{4.38}$$

$$i \in N_0, j \in N \wedge a_i + s_i + t_{ij}^{min} > b_j, \tag{4.39}$$

$$i \in N_0, j \in N \wedge a_i + s_i + t_{ij}^{min} + s_j + t_{j\,n+1}^{min} > T. \tag{4.40}$$

The inequality (4.38) is another ”well-known preprocessing step” (Schneider et al., 2013) exploiting customer demands and vehicle capacities. This particular step is applicable only with the customer demands. The inequalities (4.39) and (4.40) are similar to the preprocessing steps (3.22) and (3.23) with the exception that instead of removing a single arc, all the non-dominated paths between the two customers are removed.

The parameter t_{ij}^{min} in (4.39) and (4.40) corresponds to the travel time of the shortest feasible path (either non-dominated or the path corresponding to the single arc $(i,j) \in A$) from i to j. This is because the shortest route via the direct arc (i,j) may be infeasible, whereas there may exist one or several feasible non-dominated paths between the two customers that visit some charging stations en route. In that case, t_{ij}^{min} corresponds to the shortest of these paths, taking into account the time needed to recharge the minimum amount of energy required to reach the destination.

4.4 Valid inequalities

Inequalities that are satisfied by any integer solution of the model (4.16) - (4.29) are called *valid*. Valid inequalities are redundant for the MIP formulation of the problem; however, they may strengthen its LP-relaxation, which may significantly speed up computing the optimal solution to the problem by branch-and-bound. The benefit of adding valid inequalities depends on the trade-off between the resulting improvement in the lower bound given by the LP-relaxation and the additional computational burden for solving it. On the one hand, it becomes slower to compute the LP-relaxation with more inequalities; on the other hand, the improved lower bound may help close the optimality gap faster.

In the following, a set of inequalities is presented that remains valid for the model (4.16) - (4.29) and may help strengthen its LP-relaxation.

Proposition 3. *The constraints*

$$x_{ij}^p + x_{ji}^p \leq 1, \quad \forall i \in N_0, j \in N_{n+1}, p \in \mathscr{P}_{ij} \tag{4.41}$$

are valid inequalities for the model (4.16) - (4.29).

Proof. Suppose that there exists a solution that violates the constraints (4.41). This can happen only if both $x_{ij}^p = 1$ and $x_{ji}^p = 1$ for some $p \in \mathscr{P}_{ij}$, $i \in N_0$ and $j \in N_{n+1}$. However, this would then mean that at some point the vehicle travels directly from i to j and also directly from j to i in the solution, resulting in customer i being visited twice. Since the constraints (4.17) - (4.18) impose that each customer is visited exactly once, this is a contradiction, and the inequalities (4.41) thus remain valid. □

4.4.1 Liftings

A further way to strengthen the LP-relaxation of the formulation (4.16) - (4.29) is to improve or *lift* some of the constraints (see, e.g., Desrochers & Laporte, 1991). The lifted constraints are of course equivalent to the original ones for the MIP formulation; however, they may improve the optimal solution of its LP-relaxation. The following describes how to lift the constraints (4.24). Similar lifting can be applied to the constraints (4.25) as well, because, apart from the recharge variable r_{ij}, these two constraints are identical.

Proposition 4. *The constraints*

$$y_j \leq y_i - c_{ij}^p x_{ij}^p + r_{ij} + Q(1 - x_{ij}^p) + (c_{ji}^p - Q)x_{ji}^p, \quad \forall i \in N_0, j \in N_{n+1}, p \in \mathscr{P}_{ij} \tag{4.42}$$

are valid inequalities for the model (4.16) - (4.29).

Proof. Since a solution cannot have both $x_{ij}^p = 1$ and $x_{ji}^p = 1$ for any $p \in \mathscr{P}_{ij}$, $i \in N_0$ and $j \in N_{n+1}$ (see the proof of Proposition 3), there are three cases to consider:

1. $x_{ij}^p = 0$ and $x_{ji}^p = 0$. The constraint (4.42) reduces to

$$y_j \leq y_i + Q + r_{ij}, \tag{4.43}$$

   which is always valid, since Q is the maximum battery capacity and $r_{ij} \geq 0$.

2. $x_{ij}^p = 1$. The constraint (4.42) becomes

$$y_j \leq y_i - c_{ij}^p + r_{ij}, \tag{4.44}$$

   which remains valid, since the vehicle travels directly from i to j via charging stations.

3. $x_{ji}^p = 1$. Now (4.42) becomes

$$y_j \leq y_i + c_{ji}^p + r_{ij}. \tag{4.45}$$

Since the vehicle travels directly from j to i, it cannot also travel directly from i to j, wherefore r_{ij} can be set to zero. Thus, (4.45) can be written as

$$y_i \geq y_j - c^p_{ji}, \tag{4.46}$$

providing a valid lower bound on the energy level upon arriving at i.

Since all feasible combinations of the path variables x^p_{ij} produce inequalities that satisfy all the constraints of the model (4.16) - (4.29), the inequalities (4.42) are valid. □

The following describes a lifting for the arrival time constraints (4.21), which can be applied to the constraints (4.22) as well, since the only difference is again the term with the recharge variable r_{ij}. Let N^p_{ij} denote the number of charging station visits along the path corresponding to the variable x^p_{ij}. These can be computed in advance for all the paths while constructing the non-dominated set. With this notation, the lifting can be written as follows.

Proposition 5. *The constraints*

$$\begin{aligned} \tau_j \geq \tau_i + (s_i + t^p_{ij})x^p_{ij} + gr_{ij} + (T_{ij} - s_j - t^p_{ji} - gQN^p_{ji})x^p_{ji} - \\ T_{ij}(1 - x^p_{ij}), \forall i \in N_0, j \in N_{n+1}, p \in \mathscr{P}_{ij} \end{aligned} \tag{4.47}$$

are valid inequalities for the model (4.16) - (4.29)*.*

Proof. Since a solution cannot have both $x^p_{ij} = 1$ and $x^p_{ji} = 1$ for any $p \in \mathscr{P}_{ij}$, $i \in N_0$ and $j \in N_{n+1}$ (see the proof of Proposition 3), there are three cases to consider:

1. $x^p_{ij} = 0$ and $x^p_{ji} = 0$. The constraint (4.47) reduces to

$$\tau_j \geq \tau_i - T_{ij} + gr_{ij}. \tag{4.48}$$

For (4.48), there are two different scenarios to consider:

(i) There exists no other $\hat{p} \in \mathscr{P}_{ij}$ for which $x^{\hat{p}}_{ij} = 1$. Hence, the vehicle does not traverse directly from i to j and r_{ij} can be set to zero. The inequality (4.48) then becomes

$$\tau_j \geq \tau_i - T_{ij}. \tag{4.49}$$

In this case, since $T_{ij} = \max\{0, b_i - a_j\}$, the inequality (4.49) holds regardless of the order in which i and j are visited. Thus, (4.48) remains valid.

(ii) There exists some other $\hat{p} \in \mathscr{P}_{ij}$ for which $x_{ij}^{\hat{p}} = 1$ and hence $gr_{ij} > 0$. However, since the vehicle travels directly from i to j in this case, gr_{ij} corresponds to the recharge time along the path and (4.48) provides a valid bound.

2. $x_{ij}^p = 1$. The constraint (4.47) becomes

$$\tau_j \geq \tau_i + s_i + t_{ij}^p + gr_{ij}, \tag{4.50}$$

which remains valid, since the vehicle travels directly from i to j via charging stations.

3. $x_{ji}^p = 1$. Now (4.47) becomes

$$\tau_j \geq \tau_i - s_j - t_{ji}^p - gQN_{ji}^p + gr_{ij}. \tag{4.51}$$

Since the vehicle travels directly from j to i, it cannot also travel directly from i to j, wherefore r_{ij} can be set to zero. Thus, (4.51) can be written as

$$\tau_j + s_j + t_{ji}^p + gQN_{ji}^p \geq \tau_i. \tag{4.52}$$

Since N_{ji}^p corresponds to the number of charging station visits along the path x_{ji}^p and Q is the maximum amount that can be recharged, it must be that $gQN_{ji}^p \geq gr_{ji}$ and thus (4.52) remains valid.

All feasible combinations of the path variables x_{ij}^p for (4.47) produce inequalities that satisfy all the constraints of the model (4.16) - (4.29). Thus, these inequalities are valid. $\square$

Finally, the following Proposition presents a lifting for the constraints (4.34) incorporating customer demands.

Proposition 6. *The constraints*

$$\begin{aligned} u_j \leq u_i - q_i x_{ij}^p + C(1 - x_{ij}^p) + (q_j - C)x_{ji}^p, \\ \forall i \in N_0, j \in N_{n+1}, p \in \mathscr{P}_{ij} \end{aligned} \tag{4.53}$$

are valid inequalities for the model (4.16) - (4.29).

Proof. There are again there cases to consider:

1. $x_{ij}^p = 0$ and $x_{ji}^p = 0$. The constraint (4.53) reduces to

$$u_j \leq u_i + C, \tag{4.54}$$

   which is always valid, since C is the maximum vehicle capacity.

2. $x_{ij}^p = 1$. The constraint (4.53) becomes

$$u_j \leq u_i - q_i, \tag{4.55}$$

   which remains valid, since the vehicle travels directly from i to j.

3. $x_{ji}^p = 1$. Now (4.53) becomes

$$u_j \leq u_i + q_j, \tag{4.56}$$

   which can be written as

$$u_i \geq u_j - q_j. \tag{4.57}$$

   Since the vehicle travels directly from j to i, (4.57) remains valid.

Since all feasible combinations of the path variables x_{ij}^p produce inequalities that satisfy all the constraints of the model (4.16) - (4.29), the inequalities (4.53) are valid. □

Chapter 5

Numerical experiments

In this Chapter, the models developed in Chapters 3 and 4 are evaluated by solving a set of previously generated test instances. These instances are presented in (Schneider et al., 2013), and they are based on the benchmark instances for the VRPTW proposed by Solomon (1987). First, the general structure of the these instances is examined and their generation procedure is presented. Subsequently, the impact of preprocessing on the number of arcs and non-dominated paths in the test instances is examined. Furthermore, the effect of incorporating the valid inequalities of Section 4.4 in the LP-relaxation of the model (4.16) - (4.29) is evaluated by comparing the optimal solutions of the relaxation with and without these inequalities. Finally, the computational results of solving the test instances are reported, and the developed models are evaluated in more detail.

5.1 Test instances

The following presents a set of 36 small instances with 5, 10 and 15 customers introduced in (Schneider et al., 2013). The number of charging stations in these instances ranges from 3 to 7. The instances are based on the benchmark instances for the VRPTW proposed by Solomon (1987), and they are divided into 3 classes depending on their customer location distribution:

- Random customer location distribution (R)
- Clustered customer location distribution (C)
- Combination of random and clustered distributions (RC)

Furthermore, the instance classes are divided into two groups. Instance groups R1, C1 and RC1 have a short planning horizon, whereas the groups R2, C2 and RC2 have a long planning horizon. This means that more vehicles are likely required to serve all customer in the instances belonging to the first group than those in the second group. Moreover, for every instance group, up to 12 different time window densities (TWD) (i.e., the fraction of customers with a time window) and average time window width (TWW) values are possible. These values are presented in Table 5.1, which is included in the appendix of (Schneider et al., 2013) and can be obtained from http://evrptw.wiwi.uni-frankfurt.de.

The names of the different test instances are formed according to the class and group labels. For example, in an instance referred to as 'RC108-15', the customers are distributed both randomly (R) and in clusters (C), the planning horizon is short (RC1), and both the time window density and time window width are obtained from Table 5.1, row 8 (corresponding to the '08' part in RC108) and column RC1. Finally, the '15' part indicates that the instance contains 15 customers.

Table 5.1: Time window densities (TWD) and average time window widths (TWW) for the Solomon benchmark instances (Solomon, 1987)

	C1		C2		R1		R2		RC1		RC2	
#	TWD	TWW	TWD	TWW	TWD	TWW	TWD	TWW	TWD	TWW	TWD	TWW
1	100%	60.76	100%	160.00	100%	10.00	100%	115.96	100%	30.00	100%	120.00
2	75%	61.27	75%	160.00	75%	10.00	75%	115.23	75%	30.00	75%	120.00
3	50%	59.90	50%	160.00	50%	10.00	50%	117.34	50%	30.00	50%	120.00
4	25%	60.63	25%	160.00	25%	10.00	25%	111.80	25%	30.00	25%	120.00
5	100%	121.61	100%	320.00	100%	30.00	100%	240.00	100%	54.33	100%	223.06
6	100%	156.08	100%	486.64	75%	30.00	75%	240.00	100%	60.00	100%	240.00
7	100%	180.00	100%	612.32	50%	30.00	50%	240.00	100%	88.21	100%	349.50
8	100%	243.28	100%	640.00	25%	30.00	25%	240.00	100%	112.33	100%	471.93
9	100%	360.00			100%	58.89	100%	349.50				
10					100%	86.50	100%	383.27				
11					100%	93.10	100%	471.94				
12					100%	117.64						

Since the original Solomon instances are for the VRPTW, Schneider et al. (2013) introduce charging stations, vehicle battery capacities, recharging rates and energy consumption rates to generate meaningful test instances for BEV routing problems. The generated instances are referred to as E-VRPTW instances in (Schneider et al., 2013).

For each test instance, the charging stations are located in a random manner; however, the possible locations are limited such that every customer can be reached from the depot (the origin and the destination depots are assumed to be the same) with at most two charging station visits. This is achieved by first constructing three circles with different radii around the depot, the largest radius corresponding to the distance to the farthest customer. Subsequently, the circles are divided into equally sized sectors whose size depends on the number of charging stations to be added. Two charging stations are randomly positioned into each sector, one between the innermost circle and the middle circle, and the other one between the middle circle and the outer circle. In addition, one charging station is placed at the same location as the depot.

The vehicle battery capacity Q is set to the maximum value of the following:

(i) 60% of the energy cost of the average vehicle route length in the best known solution to the corresponding original Solomon instance

(ii) Twice the energy cost of the longest arc between a customer and a charging station.

The energy consumption rate is set to 1.0 (i.e., $K = 1.0$ in (3.1)). The vehicle speed v is also set to 1.0 in all of the instances. The recharging rate g is set so that a full recharge requires three times the average customer service time in the corresponding instance.

Since the BEVs must recharge their batteries en route between customer visits, detours to charging stations and the time required for recharging render some of the original Solomon instances infeasible with regard to the initial customer time windows, especially with the fixed recharging scheme used in (Schneider et al., 2013). Therefore, to ensure the feasibility of the constructed instances, Schneider et al. (2013) generate new time windows for each customer. The applied procedure is closely related to the original method proposed by Solomon (1987), and it is described in the following.

First, the feasible time window range of each customer is computed, that is, the range between the earliest time at which the customer can be reached from the depot and the latest time a vehicle can depart from the customer and still reach the end depot in time. For the instance classes R and RC, the time window centers are randomly drawn from the feasible time window ranges. For the instance class C, on the other hand, the time window centers are determined from real arrival times that are obtained by solving the corresponding instances without time windows. Subsequently, the time window widths for all the instance classes are chosen according to the original Solomon instances (see Table 5.1). In case any of the generated customer time windows is not included in the feasible range that was computed earlier, the violated part is cut and the corresponding time window is extended to the opposite direction.

Some of the test instances presented in (Schneider et al., 2013) include customer demands. Thus, in order to use the test instances in evaluating the developed models, this extension must first be adopted. Sections 3.3.2 and 4.2.1 describe how to implement customer demands for the standard formulation (3.2) - (3.16) and the improved formulation (4.16) - (4.29), respectively.

5.2 Impact of preprocessing

In the following, the effectiveness of the preprocessing steps and the valid inequalities presented in Sections 3.4, 4.3 and 4.4 are evaluated computationally on the test instances described in Section 5.1.

5.2.1 Effect of arc elimination

Before solving the test instances, the preprocessing steps presented in Sections 3.4 and 4.3 are applied to eliminate redundant arcs and non-dominated paths that cannot be part of a feasible solution. In the following, the effect of the preprocessing steps (3.22) - (3.25) on the number of arcs in the initial network graph G is examined. Moreover, the combined effect of (3.22) - (3.25) and (4.38) - (4.40) on the number of non-dominated paths in the multigraph $\overline{G}$ is evaluated. Since the non-dominated paths are defined for every customer-customer pair (counting the origin and the destination depots as customers as well), the average number of non-dominated paths per each such pair is also evaluated.

Table 5.2 presents the number of arcs (Arcs), non-dominated paths (NDP) and the average number of non-dominated paths per customer-customer pair (NDP/C) before and after applying the preprocessing steps on each test instance. Additionally, the relative reductions in the number of arcs ($\Delta_{Arcs}(\%)$) and non-dominated paths ($\Delta_{NDP}(\%)$), and the absolute reductions in the number of non-dominated paths per customer-customer pair ($\Delta_{NDP/C}$) on each test instance are presented. Specifically, these are computed as

$$\Delta_{\text{Arcs}}(\%) = \left(1 - \frac{\text{Arcs after preprocessing}}{\text{Arcs before preprocessing}}\right) \times 100,$$

$$\Delta_{\text{NDP}}(\%) = \left(1 - \frac{\text{NDP after preprocessing}}{\text{NDP before preprocessing}}\right) \times 100,$$

and $\Delta_{\text{NDP/C}}$ = (NDP/C after preprocessing) − (NDP/C before preprocessing).

Table 5.2: Effect of preprocessing on the number of arcs and non-dominated paths (NDP) in the E-VRPTW test instances of (Schneider et al., 2013).

	Before preprocessing			After preprocessing			Reductions		
Instance	Arcs	NDP	NDP/C	Arcs	NDP	NDP/C	$\Delta_{Arcs}(\%)$	$\Delta_{NDP}(\%)$	$\Delta_{NDP/C}$
C101-5	73	122	2.90	56	62	1.48	23.29	49.18	1.43
C103-5	57	82	1.95	47	67	1.60	17.54	18.29	0.36
C206-5	91	133	3.17	76	89	2.12	16.48	33.08	1.05
C208-5	73	106	2.52	63	86	2.05	13.70	18.87	0.48
R104-5	73	134	3.19	62	116	2.76	15.07	13.43	0.43
R105-5	73	116	2.76	57	68	1.62	21.92	41.38	1.14
R202-5	73	108	2.57	63	93	2.21	13.70	13.89	0.36
R203-5	91	122	2.90	72	100	2.38	20.88	18.03	0.52
RC105-5	91	120	2.86	78	77	1.83	14.29	35.83	1.02
RC108-5	91	131	3.12	74	96	2.29	18.68	26.72	0.83
RC204-5	91	124	2.95	82	113	2.69	9.89	8.87	0.26
RC208-5	73	110	2.62	73	110	2.62	0.00	0.00	0.00
C101-10	241	508	3.85	174	243	1.84	27.80	52.17	2.01
C104-10	211	478	3.62	180	445	3.37	14.69	6.90	0.25
C202-10	241	465	3.52	194	301	2.28	19.50	35.27	1.24
C205-10	183	418	3.17	123	237	1.80	32.79	43.30	1.37
R102-10	211	466	3.53	146	277	2.10	30.81	40.56	1.43
R103-10	183	390	2.95	153	329	2.49	16.39	15.64	0.46
R201-10	211	430	3.26	160	278	2.11	24.17	35.35	1.15
R203-10	241	504	3.82	182	419	3.17	24.48	16.87	0.64
RC102-10	211	348	2.64	134	153	1.16	36.49	56.03	1.48
RC108-10	211	408	3.09	155	312	2.36	26.54	23.53	0.73
RC201-10	211	466	3.53	155	274	2.08	26.54	41.20	1.45
RC205-10	211	444	3.36	145	292	2.21	31.28	34.23	1.15
C103-15	421	1196	4.40	343	935	3.44	18.53	21.82	0.96
C106-15	343	902	3.32	231	516	1.90	32.65	42.79	1.42
C202-15	421	1168	4.29	303	873	3.21	28.03	25.26	1.08
C208-15	381	920	3.38	247	553	2.03	35.17	39.89	1.35
R102-15	553	1346	4.95	388	606	2.23	29.84	54.98	2.72
R105-15	463	1221	4.49	312	546	2.01	32.61	55.28	2.48
R202-15	463	1322	4.86	320	1010	3.71	30.89	23.60	1.15
R209-15	421	1290	4.74	308	1005	3.69	26.84	22.09	1.05
RC103-15	421	1082	3.98	323	788	2.90	23.28	27.17	1.08
RC108-15	421	1150	4.23	291	964	3.54	30.88	16.17	0.68
RC202-15	421	1103	4.06	286	700	2.57	32.07	36.54	1.48
RC204-15	507	1497	5.50	429	1355	4.98	15.38	9.49	0.52
Average	243	581	3.50	180	402	2.47	23.14	29.27	1.03

NDP: number of non-dominated paths; NDP/C: number of ND paths per customer-customer pair.

It can be seen that the number of arcs is reduced in all but one instance. On average, the relative number of arcs eliminated over all of the test instances is approximately 23.14%. The reductions appear to become more effective as the number of customers increases: relatively more arcs are eliminated in larger instances.

It can be further observed that a significant number of non-dominated paths are removed in most of the test instances. Specifically, over 50% of non-dominated paths are removed in four instances, and the average reduction over all of the test instances is approximately 29.27%. In addition, the average number of non-dominated paths per customer-customer pair over all of the instances is reduced by approximately 1.03.

5.2.2 Impact of valid inequalities

The impact of incorporating the valid inequalities of Section 4.4 in the improved formulation (4.16) - (4.29) is evaluated by computing the optimal solution to its LP-relaxation at the root node of the branch-and-bound tree with and without these inequalities for all the test instances. No CPLEX cuts or preprocessing steps other than those presented in this thesis are used in the computations. The optimal solution of the LP-relaxation corresponds to the initial lower bound in the branch-and-bound algorithm. Note that no limit is set on the number of vehicles when computing these bounds (i.e., the constraint (4.17) is removed completely).

Table 5.3 presents the initial lower bounds (LB) in the branch-and-bound tree and the corresponding computation times (t_{LB}) for each test instance with and without incorporating the valid inequalities (liftings) of Section 4.4 in the improved formulation (4.16) - (4.29). In addition, the relative improvements in the lower bounds ($\%LB$) and the absolute increments in computation times (Δt_{LB}) are presented for each test instance. The relative lower bound improvements are computed as

$$\%LB = \left(\frac{LB \text{ with liftings}}{LB \text{ without liftings}} - 1 \right) \times 100.$$

According to Table 5.3, incorporating the valid inequalities improves the initial lower bound in almost all of the test instances. The most significant improvement corresponds to an increase of 15.14%, whereas the average improvement over all of the test instances is approximately 4.26%. Additionally, the time to solve the LP-relaxation increases by 0.01 seconds on average.

Table 5.3: Optimal solutions to the LP-relaxation of the formulation (4.16) - (4.29) with and without valid inequalities and liftings. The optimal solutions correspond to the initial lower bounds (LB) in the branch-and-bound algorithm.

	No liftings		Liftings		Difference	
Instance	LB	t_{LB}	LB	t_{LB}	$\%LB$	Δt_{LB}
C101-5	234.72	0.00	234.72	0.00	0.00	0.00
C103-5	146.57	0.00	152.64	0.00	4.14	0.00
C206-5	233.96	0.00	233.96	0.00	0.00	0.00
C208-5	110.18	0.00	110.18	0.00	0.00	0.00
R104-5	85.23	0.00	85.33	0.00	0.12	0.00
R105-5	153.01	0.00	153.01	0.00	0.00	0.00
R202-5	117.22	0.00	125.89	0.00	7.40	0.00
R203-5	165.06	0.00	169.92	0.00	2.94	0.00
RC105-5	203.27	0.00	203.33	0.00	0.03	0.00
RC108-5	173.90	0.00	178.18	0.01	2.46	0.01
RC204-5	96.73	0.00	100.96	0.00	4.37	0.00
RC208-5	128.73	0.00	133.52	0.00	3.72	0.00
C101-10	366.41	0.00	366.41	0.00	0.00	0.00
C104-10	221.06	0.00	225.73	0.02	2.11	0.02
C202-10	231.47	0.00	231.47	0.00	0.00	0.00
C205-10	194.72	0.00	224.20	0.00	15.14	0.00
R102-10	188.13	0.00	196.62	0.01	4.51	0.01
R103-10	142.01	0.00	146.95	0.01	3.48	0.01
R201-10	195.32	0.00	199.74	0.00	2.26	0.00
R203-10	156.16	0.00	173.41	0.02	11.05	0.02
RC102-10	377.26	0.00	390.69	0.00	3.56	0.00
RC108-10	253.70	0.00	272.11	0.01	7.26	0.01
RC201-10	304.00	0.00	304.00	0.00	0.00	0.00
RC205-10	305.16	0.00	306.79	0.01	0.53	0.01
C103-15	244.26	0.02	251.87	0.04	3.12	0.02
C106-15	239.37	0.01	262.53	0.01	9.68	0.00
C202-15	274.09	0.01	298.63	0.04	8.95	0.03
C208-15	234.12	0.01	255.59	0.02	9.17	0.01
R102-15	354.39	0.01	355.06	0.02	0.19	0.01
R105-15	312.54	0.00	312.54	0.01	0.00	0.01
R202-15	263.10	0.01	276.58	0.06	5.12	0.05
R209-15	206.51	0.01	225.74	0.04	9.31	0.03
RC103-15	240.47	0.02	265.32	0.03	10.33	0.01
RC108-15	179.89	0.01	204.28	0.04	13.56	0.03
RC202-15	323.32	0.01	342.97	0.04	6.08	0.03
RC204-15	211.64	0.02	217.55	0.09	2.79	0.07
Average	218.55	0.00	227.46	0.01	4.26	0.01

LB: optimal solution to the LP-relaxation at the root node without CPLEX cuts.
t_{LB}: computation time is seconds.

5.3 Computational results

This section presents the computational results for the test instances. Computations were performed on an Intel i5-3570K desktop clocked at 3.40 GHz with 8 Gb RAM running Windows 7 Home Premium x64 Edition. In the following, the standard formulation (3.2) - (3.16) presented in Chapter 3 is referred to as 'Model 1' and the improved formulation (4.16) - (4.29) developed in Chapter 4 as 'Model 2'.

First, the two models are validated by comparing their results to those reported in (Schneider et al., 2013). Note that Schneider et al. (2013) solve the test instances using both CPLEX (with a 2 hour time limit) and the developed VNS/TS heuristic, but they use a hierarchical objective, in which the primary objective is to minimize the number of vehicles required to service all the customers, and the secondary objective is to minimize the total energy cost. Since the models developed in this thesis focus on strict energy cost minimization, a direct comparison is not possible. However, by setting the upper limit m for the number of vehicles equal to that used in the best solutions reported in (Schneider et al., 2013), it is possible to examine the potential improvements of using the variable recharging scheme over the fixed recharging scheme when the vehicle fleet is limited. Therefore, the computational results are reported for both the case where $m = \infty$ (Table 5.6), and the case where $m = \overline{m}$, $\overline{m}$ being the number of vehicles in the best solution found by Schneider et al. (2013) (Tables 5.4 and 5.5).

Table 5.4 presents the best known solutions reported by Schneider et al. (2013) using both CPLEX and the VNS/TS heuristic, and the smallest number of vehicles $\overline{m}$ used in those solutions. Table 5.4 further presents the best solutions obtained by Models 1 and 2 using both the fixed recharging scheme (FIX) and the variable recharging scheme (VAR). The upper limit for the number of vehicles was set to $\overline{m}$ when computing these results: this enables estimating the improvements of using the variable recharging scheme over the fixed one with a limited number of vehicles. For all the instances, the solution obtained involves exactly $\overline{m}$ vehicles, wherefore this information is not reported separately in Table 5.4. Note, however, that the optimal solution to the instance 'RC108-5' requires two vehicles instead of one as initially reported in (Schneider et al., 2013). A time limit of 7200 seconds is imposed to the branch-and-cut algorithm; if this time limit is reached, optimality is not guaranteed.

The best known solutions reported by Schneider et al. (2013) are presented in the columns CPLEX and VNS/TS, respectively, and the number of vehicles used in those solutions are reported in the column $\overline{m}$. The best solutions obtained by Models 1 and 2 using both the fixed recharging scheme and the variable recharging scheme are presented in the columns FIX and VAR, respectively, and the corresponding computation times are reported in the columns t_{FIX} and t_{VAR}, respectively. If no integer solution is found, the relative gap between the best obtained lower bound and the best known integer solution is reported instead. Finally, the potential improvements of using the variable recharging scheme over the fixed one are reported in column %Δ (%Δ = (VAR/FIX − 1) × 100). These improvements are reported only for Model 2, because it solves more instances to optimality than Model 1.

Table 5.4: Results obtained with Model 1 and Model 2 on the E-VRPTW test instances of Schneider et al. (2013).

	Schneider et al. (Hierarchical obj. function)			MODEL 1 ($m = \overline{m}$)				MODEL 2 ($m = \overline{m}$)				
Instance	$\overline{m}$	CPLEX	VNS/TS	FIX	VAR	t_{FIX}	t_{VAR}	FIX	VAR	%Δ	t_{FIX}	t_{VAR}
C101-5	2	257.75	257.75	257.75	257.75	0.29	0.36	257.75	257.75	0.00	0.05	0.06
C103-5	1	176.05	176.05	176.05	175.37	0.15	0.20	176.05	175.37	-0.39	0.06	0.06
C206-5	1	242.55	242.56	242.55	242.55	0.81	0.48	242.55	242.55	0.00	0.04	0.04
C208-5	1	158.48	158.48	158.48	158.48	0.28	0.28	158.48	158.48	0.00	0.09	0.10
R104-5	2	136.69	136.69	136.69	136.69	0.19	0.24	136.69	136.69	0.00	0.07	0.07
R105-5	2	156.08	156.08	156.08	156.08	0.16	0.14	156.08	156.08	0.00	0.03	0.02
R202-5	1	128.78	128.78	128.78	128.78	0.19	0.12	128.78	128.78	0.00	0.04	0.05
R203-5	1	179.06	179.06	179.06	179.06	0.39	0.49	179.06	179.06	0.00	0.04	0.05
RC105-5	2	241.30	241.30	241.30	233.77	0.96	0.48	241.30	233.77	-3.12	0.06	0.08
RC108-5	2	253.93	253.93	253.93	253.93	1.77	0.92	253.93	253.93	0.00	0.08	0.08
RC204-5	1	176.39	176.39	176.39	176.39	0.78	1.10	176.39	176.39	0.00	0.11	0.11
RC208-5	1	167.98	167.98	167.98	167.98	0.33	0.38	167.98	167.98	0.00	0.12	0.13
C101-10	3	393.76	393.76	393.77	388.25	34.38	27.32	393.77	388.25	-1.40	0.17	0.12
C104-10	2	273.93	273.93	273.93	273.93	46.36	21.90	273.93	273.93	0.00	1.62	1.35
C202-10	1	304.06	304.06	304.06	304.06	371.60	855.10	304.06	304.06	0.00	0.18	0.19
C205-10	2	228.28	228.28	228.28	228.28	0.64	0.66	228.28	228.28	0.00	0.06	0.05
R102-10	3	249.19	249.19	249.19	249.19	32.21	44.71	249.19	249.19	0.00	0.37	0.34
R103-10	2	207.05	207.05	207.05	206.12	74.96	119.12	207.05	206.12	-0.45	4.59	2.80
R201-10	1	241.51	241.51	241.51	241.51	78.21	95.11	241.51	241.51	0.00	0.21	0.15
R203-10	1	218.21	218.21	218.21	218.21	26.76	50.71	218.21	218.21	0.00	0.72	0.60
RC102-10	4	423.51	423.51	423.51	423.51	4.15	8.45	423.51	423.51	0.00	0.09	0.08
RC108-10	3	345.93	345.93	345.92	345.92	25.48	20.65	345.92	345.92	0.00	0.43	0.42
RC201-10	1	412.86	412.86	412.86	412.86	2749.25	3162.22	412.86	412.86	0.00	0.13	0.16
RC205-10	2	325.98	325.98	325.98	325.98	6.16	5.21	325.98	325.98	0.00	0.16	0.11
C103-15	3	384.29	384.29	399.35	348.46	7200.00	7200.00	384.28	348.46	-9.32	141.88	12.02
C106-15	3	275.13	275.13	275.13	275.13	13.58	12.35	275.13	275.13	0.00	0.22	0.22
C202-15	2	383.62	383.62	383.61	383.61	6712.48	7200.00	383.61	383.61	0.00	12.68	7.07
C208-15	2	300.55	300.55	300.55	300.55	51.34	78.33	300.55	300.55	0.00	0.23	0.19
R102-15	5	413.93	413.93	413.93	412.78	7200.00	7200.00	413.93	412.78	-0.28	1.28	1.14
R105-15	4	336.15	336.15	336.15	336.15	945.49	1283.45	336.15	336.15	0.00	0.42	0.31
R202-15	2	358.00	358.00	358.00	358.00	7200.00	7200.00	358.00	358.00	0.00	6.72	5.86
R209-15	1	313.24	313.24	313.24	313.24	7200.00	7200.00	313.24	313.24	0.00	101.12	37.16
RC103-15	4	397.67	397.67	397.67	397.67	7200.00	7200.00	397.67	397.67	0.00	25.54	39.69
RC108-15	3	370.25	370.25	(19.22%)	(20.93%)	7200.00	7200.00	370.24	370.24	0.00	253.07	167.61
RC202-15	2	394.39	394.39	394.39	394.39	1352.77	891.91	394.39	394.39	0.00	0.47	0.43
RC204-15	1	407.45	384.86	(37.63%)	(36.94%)	7200.00	7200.00	384.86	382.22	-0.69	7200.00	7200.00
Average						1748.11	1785.62			-0.43	215.37	207.75

$\overline{m}$: number of vehicles used in the best solution of Schneider et al.
CPLEX / VNS/TS: best known solution (routing cost) reported in (Schneider et al., 2013).
FIX: best solution (routing cost) with the fixed recharging scheme. t_{FIX}: solution time (s) for FIX
VAR: best solution (routing cost) with the variable recharging scheme. t_{VAR}: solution time (s) for VAR.
%Δ: improvement of using the variable recharging scheme over the fixed one.

Model 2 is significantly faster than Model 1 and solves more instances to optimality. Model 1 appears to be faster with the fixed recharging scheme, whereas Model 2 seems to benefit from the variable recharging scheme.

It can be further observed that adopting the variable recharging scheme improves the best known solutions in some of the instances. The most significant improvement occurs with 'C103-15': the route length is reduced as much as 9.32%. In addition, in the 5 customer instance 'RC105-5', the optimal route length is reduced by 3.12%. On average, the improvement over all of the test instances is approximately 0.43%. Even though this may not seem like much, the differences can be significant in individual instances. Moreover, greater improvements are likely to occur in larger instances with more charging stations and customers, especially if the customer time windows are tight. This is fairly common, for example, in the small package shipping (SPS) industry, where customers have narrow time windows, and service times are typically very small compared to the time needed for a full recharge. Thus, since recharging times obviously affect the route planning, considerable improvements can be obtained by adopting the variable recharging scheme in real-world BEV routing problems.

Table 5.5 evaluates the performances of the two models in more detail. The results of this table correspond to those presented in Table 5.4 for the variable recharging scheme (i.e., at most $\overline{m}$ vehicles can be used and the variable recharging scheme is adopted). Table 5.5 presents the initial lower bounds (LB) corresponding to the optimal solution of the LP-relaxation at the root node of the branch-and-bound tree, the percentage ratio ($\%LB$) between the initial lower bound and the best known integer solution (computed as $\%LB = (LB/f^*) \times 100$), and the computation times (t_{LB}) for the lower bounds. Furthermore, Table 5.5 presents the number of nodes (#nodes) in the branch-and-bound tree, the cost of the best integer solution obtained (f^*) and the total computation time (t_{TOT}). In case no integer solution is found, the relative gap between the best obtained lower bound and the best known integer solution, computed as $(LB^*/f^*) \times 100$, is presented, where LB^* denotes the best obtained lower bound. These bounds are not presented explicitly in the table, because only two cases exist in which an integer solution is not found. The time limit is set to 7200 seconds as before.

According to Table 5.5, the lower bounds obtained with Model 2 are significantly stronger than those obtained with Model 1: on average, the percentage ratio between the initial lower bound and the best known integer solution increases by approximately 33.09%. This indicates that the improved formulation (4.16) - (4.29) of Model 2 is much stronger than the standard formulation (3.2) - (3.16). Moreover, computing the initial lower bounds is faster with Model 2. The number of nodes in the branch-and-bound tree and the total computation times further support these observations: solving the instances with Model 2 requires much less nodes and the computation times are much lower than with Model 1. Interestingly, the number of nodes in the last instance 'RC204-15' is considerably larger with Model 2. The reason for this is that since computing the lower bound is faster with Model 2, it can also evaluate more nodes in the branch-and-bound tree than Model 1 within the given time (both models reached the 7200 s limit).

Table 5.5: Comparison of Model 1 and Model 2.

	MODEL 1						MODEL 2					
Instance	LB	$\%LB$	t_{LB}	#nodes	f^*	t_{TOT}	LB	$\%LB$	t_{LB}	#nodes	f^*	t_{TOT}
C101-5	180.50	70.03	0.00	760	257.75	0.36	245.32	95.18	0.00	0	257.75	0.06
C103-5	121.64	69.36	0.00	453	175.37	0.20	152.38	86.89	0.00	5	175.37	0.06
C206-5	163.62	67.46	0.00	455	242.55	0.48	234.03	96.48	0.01	0	242.55	0.04
C208-5	83.28	52.55	0.01	361	158.48	0.28	110.18	69.53	0.00	0	158.48	0.10
R104-5	85.23	62.35	0.00	153	136.69	0.24	85.33	62.42	0.00	0	136.69	0.07
R105-5	118.51	75.93	0.00	94	156.08	0.14	153.01	98.03	0.01	0	156.08	0.02
R202-5	105.23	81.71	0.00	62	128.78	0.12	125.88	97.75	0.00	0	128.78	0.05
R203-5	121.40	67.80	0.01	437	179.06	0.49	169.92	94.90	0.01	0	179.06	0.05
RC105-5	117.05	50.07	0.01	464	233.77	0.48	202.82	86.76	0.00	0	233.77	0.08
RC108-5	134.04	52.79	0.00	1365	253.93	0.92	178.04	70.11	0.01	0	253.93	0.08
RC204-5	84.23	47.75	0.00	1968	176.39	1.10	100.96	57.24	0.00	219	176.39	0.11
RC208-5	87.59	52.14	0.00	987	167.98	0.38	133.52	79.49	0.00	0	167.98	0.13
C101-10	187.89	48.39	0.04	10813	388.25	27.32	366.36	94.36	0.01	0	388.25	0.12
C104-10	177.53	64.81	0.03	18098	273.93	21.90	225.73	82.40	0.01	2745	273.93	1.35
C202-10	158.69	52.19	0.04	428454	304.06	855.10	231.47	76.13	0.00	0	304.06	0.19
C205-10	161.42	70.71	0.01	131	228.28	0.66	224.20	98.21	0.00	0	228.28	0.05
R102-10	170.15	68.28	0.02	36769	249.19	44.71	195.57	78.48	0.00	60	249.19	0.34
R103-10	129.08	62.63	0.02	127888	206.12	119.12	146.58	71.12	0.00	11841	206.12	2.80
R201-10	169.00	69.98	0.03	74656	241.51	95.11	212.97	88.18	0.00	0	241.51	0.15
R203-10	134.14	61.47	0.04	13599	218.21	50.71	173.09	79.32	0.01	0	218.21	0.60
RC102-10	296.38	69.98	0.02	1652	423.51	8.45	390.27	92.15	0.00	1	423.51	0.08
RC108-10	210.45	60.84	0.02	23048	345.92	20.65	268.47	77.61	0.01	223	345.92	0.42
RC201-10	177.86	43.08	0.02	1714925	412.86	3162.22	333.26	80.72	0.00	11	412.86	0.16
RC205-10	239.89	73.59	0.02	3407	325.98	5.21	306.79	94.11	0.01	0	325.98	0.11
C103-15	205.06	58.85	0.10	771646	348.46	7200.00	251.29	72.11	0.02	8558	348.46	12.02
C106-15	217.18	78.94	0.03	3902	275.13	12.35	262.53	95.42	0.01	16	275.13	0.22
C202-15	249.28	64.98	0.06	1653723	383.61	7200.00	297.83	77.64	0.02	7623	383.61	7.07
C208-15	199.07	66.24	0.05	17936	300.55	78.33	255.59	85.04	0.02	2	300.55	0.19
R102-15	227.14	55.03	0.17	527130	412.78	7200.00	354.91	85.98	0.02	1490	412.78	1.14
R105-15	206.22	61.35	0.13	101241	336.15	1283.45	312.48	92.96	0.00	46	336.15	0.31
R202-15	214.43	59.90	0.09	934308	358.00	7200.00	276.51	77.24	0.02	3880	358.00	5.86
R209-15	192.95	61.50	0.06	1637948	313.24	7200.00	223.66	71.40	0.02	48279	313.24	37.16
RC103-15	173.36	43.70	0.06	1026486	397.67	7200.00	264.45	66.50	0.01	63513	397.67	39.68
RC108-15	170.09	45.94	0.09	1166358	(20.93%)	7200.00	204.28	55.18	0.03	179056	370.24	167.61
RC202-15	222.71	56.47	0.06	344598	394.39	891.91	342.18	86.76	0.01	70	394.39	0.43
RC204-15	202.22	52.91	0.13	1054389	(36.94%)	7200.00	216.56	56.66	0.03	5071665	382.22	7200.00
Average		61.16	0.04	325018		1785.62		81.40	0.01	149981		207.75

LB: initial lower bound; $\%LB$: percentage ratio between the lower bound and the best known integer solution
#nodes: number of nodes in the branch-and-bound tree; f^*: best obtained integer solution.
t_{LB}: time to compute the lower bound (s); t_{TOT}: total computation time (s).

Finally, Table 5.6 presents the computational results for the test instances with and without limiting the number of vehicles. The solutions where the number of vehicles is limited correspond to those presented in Table 5.4 (i.e., the best solutions with the variable recharging scheme and at most $m = \overline{m}$ vehicles). The solution requiring the least number of vehicles is also often the one with least energy costs; however, as is shown in Table 5.6, this is not generally true: lower energy costs may be obtained with more vehicles. This can happen, for example, if some vehicles are forced to perform long detours to service customers which are located far from each other.

Table 5.6: Results obtained with Model 2 with and without limiting the number of vehicles. Setting no limit on the number of vehicles (case $m = \infty$) produces solutions with the smallest energy costs.

	Case $m = \overline{m}$			Case $m = \infty$			Difference		
Instance	m	f^*	$t(s)$	m	f^*	$t(s)$	Δm	$\Delta f^*(\%)$	$\Delta t(s)$
C101-5	2	257.75	0.06	3	247.15	0.03	1	-4.11	-0.03
C103-5	1	175.37	0.06	2	165.67	0.03	1	-5.53	-0.03
C206-5	1	242.55	0.04	2	236.58	0.02	1	-2.46	-0.02
C208-5	1	158.48	0.10	1	158.48	0.03	0	0.00	-0.07
R104-5	2	136.69	0.07	2	136.69	0.04	0	0.00	-0.03
R105-5	2	156.08	0.02	2	156.08	0.02	0	0.00	0.00
R202-5	1	128.78	0.05	1	128.78	0.05	0	0.00	0.00
R203-5	1	179.06	0.05	1	179.06	0.03	0	0.00	-0.02
RC105-5	2	233.77	0.08	2	233.77	0.05	0	0.00	-0.03
RC108-5	2	253.93	0.08	2	253.93	0.05	0	0.00	-0.03
RC204-5	1	176.39	0.11	1	176.39	0.10	0	0.00	-0.01
RC208-5	1	167.98	0.13	1	167.98	0.10	0	0.00	-0.03
C101-10	3	388.25	0.12	3	388.25	0.08	0	0.00	-0.04
C104-10	2	273.93	1.35	2	273.93	1.65	0	0.00	0.30
C202-10	1	304.06	0.19	2	243.20	0.08	1	-20.02	-0.11
C205-10	2	228.28	0.05	2	228.28	0.03	0	0.00	-0.02
R102-10	3	249.19	0.34	3	249.19	0.21	0	0.00	-0.13
R103-10	2	206.12	2.80	3	202.85	1.33	1	-1.59	-1.47
R201-10	1	241.51	0.15	3	217.68	0.10	2	-9.87	-0.05
R203-10	1	218.21	0.60	1	218.21	0.66	0	0.00	0.06
RC102-10	4	423.51	0.08	4	423.51	0.07	0	0.00	-0.01
RC108-10	3	345.92	0.42	3	345.92	0.31	0	0.00	-0.11
RC201-10	1	412.86	0.16	3	310.06	0.07	2	-24.90	-0.09
RC205-10	2	325.98	0.11	2	325.98	0.09	0	0.00	-0.02
C103-15	3	348.46	12.02	3	348.46	6.19	0	0.00	-5.83
C106-15	3	275.13	0.22	3	275.13	0.20	0	0.00	-0.02
C202-15	2	383.61	7.07	3	369.57	2.36	1	-3.66	-4.71
C208-15	2	300.55	0.19	2	300.55	0.14	0	0.00	-0.05
R102-15	5	412.78	1.14	5	412.78	1.54	0	0.00	0.40
R105-15	4	336.15	0.31	4	336.15	0.32	0	0.00	0.01
R202-15	2	358.00	5.86	2	358.00	4.13	0	0.00	-1.73
R209-15	1	313.24	37.16	2	293.20	4.03	1	-6.40	-33.13
RC103-15	4	397.67	39.69	4	397.67	18.43	0	0.00	-21.26
RC108-15	3	370.24	167.61	3	370.24	116.04	0	0.00	-51.57
RC202-15	2	394.39	0.43	2	394.39	0.51	0	0.00	0.08
RC204-15	1	382.22	7200.00	2	310.57	625.95	1	-18.75	-6574.05
Average							0.33	-2.70	-185.94

m: number of vehicles used; f^*: best obtained solution; $t(s)$: computation time.

Table 5.6 presents the number of vehicles used (m), the costs of the best integer solutions obtained (f^*), and the corresponding computation times ($t(s)$) with and without limiting the number of vehicles for each test instance.

In addition, the absolute increments in the number of vehicles (Δm), the relative increases in the routing costs ($\Delta f^*(\%)$) and the absolute increases in the computation times ($\Delta t(s)$) for each test instance are presented. The relative increase in the routing cost is computed as

$$\Delta f^*(\%) = \left(\frac{f^*(\text{case } m = \infty)}{f^*(\text{case } m = \overline{m})} - 1 \right) \times 100$$

As can be seen in Table 5.6, the energy costs can be significantly reduced in some instances by using more vehicles than the minimum required. For example, in the instance 'C202-10', using two vehicles instead of one results in a 20.02% reduction in energy costs. Moreover, in 'RC201-10', a 24.90% reduction in energy costs is possible by using three vehicles instead of one. Note that also the last instance 'RC204-15' is now solved to optimality: the optimal solution without limiting the number of vehicles is obtained with two vehicles instead of one; the improvement over the best known single-vehicle solution is approximately 18.75%.

The are a few more instances where the energy costs can be reduced by using more vehicles. However, in most instances the two solutions are identical. On average, the energy costs can be reduced by as much as 2.70%. To compensate for this reduction, the number of vehicles required increases on average by 0.33. As mentioned before, even though the average reduction seems insignificant, the differences can be significant in individual problem instances.

Chapter 6

Case study

This Chapter presents an illustrative case study that attempts to simulate potential real-world BEV routing problems. Towards this end, a test instance based on the road network of southwestern Finland is created using the network data obtained from `openstreepmap.org`. Subsequently, a set of small test cases are constructed that simulate potential real-world BEV routing problems utilizing the existing charging infrastructure. Locations of the existing charging stations are obtained from `electrictraffic.fi`. Finally, larger test cases with more customers and randomly generated time windows are constructed based on the created test instance. All of the test cases are solved using the improved formulation developed in Chapter 4. Computations were performed on an Intel i5-3570K desktop clocked at 3.40 GHz with 8 Gb RAM running Windows 7 Home Premium x64 Edition.

6.1 Test instance

The structure of the test instance is presented in Figure 6.1. The corresponding road network is derived from that of southwestern Finland such that only the highways and other 'big roads' are included. Longer road segments are simplified to reduce the network size: the simplification reduces the number of vertices significantly while ensuring that the lengths of the modified road segments deviate by at most 1 km from their original length. The simplification was performed with JOSM (Scholz & Stöcker, 2013) using the tool 'simplify-roads' and the add-on 'simplify-area' that allow setting an upper limit on the distance deviation between two points.

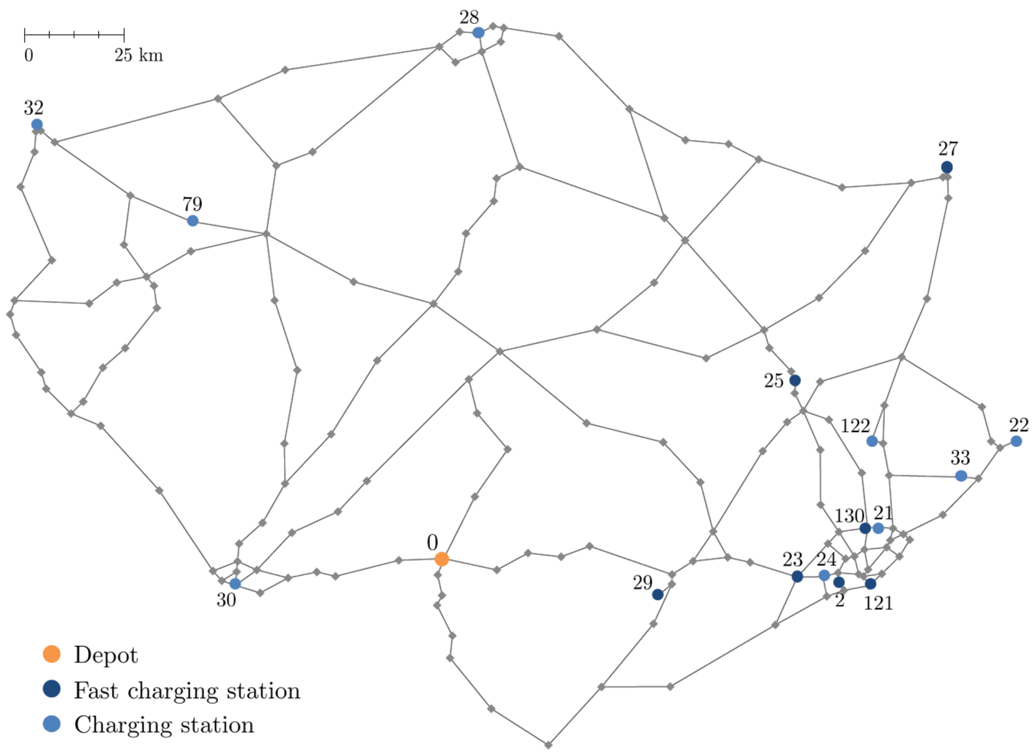

Figure 6.1: Test instance based on the road network of southwestern Finland.

In Figure 6.1, the charging stations are located based on their actual locations; however, not all of them are presented: in particular, those in close proximity are aggregated into a single station. In addition, the vertex numbers are presented by each charging station to facilitate referring to them. The selected depot represents both the origin and the destination depots.

Since battery recharging is rather time-consuming, only the fast charging stations are included in creating the test instances. However, as can be seen in Figure 6.1, only seven such charging stations exist in this area. Moreover, they are all aggregated towards the right side of the map, rendering it difficult to efficiently service customers located at the opposite side. Therefore, in order to create meaningful test instances, it is assumed that some of the normal charging stations are upgraded to provide fast recharging.

6.2 Test cases

In this Section, several test cases are generated by first selecting a set of customers from the created test instance, subsequently setting the vehicle battery capacity, and finally incorporating randomly generated time windows for the customers. All the fast charging stations are included. Also, it is assumed that the charging station '79' is upgraded to provide fast recharging.

Initially, no time windows are set for the customers, the only time-related constraint being the maximum route duration T. Subsequently, customer time windows are randomly generated and optimal routing costs (with regard to traveled distance and thus energy consumption) are compared to those obtained without time windows. Furthermore, the impact of the vehicle battery capacity Q in conjunction with customer time windows is examined by fixing a set of time windows and solving the generated instance with different values of Q. Initially, the following assumptions are made:

- Maximum route duration $T = 12$ hours.
- Customer service time $s_i = 5$ minutes for each customer $i \in N$.
- Vehicle speed $v = 90$ km/h.
- The (fast) recharging rate $g = 5$ km/min.
- Vehicle battery capacity $Q = 200$ km.
- Vehicle load capacity $C = \infty$ (i.e., the vehicles can service any number of customers within given time limits).

The vehicle battery capacity Q and the recharging rate g are presented in distance units for simplicity. This does not alter the computation or affect the optimal routing plan, since energy consumption is assumed to be directly proportional to the traveled distance by (3.1). The fast recharging rate is estimated based on the assumption that the vehicle battery can be recharged from empty to approximately 80% within 30 - 45 minutes with almost a constant rate, whereafter the charging rate begins to gradually decrease.

An example charging profile is presented in Figure 6.2 for the 'Tesla Supercharger' fast charging station. As can be seen in the figure, the charging rate exhibits the aforementioned behavior. This provides a possible avenue for future research to separately model the recharging behavior as linear (i.e., with a constant rate) up to 80% state-of-charge and as a piece-wise linear approximation for the remaining 20% to capture the non-linear behavior.

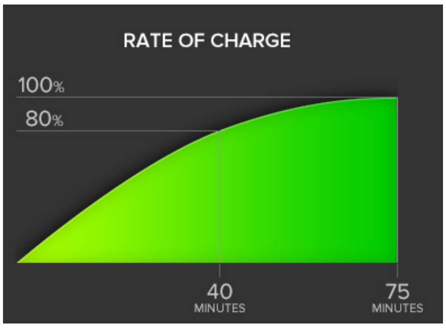

Figure 6.2: Charging profile of the Tesla Supercharger fast charging station. Obtained from www.teslamotors.com/supercharger.

6.2.1 First test case

Consider the following test instance presented in Figure 6.3. Initially, no specific time windows are set, apart from those of the form $[0, T]$, where $T = 720$ minutes denotes the maximum route duration. In the following, this test instance is referred to as 'A1-Q200', where 'Q200' denotes the battery capacity value $Q = 200$ km that is initially used in solving the instance.

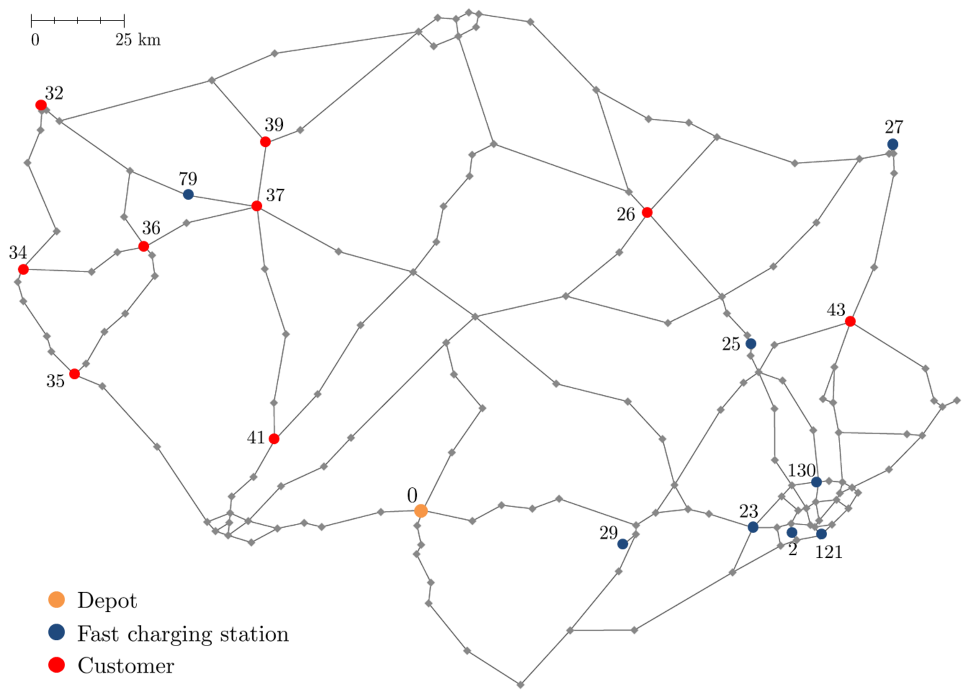

Figure 6.3: The test instance A1-Q200 without time windows.

As can be seen in Figure 6.3, there are only nine customers to be serviced. However, due to the nature of the problem, even with such a small instance it is not immediately clear in which order the customers should be serviced; when, where, and how much the vehicle battery should be recharged; and how many vehicles should be used in order to minimize the total routing cost. The developed model provides this information in less than one second.

The optimal solution is presented in Figure 6.4. It turns out that the minimum routing cost is obtained by using only one vehicle. The order in which the customers and charging stations are visited is indicated by arrows and small numbers. It is assumed that the vehicle always travels the shortest paths in the road network between any pair of customers and/or charging stations; therefore, the arrows only indicate the visiting order. The length of the optimal route is 823.26 km and the total duration is 718.49 minutes.

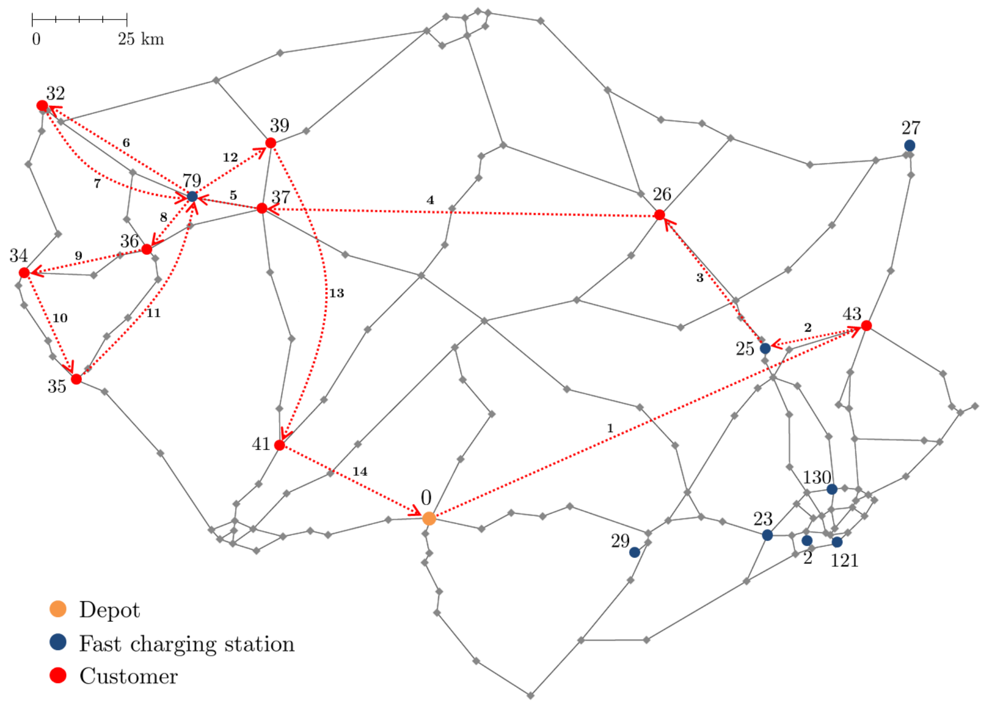

Figure 6.4: Optimal solution of the test instance A1-Q200 ($Q = 200$ km).

The charging station '79' must be visited three times in the optimal solution to prevent battery depletion. Note that the path 79-32-34-35-36-79 would require one charging station visit less than the path 79-32-79-36-34-35-79 traversed in the optimal solution; however, the length of the former path exceeds the maximum driving range of the vehicle and is therefore infeasible.

6.2.1.1 Fixed recharging scheme

A full recharge is not necessary at all of the charging station visits. In the obtained solution, the battery is recharged to full only at the first station '25', after which the minimum required amount is recharged. Since the duration of the optimal route is close to the maximum allowed, it is interesting to examine how the optimal solution changes if the fixed recharging scheme that enforces a full recharge at every station visit is used instead.

The optimal solution to the instance A1-Q200 with the fixed recharging scheme is presented in Figure 6.5. It can be seen that two vehicles are now required instead of one. Moreover, the total length of the optimal vehicle routes is now 883.53 km, resulting in a 7.32% increase in the routing cost. This small example demonstrates how the fixed recharging scheme used in the previous studies may produce inferior solutions even for routing problems without specific time windows (apart from those imposed by the maximum route duration).

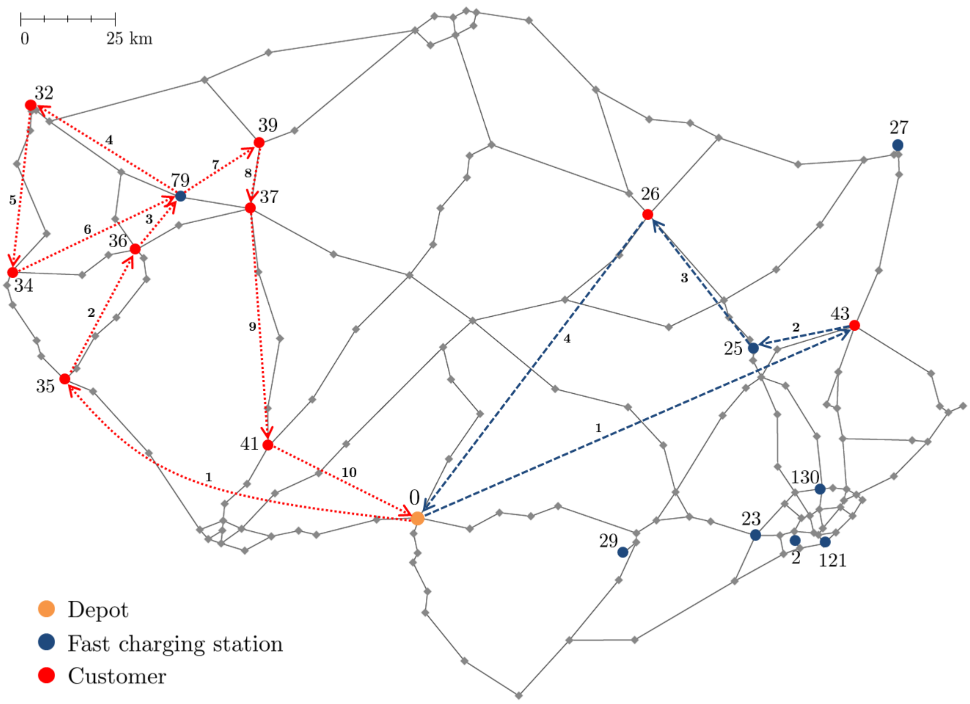

Figure 6.5: Optimal solution of the test instance A1-Q200 (Q = 200 km) using the fixed recharging scheme. The different colored tours represent separate vehicle routes.

6.2.2 Varying battery capacity

This section examines the impact of varying the battery capacity Q on the solution quality. Towards this end, the test instance A1-Q is solved by using different values of Q, and the obtained results are evaluated. The optimal routing plans of two test instances A1-Q350 ($Q = 350$ km) and A1-Q160 ($Q = 160$ km) are also presented graphically. Throughout this section, it is assumed that the variable recharging scheme is adopted.

First, suppose that the battery capacity is changed to $Q = 160$ km (~100 miles), which, according to some studies, corresponds to a range that is sufficient for individual consumers to consider switching to BEVs and is also used as a basis for some business models for an electric transportation system (see, e.g., Skippon & Garwood, 2011; Becker et al., 2009). The optimal solution to the test instance A1-Q160 is presented in Figure 6.6.

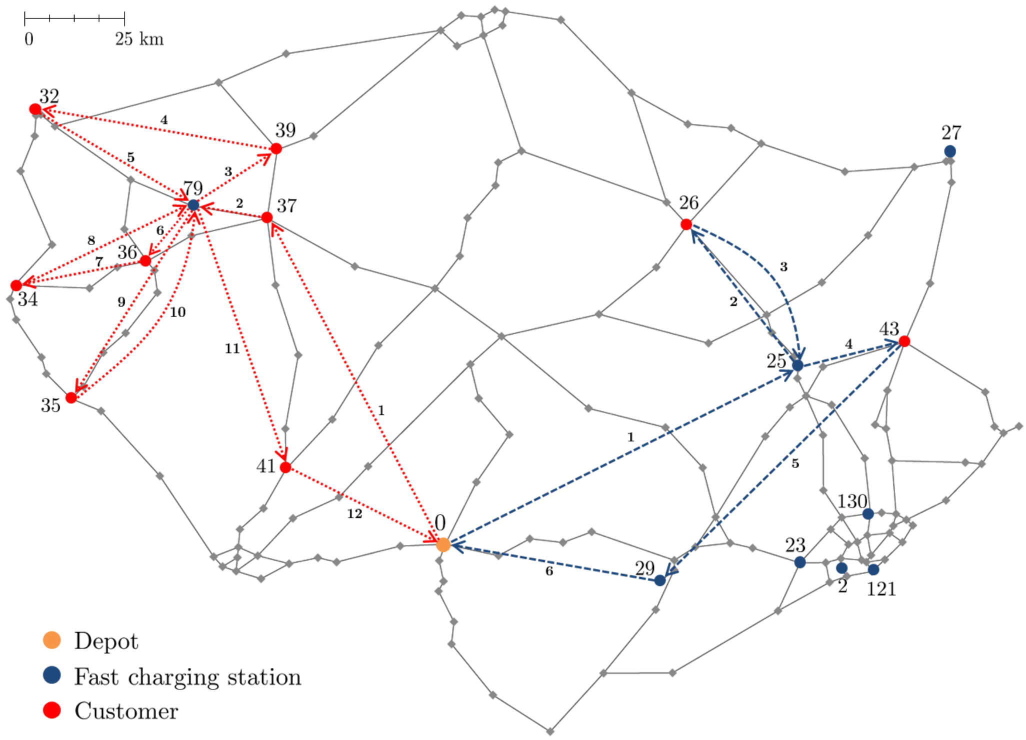

Figure 6.6: Optimal solution of the test instance A1-Q160 ($Q = 160$ km). The different colored tours correspond to distinct vehicle routes.

As can be seen, two vehicles are required instead of one as in the test instance A1-Q200 presented in Figure 6.4. Moreover, the total length of the optimal vehicle routes is now 1148.08 km, resulting in a 39.46% increase in the routing cost. This is, of course, due to the shorter driving range: more visits to charging stations are required to prevent battery depletion. Specifically, the charging station '79' is now visited four times, whereas the station '25' is visited twice; furthermore, a previously unvisited charging station '29' is now visited in the optimal routing plan.

To investigate how the optimal solution changes with a larger battery capacity, let $Q = 350$ km, which is currently close to the maximum driving range of any commercially available BEV (see, e.g., Mangram, 2012). The new optimal solution is presented in Figure 6.7.

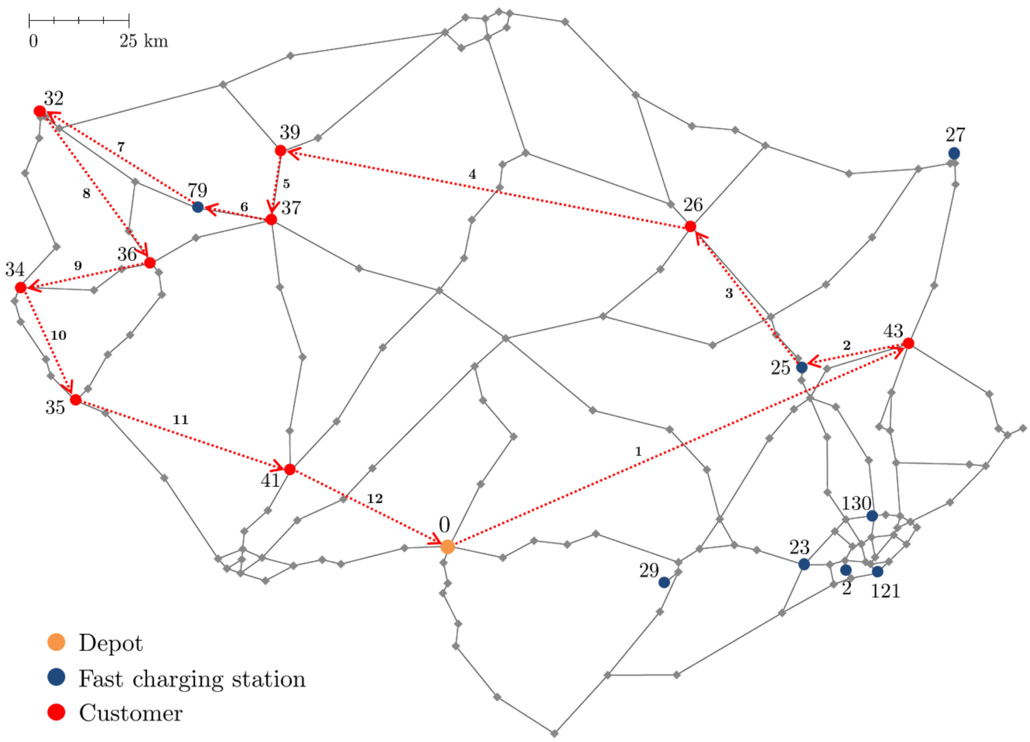

Figure 6.7: Optimal solution of the test problem A1-Q350 ($Q = 350$ km).

It can be seen that only one vehicle is used in the optimal solution. Moreover, due to the large battery capacity, only two charging stations visits are needed. The length of the optimal route is now 712.43 km, while the total duration amounts to 592.35 minutes. Hence, compared to the optimal solution of the test instance A1-Q200 presented in Figure 6.4, the routing cost decreases by 13.46% and the total duration by 17.56%.

These small examples demonstrate the impact of the battery capacity on the optimal routing cost and duration. A more detailed analysis is provided in Figure 6.8, which presents the optimal routing cost $c(Q)$ with different values of battery capacity Q up to the case where no charging station visits are required. The test instance A1-Q was solved by using values $Q \in \{160, 165, \ldots 1000\}$, and the points where the optimal solution changes are plotted in the Figure 6.8. The adjacent table presents the used battery capacity Q, the number of vehicles m used in the solution, the optimal routing cost $c(Q)$, and the relative increase in the routing cost $\Delta\%$ with respect to the case $Q = \infty$, which corresponds to the regular TSP solution, since only one vehicle is required to service all the customers.

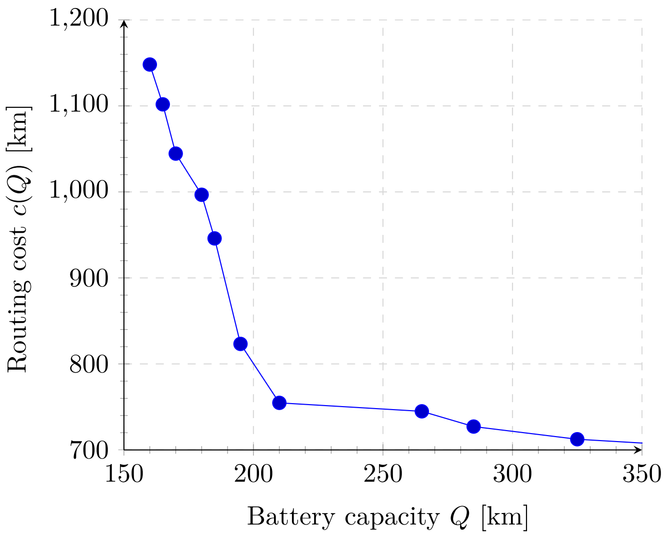

	Optimal solution		
Q	m	$c(Q)$	$\Delta\%$
160	2	1148.08	65.26
165	2	1101.81	58.60
170	2	1044.52	50.35
180	2	996.67	43.47
185	2	945.93	36.16
195	1	823.26	18.50
210	1	754.73	8.64
265	1	744.89	7.22
285	1	727.17	4.67
325	1	712.43	2.55
520	1	694.71	0.00
∞	1	694.71	0.00

$\Delta\%$: increase in routing cost compared to the case $Q = \infty$.

Figure 6.8: Optimal routing cost $c(Q)$ of the test instance A1-Q with different values of battery capacity Q. The table presents the number of vehicles m and the increase in the routing cost $\Delta\%$ with respect to the case $Q = \infty$.

It can be seen that the optimal routing cost decreases rapidly in the beginning when the battery capacity is increased. Initially with $Q = 160$ km, the routing cost is 65.26% higher compared to the case where $Q = \infty$ (i.e., where no recharging is required). When $Q \geq 210$ km, the optimal routing cost decreases significantly slower when the battery capacity is further increased. With $Q = 210$ km, the optimal routing cost is only 8.64% higher than with $Q = \infty$. When $Q = 700$ km, no charging stations visits are required. Conversely, the problem becomes infeasible with $Q < 160$.

In the absence of time-related constraints, only the detours to the charging stations contribute to the increase in the routing cost and not the recharged amount itself. In this case, the optimal solution depends only on the placement and the number of charging stations. For example, with $Q = 520$ km, the vehicle must stop to recharge at some point to prevent battery depletion. Still, the optimal solution is the same as with $Q = \infty$: the charging station '25' is located along the shortest path between the customers '26' and '43', wherefore stopping to recharge at '25' does not affect the routing cost if there are no time-related constraints.

6.2.3 Customer time windows

In this section, a procedure for generating customer time windows for the created test instance is presented. The procedure is similar to that presented in (Solomon, 1987). Subsequently, randomly generated customer time windows are included in the previous test cases with different battery capacities, and the new optimal solutions are evaluated. It turns out that all the example problems in this section can be solved in less than one second using the improved formulation.

The following procedure is used in generating the customer time windows. First, the feasible time window range is computed for each customer; i.e., the range between the earliest time a vehicle can arrive at the customer directly from the origin depot, and the latest time a vehicle can depart from the customer and reach the destination depot in time. Subsequently, the time window center is randomly drawn for each customer from the corresponding feasible time window range. Finally, the time window width (TWW) is randomly chosen from three alternatives w_i, $i = \{1, 2, 3\}$, each associated with a probability $P(w_i)$ of being selected. However, if some part of the generated time window falls outside the feasible time window range, the violated part is cut and the time window is extended to the opposite direction by the violated amount. The time windows widths and the corresponding selection probabilities are presented in Table 6.1. As before, it is assumed that $T = 720$ minutes.

Table 6.1: Time window widths w_i, $i = \{1, 2, 3\}$, and selection probabilities $P(w_i)$ for the customer time windows.

TWW (minutes)	Probability
$w_1 = 0.10 \times T = 72$	$P(w_1) = 0.20$
$w_2 = 0.15 \times T = 108$	$P(w_2) = 0.50$
$w_3 = 0.30 \times T = 216$	$P(w_3) = 0.30$

6.2.3.1 Random time windows

In this section, randomly drawn customer time windows are incorporated in the test instance A1-Q with different values of Q. The test instance with a specific value of Q and a specific set of time windows TW is referred to as A1-Q-TW. Note that the set of customers remains the same in all of the test instances; only the battery capacity and customer time windows change. Initially, four different test instances are generated and their optimal solutions are presented graphically. The randomly generated customer time windows used in the test instances are presented in Table 6.2. The time windows are presented in the form $[a \;\; b]$, a denoting the start time and b the end time of the time window. The corresponding time window widths $(b-a)$ are also presented in the table.

Table 6.2: Customer time windows used in the test instances.

	TW1			TW2			TW3			TW4		
Customer	[a	b]	b-a	[a	b]	b-a	[a	b]	b-a	[a	b]	b-a
26	[77	293]	216	[77	185]	108	[77	293]	216	[279	495]	216
32	[372	588]	216	[339	555]	216	[278	494]	216	[480	588]	108
34	[403	619]	216	[403	619]	216	[350	422]	72	[459	531]	72
35	[541	613]	72	[383	455]	72	[151	367]	216	[224	332]	108
36	[158	230]	72	[520	592]	72	[504	612]	108	[504	612]	108
37	[83	299]	216	[83	191]	108	[210	318]	108	[142	250]	108
39	[511	619]	108	[95	203]	108	[271	379]	108	[390	498]	108
41	[512	620]	108	[557	665]	108	[357	429]	72	[472	580]	108
43	[361	469]	108	[153	261]	108	[458	566]	108	[222	330]	108

a: time window start time (min). b: time window end time (min). b-a: time window width (min).

Figure 6.9 presents the optimal solution to the test instance A1-Q200-TW1 (i.e., the battery capacity is set to $Q = 200$ km and the customer time windows are designated according to the set TW1 presented in Table 6.2). The length of the vehicle routes in the optimal solution is 1090.79 km, resulting in a 32.50% increase in the routing cost compared to the optimal solution of the instance A1-Q200 without time windows presented in Figure 6.4. Interestingly, it is beneficial to let the blue vehicle service the customer '35' instead of sending a third, separate vehicle to service it. Consequently, the blue vehicle must perform a long detour to service the last customer. It can be further noted that the blue vehicle must visit two charging stations successively to reach the customer '35' before returning to the depot.

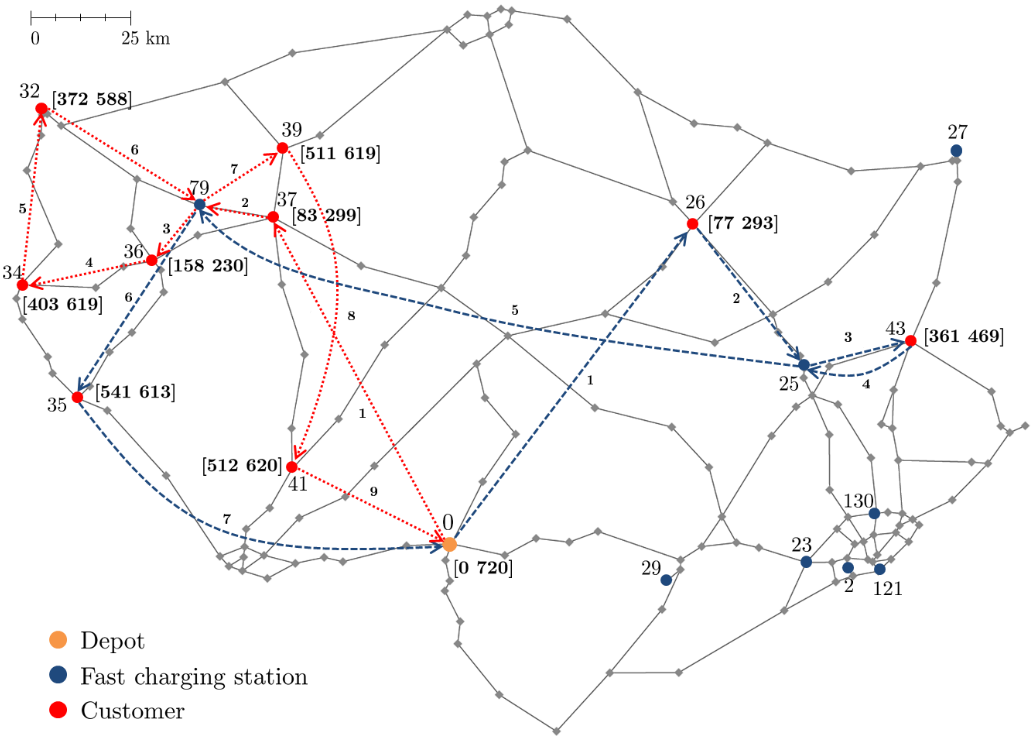

Figure 6.9: Optimal solution of the test instance A1-Q200-TW1. The different colored tours represent distinct vehicle routes. The customer time windows are displayed in brackets.

Figure 6.10 presents the optimal solution to the test instance A1-Q180-TW2 with customer time windows designated according to the set TW2 in Table 6.2 and battery capacity set equal to $Q = 180$ km. As in the previous test instance A1-Q200-TW1, the optimal routing cost is obtained with only two vehicles. In this test instance, however, the customers are distributed more evenly among the two vehicles. The total length of the optimal vehicle routes amounts to 1203.94 km, which is approximately 20.80% more than the optimal routing cost of the same instance without time windows, which is 996.67 km (see Figure 6.8). Since the time windows of A1-Q180-TW2 are different than those of A1-Q200-TW1, no comparison is made with regard to the routing costs between these two instances. Routing cost comparisons using the same time windows are presented in the following Section 6.2.3.2.

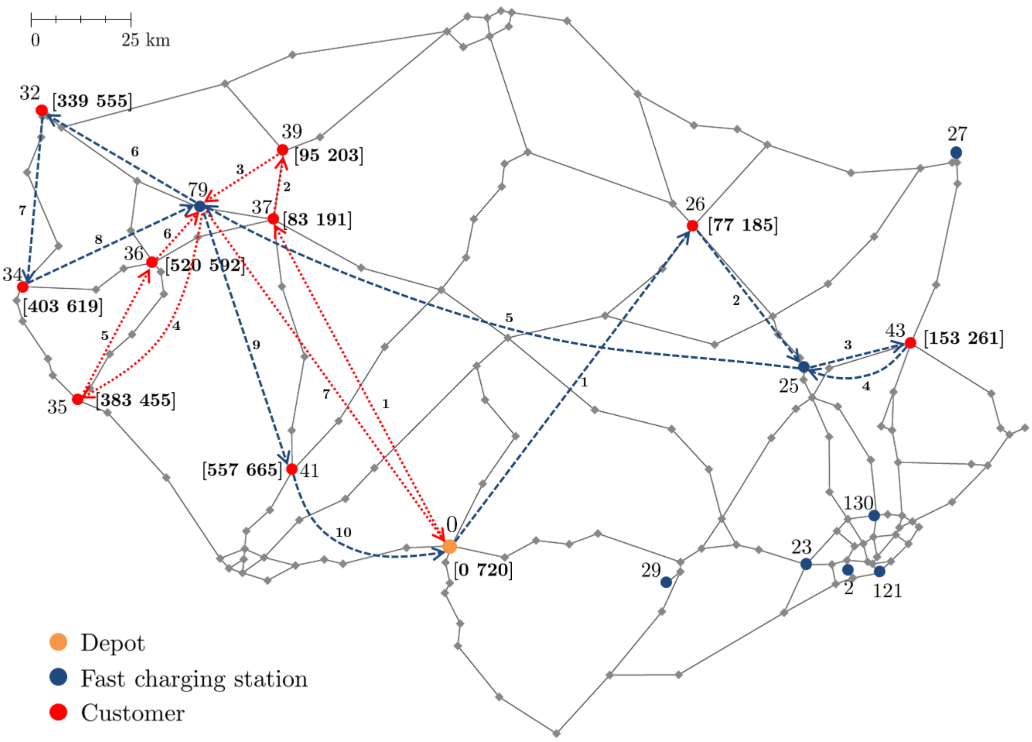

Figure 6.10: Optimal solution of the test instance A1-Q180-TW2. The different colored tours represent distinct vehicle routes. The customer time windows are displayed in brackets.

Two more test instances A1-Q160-TW3 and A1-Q350-TW4 are presented in Figures 6.11 and 6.12, respectively. Similarly to the previous test instances, the customer time windows are designated according to the sets TW3 and TW4 presented in Table 6.2, and the battery capacities are set equal to $Q = 160$ km and $Q = 350$ km.

Figure 6.11 presents the optimal solution to the test instance A1-Q160-TW3. It can be seen that the minimum routing cost is obtained by using three vehicles, whereas in the optimal solution of A1-Q160 presented in Figure 6.6, two vehicles are sufficient. Due to the shorter driving range and the presence of customer time windows, the charging station '79' is now visited a total of six times, whereas in the solution of A1-Q160, only four visits are required. Note that a single vehicle services most of the customers located at the left side of the map; only the customer closest to the depot, customer '41', is serviced by using an additional vehicle. The total length of the optimal vehicle routes amounts to 1373.80 km, resulting in a 19.66% increase in the routing cost compared to the corresponding instance without time windows.

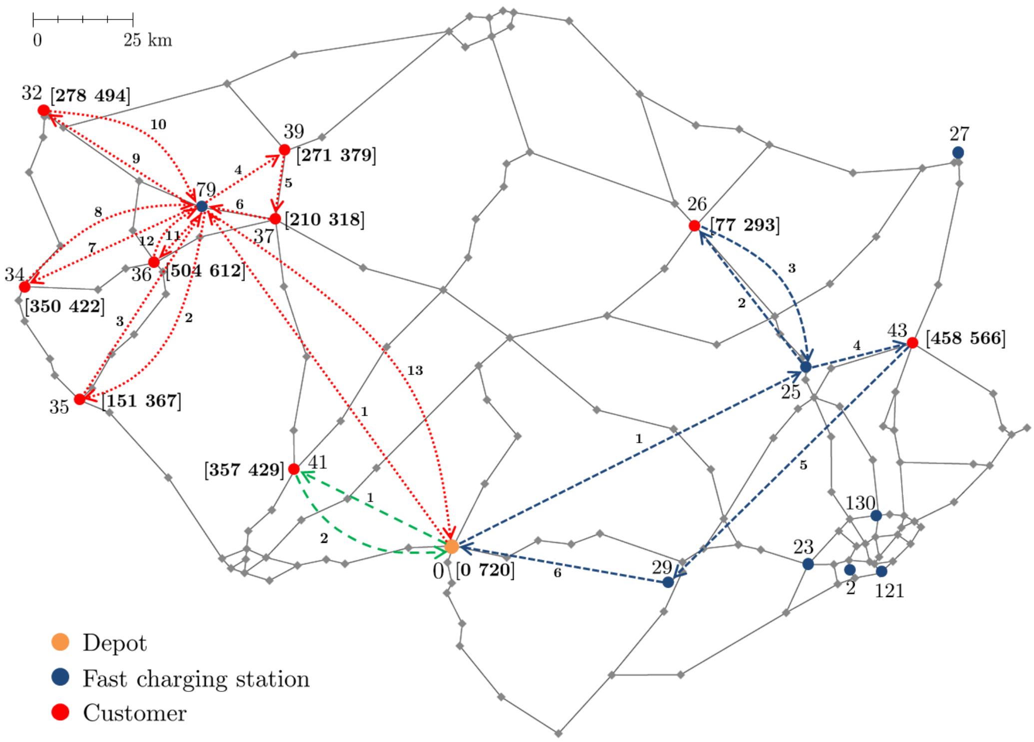

Figure 6.11: Optimal solution of the test instance A1-Q160-TW4. The different colored tours represent distinct vehicle routes. The customer time windows are displayed in brackets.

Notice that due to the number of visits to the charging station ’79’, the optimal solution cannot be obtained if an artificial upper bound (less than six in this case) is imposed on the number of stops to a single station. Moreover, even by setting this upper bound appropriately, solving the problem by using the standard formulation presented in Section 3 takes over 7200 seconds with the same implementation that was used in Chapter 5, whereas the problem can be solved in less than one second with the improved formulation. This small example emphasizes the benefit of the new formulation, since no upper bound is required on the number of station visits.

Finally, Figure 6.12 presents the optimal solution to the test instance A1-Q350-TW4. Despite the long driving range, one vehicle is no longer enough to service all the customers as in the corresponding instance without time windows A1-Q350 presented in Figure 6.7; instead, two vehicles are required to service all the customers in time. Due to the longer driving range, only one charging station visit is needed in both of the vehicle routes. The combined length of these vehicle routes is 1028.03 km, resulting in a 44.30% increase in the routing cost compared to the optimal solution of the corresponding instance without time windows presented in Figure 6.7.

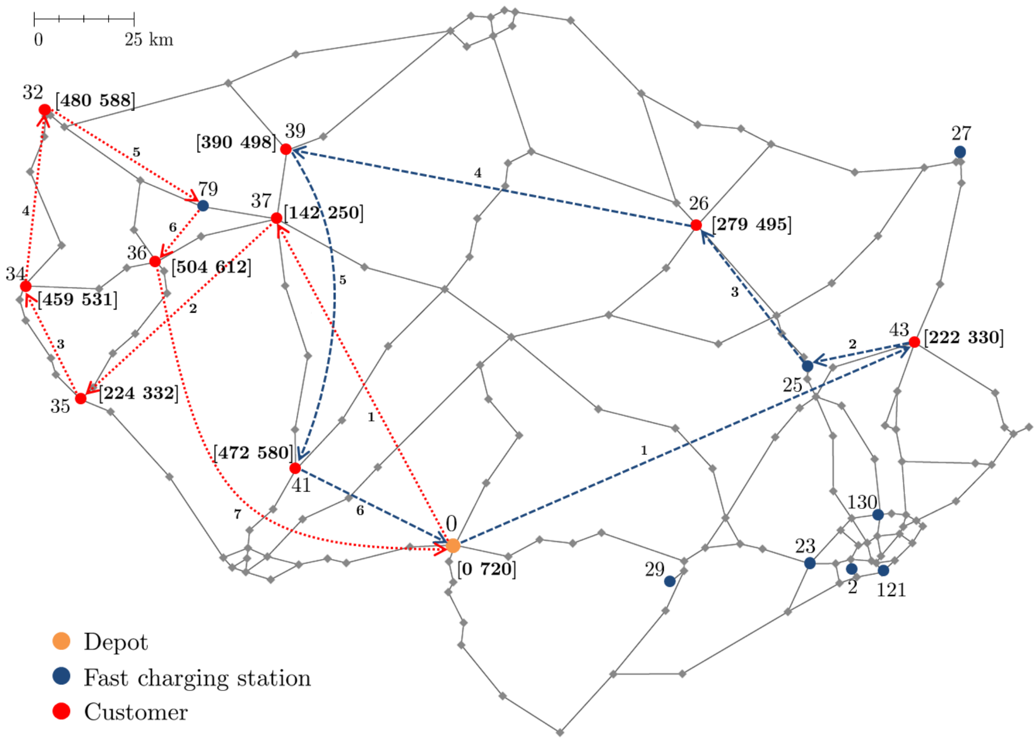

Figure 6.12: Optimal solution of the test instance A1-Q350-TW4. The different colored tours represent distinct vehicle routes. The customer time windows are displayed in brackets.

6.2.3.2 Fixed time windows

In this section, the impact of the vehicle battery capacity Q in conjunction with customer time windows is examined by fixing the time windows according to the set TW4 presented in Table 6.2 and comparing the optimal routing costs with different values of Q. The optimal solutions of two test instances A1-Q200-TW4 (Q = 200 km) and A1-Q160-TW4 (Q = 160 km) are also presented graphically. Note that Figure 6.12 presents the optimal solution to the instance A1-Q350-TW4 with the same set of time windows TW4 but with $Q = 350$ km.

Figure 6.13 presents the optimal solution to the test instance A1-Q200-TW4. As in the optimal solution of the test instance A1-Q350-TW4 presented in

Figure 6.12, two vehicles are sufficient in servicing all the customers even though the battery capacity is considerably smaller. However, the blue vehicle must now also service some of the customers located at the left side; due to the shorter driving range, the red vehicle must stop to recharge more frequently, wherefore it cannot service all those customers in time. The total length of the optimal vehicle routes is 1163.08. With respect to the optimal solution of the corresponding instance without time windows (i.e., A1-Q200 presented in Figure 6.4), the routing cost increases by 41.28%. Furthermore, in comparison to the optimal solution of the instance A1-Q350-TW4, the optimal routing cost increases by 13.14%.

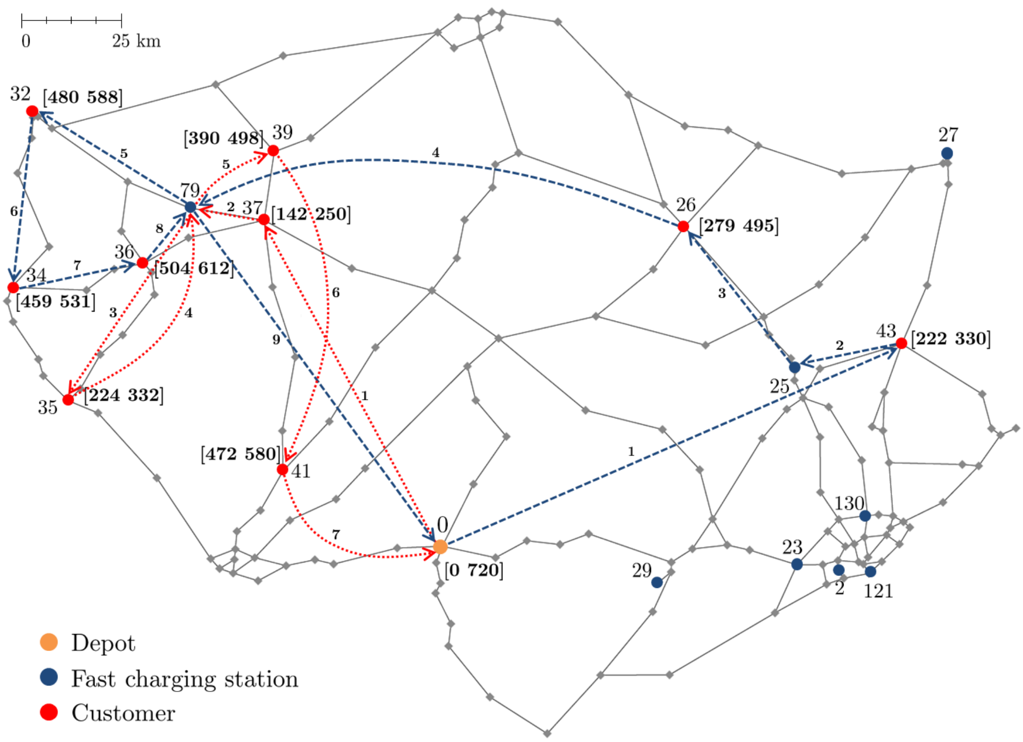

Figure 6.13: Optimal solution of the test instance A1-Q200-TW4. The different colored tours represent distinct vehicle routes. The customer time windows are displayed in brackets.

Figure 6.14 presents the optimal solution to the instance A1-Q160-TW4. It can be observed that four vehicles are used in the optimal solution to service all the customers. Further tests indicate that four vehicles are actually required, since the problem becomes infeasible by limiting the number of vehicles to three (for this small example, the infeasibility is determined in a fraction of a second with the improved model). As can be seen, two vehicles are now dispatched to service the customers located at the left. Moreover, the customer '41' must now be serviced by a separate vehicle, because otherwise it cannot be serviced in time. The customers located at the right side of the map are also serviced by a separate vehicle: the distance between the charging stations '25' and '79' exceeds the driving range of 160 km.

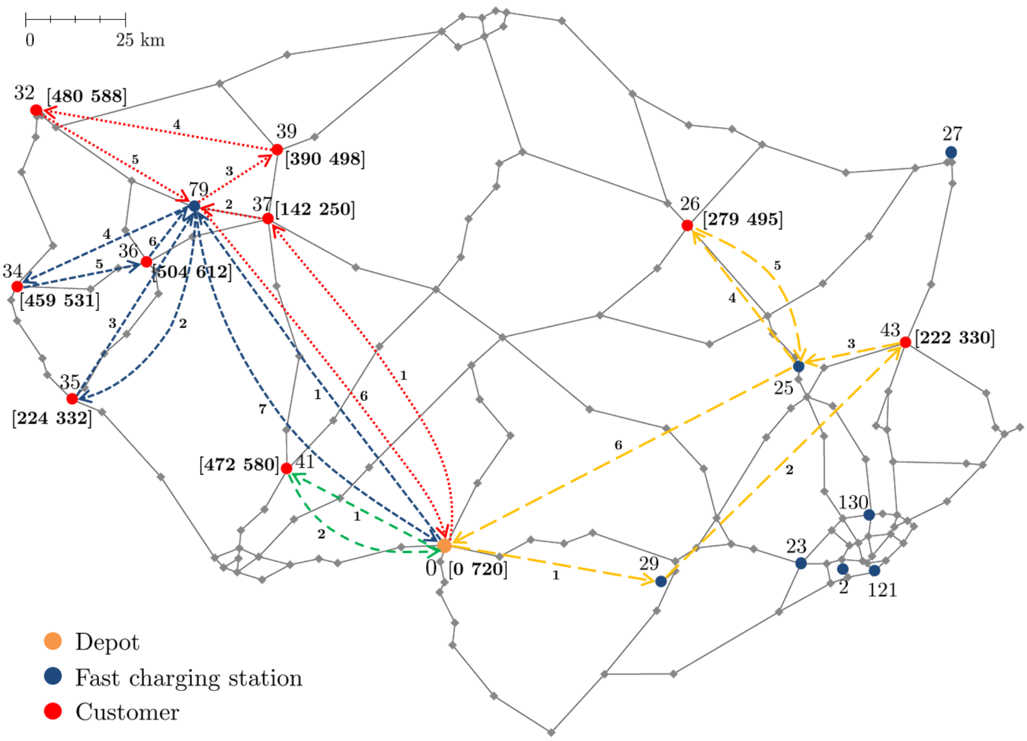

Figure 6.14: Optimal solution of the test instance A1-Q160-TW4. The different colored tours correspond to distinct vehicle routes. The customer time windows are displayed in brackets.

The aggregate length of the optimal vehicle routes amounts to 1575.74 km, which results in a 37.25% increase in the routing cost compared to the corresponding instance without time windows (A1-Q160) presented in Figure 6.6. Also, with respect to the instances A1-Q350-TW4 and A1-Q200-TW4 with the same set of time windows TW4, the optimal routing cost is approximately 53.28% and 35.48% higher, respectively.

These small test instances demonstrate the impact of varying the battery capacity in conjunction with fixed customer time windows on the solution quality. A more comprehensive analysis is provided in Figure 6.15, which presents the optimal routing cost $c(Q)$ with different values of battery capacity Q. The customer time windows are fixed according to the set TW4 of Table 6.2 when computing the results. The problem was solved by using values $Q \in \{160, 165, \dots 1000\}$, and the points where the optimal solution changes are plotted if the figure. The optimal routing costs without customer time windows are also presented for comparison. The adjacent table reports the used battery capacity Q, the number of vehicles m, the optimal routing cost $c(Q)$, and the relative increase in the routing cost $\Delta\%$ with respect to the case $Q = \infty$ (i.e., $\Delta\% = (c(Q)/c(\infty) - 1) \times 100$).

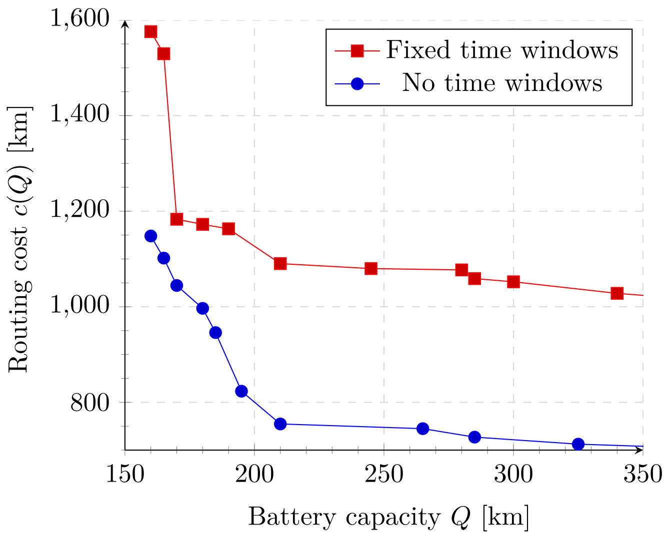

Fixed time windows TW4

	Optimal solution		
Q	m	$c(Q)$	$\Delta\%$
160	4	1575.74	58.28
165	4	1529.47	53.63
170	3	1183.10	18.84
180	3	1172.42	17.76
190	2	1163.08	16.83
210	2	1090.27	9.51
245	2	1079.88	8.47
280	2	1077.09	8.19
285	2	1058.91	6.36
300	3	1052.24	5.69
340	2	1028.03	3.26
365	2	1017.63	2.22
485	2	995.57	0.00
∞	2	995.57	0.00

$\Delta\%$: increase in routing cost compared to the case $Q = \infty$.

Figure 6.15: Optimal routing cost $c(Q)$ of the test problem with different values of battery capacity Q and fixed time windows TW4. The table presents the number of vehicles m and the increase in routing cost $\Delta\%$ with respect to the case $Q = \infty$. The optimal solutions without time windows are also presented for comparison.

As can be seen in Figure 6.15, the optimal routing cost decreases more rapidly in the beginning with the fixed time windows. Initially with $Q = 160$ km, the optimal routing cost is 58.28% higher than with $Q = \infty$. However, when the battery capacity is increased by 10 km (i.e., by setting $Q = 170$ km), this difference reduces to 18.84%.

Comparing the solutions with and without the customer time windows, the differences in the optimal routing costs appear to change unevenly with regard to the battery capacity Q. Initially with $Q = 160$ km, the optimal routing cost is 37.25% higher with the time windows, whereas with $Q = 170$ km this difference is only 13.27%. After this point, the gap between these two cases becomes larger. Eventually with $Q = \infty$, this difference is 43.31%.

6.2.4 Outcome evaluation

These small examples demonstrate the potential impact that customer time windows and different battery capacities can have on the optimal routing plan. Unlike with regular VRPTW instances, the recurring need to recharge in conjunction with relatively long recharging times complicate the route planning considerably. In particular, complications arise with determining:

1. When and where to recharge?
2. How much should be recharged?
3. How many vehicles should be used?

From the previous examples it should be obvious how difficult even small BEV routing problems can be without proper decision support, especially when customer time windows are included.

6.3 Larger test cases

In this Section, a larger test instance is constructed by selecting 26 customers from the road network and generating time windows for the customers based on Table 6.1. Several test cases are subsequently generated by varying the battery capacity Q but keeping the time windows fixed. Initially, the optimal solutions of two different test instances are presented graphically. Subsequently, the optimal solutions with different values of Q are computed and the corresponding routing costs are reported.

Figure 6.16 presents the test instance with 26 customers and randomly generated customer time windows. The same set of charging stations is used as before. Due to the large number of customers, designing an optimal routing plan is practically impossible without decision support (see the three questions in 6.2.4). Fortunately, by using the developed model, the optimal solution can be computed in a reasonable time for different values of Q.

The larger test instances are referred to as A2-QX-TW, where X denotes the battery capacity value $Q = \text{X}$ that is used in solving the instance. The TW part is always the same, since only a single set of customer time windows is used. These time windows are displayed in brackets next to the selected customers in Figure 6.16.

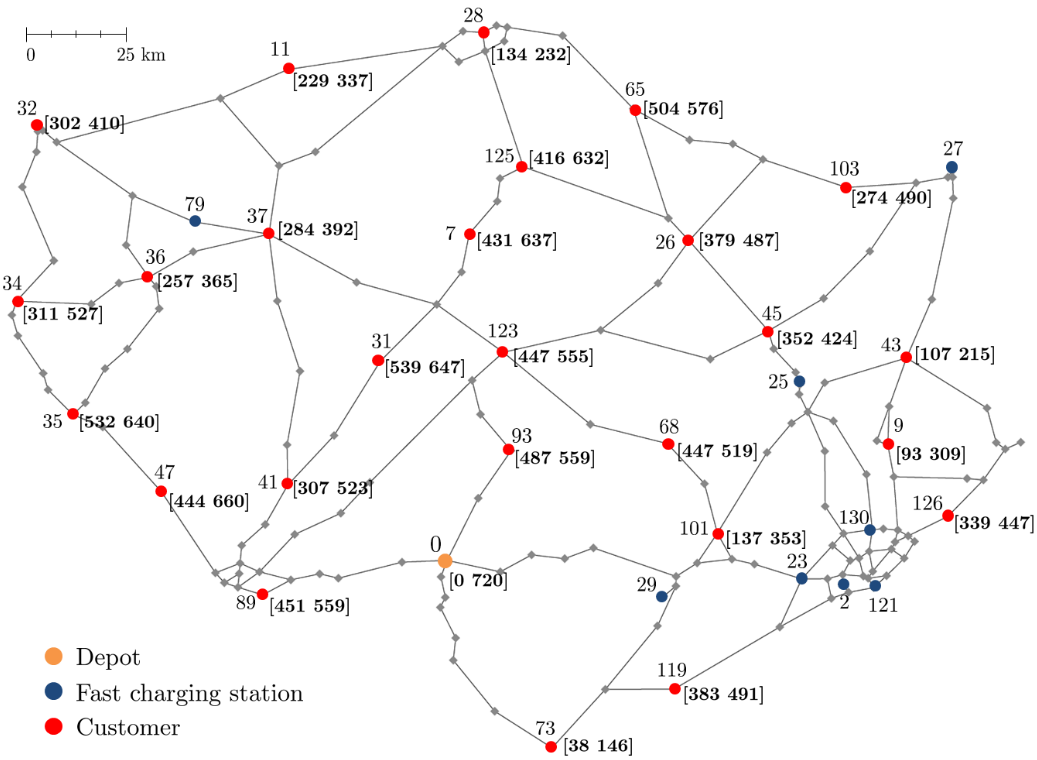

Figure 6.16: Test instance with 26 customers and randomly generated customer time windows.

Figure 6.17 presents the optimal solution to the test instance A2-Q200-TW (i.e., with the battery capacity set equal to $Q = 200$ km). The optimal solution was computed in 222.04 seconds. As can be seen, five vehicles are used in the optimal routing plan. The total length of the optimal vehicle routes amounts to 2520.98 km. It can be further observed that 12 charging station visits are required in the optimal solution, the charging station '79' being visited six times in total by three different vehicles. Additionally, the previously unused charging stations '23', '130' and '27' are now utilized in the optimal routing plan to help achieve lower routing costs. As an example of how a less frequently used charging station may affect the route planning, the removal of the charging station '27' from the network causes an increase in the optimal routing cost of approximately 5.60%.

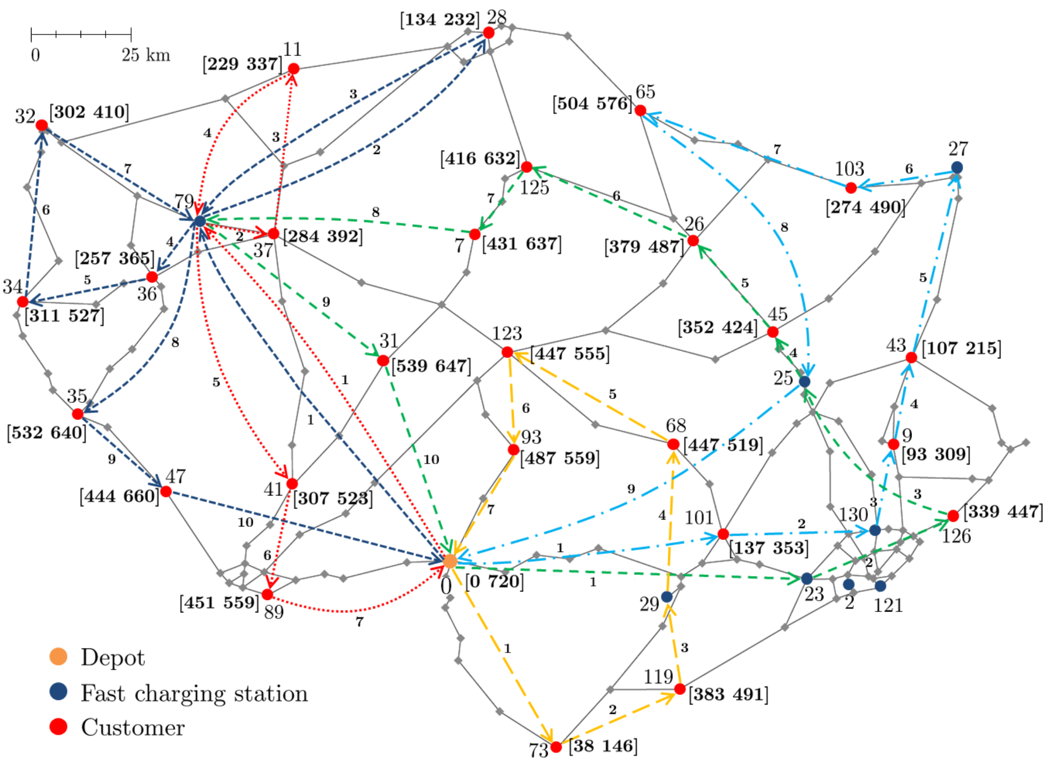

Figure 6.17: Optimal solution of the 26-customer test instance A2-Q200-TW. The different colored tours represent distinct vehicle routes.

Figure 6.18 presents the optimal solution to the test problem A2-Q350-TW. It can be seen that only four vehicles are now used instead of five as in the previous instance in Figure 6.17. In addition, due to the longer driving range, only four charging station visits are required in the optimal solution. Consequently, the optimal routing cost is considerably smaller: the aggregate length of the optimal vehicle routes amounts to 1753.51 km, resulting in a 30.44% reduction in the routing cost.

The same time windows as in the previous instance were used in computing the optimal solution. However, for this instance, the optimal solution was obtained in only 76.73 seconds, whereas for the previous instance it took 222.04 seconds. This difference in computation times is not entirely intuitive, since not only the number of non-dominated paths is considerably larger, but also the preprocessing steps based on battery capacity are relatively weaker with higher values of Q. The impact of varying the battery capacity on the computation time is further examined in Figure 6.19.

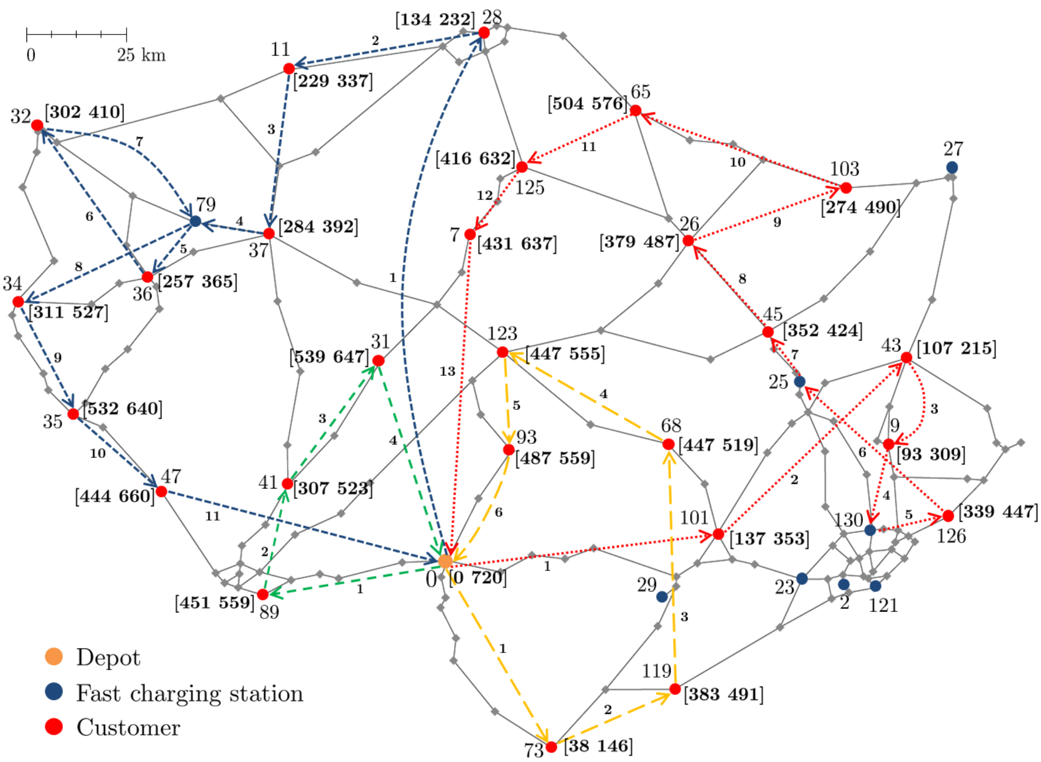

Figure 6.18: Optimal solution of the 26-customer test instance A2-Q350-TW. The different colored tours represent distinct vehicle routes.

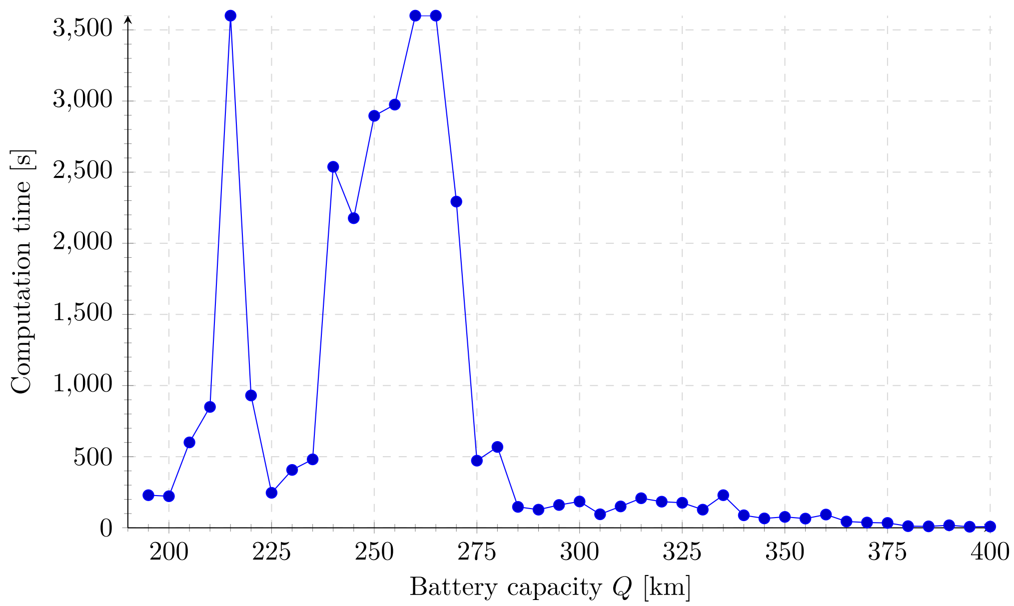

Figure 6.19: Computation times of the 26-customer test instances with varying Q.

According to Figure 6.19, the computation times are heavily dependent on the used battery capacity: as a trend, the larger Q becomes, the faster the optimal solution can be computed. For example, when Q becomes large enough so that no charging station visits are needed, the problem becomes a regular VRPTW and the optimal solution can be obtained in approximately one second. However, there are two values of Q (approximately $Q = 215$ and $Q = 265$) around which the problem becomes very difficult.

In the following, the test instance of Figure 6.16 is solved with several different values of battery capacity Q and the optimal routing costs are reported. According to the developed model, the problem is infeasible for values of $Q \leq 190$ km; this information was obtained in a fraction of a second upon attempting to solve the problem for values $Q = 150 \ldots 190$ km. Figure 6.20 presents the optimal routing costs $c(Q)$ for both the fixed and variable recharging schemes. The points where the optimal solution changes are plotted in the figure. The adjacent table presents the used battery capacity Q, the number of vehicles m used in the solution, the optimal routing cost $c(Q)$, and the relative increase in the routing cost $\Delta\%$ with respect to the case $Q = \infty$ (i.e., $\Delta\% = (c(Q)/c(\infty) - 1) \times 100$), which corresponds to the regular VRPTW solution. This information is presented for the variable recharging scheme only; the optimal routing costs with the fixed recharging scheme are presented only for comparison.

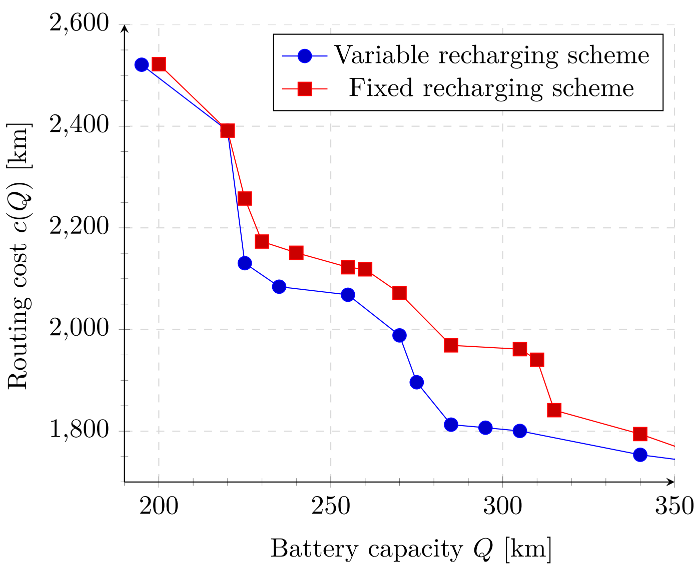

Variable recharging scheme

	Optimal solution		
Q	m	$c(Q)$	$\Delta\%$
195	5	2520.98	55.37
220	6	2391.30	47.38
225	5	2130.53	31.31
235	5	2084.25	28.46
255	5	2068.37	27.48
270	4	1988.45	22.55
275	4	1896.20	16.87
285	4	1812.82	11.73
295	4	1806.81	11.36
305	4	1800.47	10.97
340	4	1753.51	8.07
360	4	1736.01	6.99
365	4	1697.06	4.59
375	4	1684.98	3.85
380	4	1660.40	2.33
425	3	1656.63	2.10
∞	3	1622.53	0.00

$\Delta\%$: increase in routing cost compared to the case $Q = \infty$.

Figure 6.20: Optimal routing cost $c(Q)$ of the 26-customer test instance with different values of battery capacity Q. The table presents the number of vehicles m and the increase in the routing cost $\Delta\%$ with respect to the case $Q = \infty$.

Chapter 7

Conclusion

This thesis examined the optimal routing of plug-in battery electric vehicles (BEVs) and presented two mathematical models to determine optimal routing plans in scenarios, where a set of locations (e.g., customers) is to be visited by one or more BEVs, and where the traveled distance exceeds the initial driving range, thus making it necessary to recharge the battery at charging stations en route to prevent it from depleting. The presented models also incorporate customer time windows, service times and vehicle capacities that represent the most relevant constraints of real-world routing problems. The models were implemented in C programming language and solved with CPLEX (ILOG, 2013) using the CPLEX 12.5 callable library interface functions.

The initial model generalizes the *Electric Vehicle Routing Problem with Time Windows* (E-VRPTW) introduced by Schneider et al. (2013) by also allowing the possibility of recharging a variable amount of energy at the charging stations (*variable recharging scheme*) rather than performing a full recharge at every visit (*fixed recharging scheme*). Computational tests performed in this thesis indicate that significant reductions in the routing cost can be obtained by adopting the variable recharging scheme over the fixed one.

A major disadvantage of the standard E-VRPTW formulation proposed by Schneider et al. (2013) is the need to model every possible charging station *visit* as a separate 'dummy' vertex in the network graph. To overcome this drawback, a new formulation for the E-VRPTW was developed that does not model the charging stations explicitly, but replaces them with a set of non-dominated energy paths between every customer pair. The new formulation was shown to reduce the number of decision variables in the model and to provide considerable computational improvements over the standard formulation. Some new preprocessing steps and valid inequalities were also presented to strengthen the new formulation.

The effect of the preprocessing steps and valid inequalities were examined, and the two models were evaluated by solving a set of small benchmark instances presented in (Schneider et al., 2013). The preprocessing steps reduced the number of decision variables considerably, and the valid inequalities were shown to improve the LP-relaxation of the new formulation.

The benchmark results indicate that the new formulation is capable of solving moderately sized instances with up to 15 customers efficiently: all but one benchmark instance were solved to optimality in less than 300 seconds. However, the number of vehicles was limited in the computations; without limiting this number, all the benchmark instances were solved to optimality and significantly lower routing costs were obtained in some instances by using 1-2 additional vehicles. The results further indicate that since recharging times affect the route planning, considerable improvements can be obtained by adopting the variable recharging scheme over the fixed one.

Finally, a test instance based on the actual road network of Finland was constructed and the improved formulation was used to solve various test cases simulating potential real-world BEV routing problems. First, a set of small test cases with nine customers was constructed by varying the battery capacity and incorporating randomly drawn customer time windows. Subsequently, a set of larger test cases with 26 customers was constructed by randomly generating time windows for the customers, and by varying the battery capacity. All the small test cases were solved in less than one second, whereas solving the larger test cases with 26 customers took up to one hour depending on the value of the battery capacity. The results were examined by presenting some of the optimal solutions graphically and plotting the optimal routing cost for different battery capacity values. The results clearly demonstrate how sensible the optimal routing cost is to small battery capacity variations, and how difficult it is to design optimal routing plans even for small test cases. The results further indicate that the value of the battery capacity may have a dramatic impact on the computation time when solving the formulation proposed in this thesis by branch-and-cut.

Since the previous studies adopted a fixed recharging scheme, the new formulation also provides a tool for estimating how much the total energy cost can be reduced without performing a full recharge at charging station visits. The developed model could also be used in evaluating the performance of a heuristic algorithm designed for similar problems, or to facilitate the calibration and design of such heuristics.

Even though this thesis focuses specifically on BEV routing, the developed model can also be used in modeling routing problems involving different types of alternative fuel vehicles (e.g., hydrogen or natural gas vehicles), especially those with a limited charging infrastructure and/or slow refueling time that must be considered in the route planning. Additionally, since the model is capable of solving regular VRPTW problems, it is possible to compare the routing costs incurred by using BEVs to those incurred by using conventional internal combustion engine (ICE) vehicles. Another possibility is to compare the routing costs incurred by using BEVs to those incurred by deploying other alternative fuel vehicles. Such information could be helpful for organization planning to convert their fleet from conventional ICE vehicles to BEVs or other alternative fuel vehicles. By performing several comparisons in problem instances reflecting real-world routing problems, potential benefits and disadvantages could be evaluated, thus facilitating such decisions.

Future avenues of research could be to also model fixed service times in addition to the variable recharging times for the charging station visits through expanding the definition of e-paths, and developing new dominance rules that allow to handle these service times efficiently. Another possibility is to focus on the hierarchical objective and develop new modeling techniques that minimize first the number of vehicles and then the total energy cost of the vehicle routes.

The models proposed in this thesis have been evaluated on relatively small instances. Further research should be devoted to the development of new models and solution methods that allow solving larger E-VRPTW instances to optimality. Towards this end, a possibility could also be to concentrate on some special cases of the E-VRPTW for which, as far as this thesis is aware of, no exact solution methods have been so far proposed in the literature, such as the problem variant without customer time windows, or the single vehicle version of the E-VRPTW.

Finally, the model can be extended to incorporate the simultaneous optimization of the routing of BEVs and the placement of new charging stations.

Bibliography

Baldacci, R., Mingozzi, A., & Roberti, R. (2012). Recent exact algorithms for solving the vehicle routing problem under capacity and time window constraints. *European Journal of Operational Research*, *218*(1), 1–6.

Bard, J. F., Huang, L., Dror, M., & Jaillet, P. (1998). A branch and cut algorithm for the VRP with satellite facilities. *IIE Transactions*, *30*(9), 821–834.

Becker, T. A., Sidhu, I., & Tenderich, B. (2009). Electric vehicles in the United States: a new model with forecasts to 2030. *Center for Entrepreneurship and Technology, University of California, Berkeley*(2009.1).

Bigliani, R., & Gallotti, G. (2009). Case study: electric vehicles using sustainable energy and open networks: the EDISON project, Denmark. Retrieved from http://ec.europa.eu/enterprise/archives/e-business-watch/studies/case_studies/documents/Case%20Studies%202009/CS09_Energy2_Edison.pdf (Accessed: 03/03/2014)

Binding, C., Gantenbein, D., Jansen, B., Sundstrom, O., Andersen, P. B., Marra, F., ... Træholt, C. (2010). Electric vehicle fleet integration in the Danish EDISON project - a virtual power plant on the island of Bornholm. In *Power and Energy Society General Meeting, 2010 IEEE* (pp. 1–8).

Chan, C. (2002). The state of the art of electric and hybrid vehicles. *Proceedings of the IEEE*, *90*(2), 247–275.

Chan, C. (2007). The state of the art of electric, hybrid, and fuel cell vehicles. *Proceedings of the IEEE*, *95*(4), 704–718.

Clarke, G. u., & Wright, J. (1964). Scheduling of vehicles from a central depot to a number of delivery points. *Operations research*, *12*(4), 568–581.

Conrad, R. G., & Figliozzi, M. A. (2011). The recharging vehicle routing problem. In *Proceedings Industrial Engineering Research Conference, Reno, NV.*

Cordeau, J.-F., Gendreau, M., Laporte, G., Potvin, J.-Y., Semet, F., et al. (2002). A guide to vehicle routing heuristics. *Journal of the Operational Research society*, *53*(5), 512–522.

Crevier, B., Cordeau, J.-F., & Laporte, G. (2007). The multi-depot vehicle routing problem with inter-depot routes. *European Journal of Operational Research*, *176*(2), 756–773.

Dantzig, G. B., & Ramser, J. H. (1959). The truck dispatching problem. *Management Science*, *6*(1), 80–91.

Daziano, R. A. (2013). Conditional-logit bayes estimators for consumer valuation of electric vehicle driving range. *Resource and Energy Economics*, *35*(3), 429 - 450. Retrieved from http://www.sciencedirect.com/science/article/pii/S0928765513000298 doi: http://dx.doi.org/10.1016/j.reseneeco.2013.05.001

Deb, K. (2001). *Multi-Objective Optimization Using Evolutionary Algorithms* (Vol. 2012). John Wiley & Sons Chichester.

Demir, E., Bektas, T., & Laporte, G. (2013). A review of recent research on green road freight transportation. *European Journal of Operational Research*.

Desrochers, M., Desrosiers, J., & Solomon, M. (1992). A new optimization algorithm for the vehicle routing problem with time windows. *Operations Research*, *40*(2), 342–354.

Desrochers, M., & Laporte, G. (1991). Improvements and extensions to the miller-tucker-zemlin subtour elimination constraints. *Operations Research Letters*, *10*(1), 27–36.

Dijkstra, E. W. (1959). A note on two problems in connexion with graphs. *Numerische Mathematik*, *1*(1), 269–271.

Edwards, J. B., McKinnon, A. C., & Cullinane, S. L. (2010). Comparative analysis of the carbon footprints of conventional and online retailing: a "last mile" perspective. *International Journal of Physical Distribution & Logistics Management*, *40*(1/2), 103–123.

Ehsani, M., Gao, Y., & Emadi, A. (2009). *Modern Electric, Hybrid Electric, and Fuel Cell Vehicles: Fundamentals, Theory, and Design*. CRC press.

Erdoğan, S., & Miller-Hooks, E. (2012). A green vehicle routing problem. *Transportation Research Part E: Logistics and Transportation Review*, *48*(1), 100–114.

Ester, M., Kriegel, H.-P., Sander, J., & Xu, X. (1996). A density-based algorithm for discovering clusters in large spatial databases with noise. In *Proceedings of the International Conference on Knowledge, Discovery and Data Mining (KDD)* (Vol. 96, pp. 226–231).

European Parliament, & European Council. (2011). Regulation (EU) No 510/2011 - Setting emission performance standards for new light commercial vehicles as part of the union's integrated approach to reduce CO_2 emissions from light-duty vehicles. Retrieved from http://eur-lex.europa.eu/LexUriServ/LexUriServ.do?uri=OJ:L:2011:145:0001:0018:EN:PDF (Accessed: 01/01/2014)

Figliozzi, M. A. (2010). An iterative route construction and improvement algorithm for the vehicle routing problem with soft time windows. *Transportation Research Part C: Emerging Technologies*, *18*(5), 668–679.

Finnegan, C., Finlay, H., O'Mahony, M., & O'Sullivan, O. (2005). Urban freight in Dublin city center, Ireland: survey analysis and strategy evaluation. *Transportation Research Record: Journal of the Transportation Research Board*, *1906*(1), 33–41.

Flood, M. M. (1956). The traveling-salesman problem. *Operations Research*, *4*(1), 61–75.

Franke, T., Neumann, I., Bühler, F., Cocron, P., & Krems, J. F. (2012). Experiencing range in an electric vehicle: understanding psychological barriers. *Applied Psychology*, *61*(3), 368–391.

Fulton, L., Cazzola, P., Cuenot, F., Kojima, K., Onoda, T., & Staub, J. (2009). *Transport, Energy and CO_2: Moving Toward Sustainability.* Paris, France: OECD/IEA.

Glover, F., & Laguna, M. (1999). *Tabu Search.* Springer.

Golden, B. L., Raghavan, S., & Wasil, E. A. (2008). *The Vehicle Routing Problem: Latest Advances and New Challenges* (Vol. 43). Springer.

Gonçalves, F., Cardoso, S., Relvas, S., & Barbosa-Póvoa, A. (2011). Optimization of a distribution network using electric vehicles: a VRP problem. In *IO2011—15 Congresso da Associação Portuguesa de Investigação Operacional.* INESC, Lisboa, Portugal.

Ichimori, T., Ishii, H., & Nishida, T. (1983). Two routing problems with the limitation of fuel. *Discrete Applied Mathematics*, *6*(1), 85–89.

ILOG. (2013). CPLEX: ILOG CPLEX 12.5 callable library.

Intergovernmental Panel on Climate Change. (2013). *Climate Change 2013: The Physical Science Basis.* Retrieved from http://www.climatechange2013.org/images/uploads/WGIAR5_WGI-12Doc2b_FinalDraft_All.pdf (Accessed: 05/01/2014)

Jha, A. (2012). *Next-Generation Batteries and Fuel Cells for Commercial, Military, and Space Applications.* Taylor & Francis. Retrieved from http://books.google.fi/books?id=HYyoizlAuiIC

Kempton, W., Udo, V., Huber, K., Komara, K., Letendre, S., Baker, S., … Pearre, N. (2008). A test of vehicle-to-grid (V2G) for energy storage and frequency regulation in the PJM system (Tech. Rep.). University of Delaware. Retrieved from http://www.udel.edu/V2G/resources/test-v2g-in-pjm-jan09.pdf (Accessed: 01/01/2014)

Kim, B.-I., Kim, S., & Sahoo, S. (2006). Waste collection vehicle routing problem with time windows. *Computers & Operations Research*, *33*(12), 3624–3642.

Kintner-Meyer, M., Schneider, K., & Pratt, R. (2007). Impacts assessment of plug-in hybrid vehicles on electric utilities and regional us power grids, part 1: technical analysis. *Pacific Northwest National Laboratory (a).*

Kontoravdis, G., & Bard, J. F. (1995). A GRASP for the vehicle routing problem with time windows. *ORSA Journal on Computing*, *7*(1), 10–23.

Laporte, G. (2009). Fifty years of vehicle routing. *Transportation Science*, *43*(4), 408–416.

Laporte, G., Desrochers, M., & Nobert, Y. (1984). Two exact algorithms for the distance-constrained vehicle routing problem. *Networks*, *14*(1), 161–172.

Laporte, G., Nobert, Y., & Arpin, D. (1984). Optimal solutions to capacitated multidepot vehicle routing problems. *Congressus Numerantium*, *44*, 283-292.

Mangram, M. E. (2012). The globalization of Tesla Motors: a strategic marketing plan analysis. *Journal of Strategic Marketing*, *20*(4), 289–312.

Mehrez, A., & Stern, H. I. (1985). Optimal refueling strategies for a mixed-vehicle fleet. *Naval Research Logistics Quarterly*, *32*(2), 315–328.

Mehrez, A., Stern, H. I., & Ronen, D. (1983). Vehicle fleet refueling strategies to maximize operational range. *Naval Research Logistics Quarterly*, *30*(2), 319–342.

Melkman, A. A., Stern, H. I., & Mehrez, A. (1986). Optimal refueling sequence for a mixed fleet with limited refuelings. *Naval Research Logistics Quarterly*, *33*(4), 759–762.

Mladenović, N., & Hansen, P. (1997). Variable neighborhood search. *Computers & Operations Research*, *24*(11), 1097–1100.

National Research Council. (2010). *Advancing the Science of Climate Change*. The National Academies Press. Retrieved from http://www.nap.edu/openbook.php?record_id=12782 (Accessed: 05/01/2014)

Polski Instytut Spraw Miedzynarodowych. (2009). *Energy Security and Climate Change : Double Challenge for Policymakers*. Polski Instytut Spraw Miedzynarodowych.

Psaraftis, H. N. (1983). Interchange procedures for local search in a precedence-constrained routing problem. *European Journal of Operational Research*, *13*(4), 391–402.

Savelsbergh, M. W. (1985). Local search in routing problems with time windows. *Annals of Operations research*, *4*(1), 285–305.

Schneider, M., Stenger, A., & Goeke, D. (2013). The electric vehicle routing problem with time windows and recharging stations (Tech. Rep.). Darmstadt Technical University, Department of Business Administration, Economics and Law, Institute for Business Studies (BWL). Retrieved from http://www.is-frankfurt.de/fileadmin/user_upload/publicationsNew/TheElectricVehicleRoutingProbl4278.pdf (Accessed: 05/01/2014)

Scholz, I., & Stöcker, D. (2013). JOSM: Java OpenStreetMap Editor. https://josm.openstreetmap.de/. (Accessed: 01/03/2014)

Skippon, S., & Garwood, M. (2011). Responses to battery electric vehicles: UK consumer attitudes and attributions of symbolic meaning following direct experience to reduce psychological distance. *Transportation Research Part D: Transport and Environment*, *16*(7), 525–531.

Solomon, M. M. (1987). Algorithms for the vehicle routing and scheduling problems with time window constraints. *Operations Research*, *35*(2), 254–265.

Tambovceva, T., & Tambovcevs, A. (2012). Interaction between environmental performance and logistic system: a case study of international company. *Wold Academy of Science, Engineering and Technology*, *68*.

Tarantilis, C. D., Zachariadis, E. E., & Kiranoudis, C. T. (2008). A hybrid guided local search for the vehicle-routing problem with intermediate replenishment facilities. *INFORMS Journal on Computing*, *20*(1), 154–168.

Thiell, M., Zuluaga, J. P. S., Montañez, J. P. M., & van Hoof, B. (2011). Green logistics: global practices and their implementation in emerging markets. *Green Finance and Sustainability: Environmentally-Aware Business Models and Technologies*, 334.

Toth, P., & Vigo, D. (2001). *The Vehicle Routing Problem*. Siam.

Wiederer, A., & Philip, R. (2010). Policy options for electric vehicle charging infrastructure in C40 cities. Retrieved from http://www.innovations.harvard.edu/cache/documents/11089/1108934.pdf (Accessed: 01/03/2014)